

**An-Najah National University
Faculty of Graduate Studies**

**Water Disinfection by Photo-Degradation
of Microorganisms Using Natural Dye-
Sensitized ZnO Catalyst**

**By
Sondos Othman Abed-Alhadi Ateeq**

**Supervisors
Prof. Hikmat Hilal
Dr. Majdi Dweikat**

**This Thesis is Submitted in Partial Fulfillment of the Requirements
for the Degree of Master of Science in Chemistry, Faculty of Graduate
Studies, An-Najah National University, Nablus, Palestine.**

2012

Water Disinfection by Photo-Degradation of Microorganisms Using Natural Dye- Sensitized ZnO Catalyst

**By
Sondos Othman Abed-Alhadi Ateeq**

This Thesis was defended successfully on 22/1/2012 and approved by:

Defense Committee Members

Signature

- | | |
|--|-------|
| 1. Prof. Hikmat Hilal / Supervisor | |
| 2. Dr. Majdi Dweikat / Co-Supervisor | |
| 3. Dr. Hatim Saleem / External Examiner | |
| 4. Dr. Mohammad Suliman / Internal Examiner | |

Dedication

To My Mother, Father, Sister, and Brothers

Also to my Husband, for their continuous support

with my appreciation

Acknowledgment

Praise be to Allah who enable me to complete this work.

Thanks and deepest appreciation to my supervisors, Prof. Hikmat Hilal for his guidelines, support and great help throughout this research, and Dr. Majdi Dweikat for his encouragement, and continuous theoretical and practical help.

Thanks for Dr. Ahed Zyoud for his continuous help and useful discussions.

I would like to thank the technical staff in Chemistry, Biology and Medical Laboratory Sciences Departments, especially Mr. Yusuf Salama, for their technical help.

Thanks for Poison and Chemical and Biological Analysis Center at An-Najah National University, and its director Dr. Amjad Ezz-Aldeen for their help in GC/MS analysis.

Thanks are due to Dr. Guy Campet (ICMCB, University of Bordeaux, France) and his group for their help in XRD and SEM measurements.

Financial support for this project from Al-Maqdisi program is acknowledged.

My great thanks for my father and mother for their endless support. I would like to thank my uncle Dr. Omar Ateeq for his encouragement and proofreading for the Arabic abstract.

I wish to thank all my friends, especially research lab mates.

الإقرار

أنا الموقعة أدناه مقدمة الرسالة التي تحمل العنوان:

Water Disinfection by Photo-Degradation of Microorganisms Using Natural Dye-Sensitized ZnO Catalyst

استخدام ZnO المطور بالأصبغ الطبيعية في تعقيم المياه بالتحطيم الضوئي للبكتيريا

أقر بأن ما اشتملت عليه هذه الرسالة هو نتاج جهدي الخاص، باستثناء ما تمت الإشارة إليه حيثما ورد، وأن هذه الرسالة ككل، أو أي جزء منها لم يقدم من قبل لنيل أية درجة أو لقب علمي أو بحثي لدي أي مؤسسة تعليمية أو بحثية أخرى.

Declaration

The work provide in this thesis, unless otherwise referenced, is the researcher's own work, and has not been submitted elsewhere for any other degree or qualification.

Student's name:

اسم الطالبة:

Signature:

التوقيع:

Date:

التاريخ:

List of Abbreviations

Symbol	Abbreviation
UV	Ultraviolet light
AOP	Advanced Oxidation Processes
DBPs	Disinfection By-Products
THMs	Trihalomethanes
TOC	Total Organic Carbon
AC	Activated Carbon
<i>E. coli</i>	<i>Escherichia coli</i>
CFU	Colony Forming Unit
CoA	Coenzyme A
VB	Valence Band
CB	Conduction Band
E_F	Fermi Level
DSSC	Dye Sensitized Solar Cell
PVC	Polyvinyl Chloride
PL	Photoluminescence
SEM	Scanning Electron Microscopy
XRD	X-Ray Diffraction
FWHM	Full Width at Half Maximum
GC-MS	Gas Chromatography-Mass Spectroscopy
eV	Electron Volt
HOMO	Highest Occupied Molecular Orbital
LUMO	Lowest Unoccupied Molecular Orbital
MDA	Malondialdehyde
E_v	Valence band Edge
E_c	Conduction band Edge
e⁻	Electron
h⁺	Hole
VB	Valence Band
CB	Conduction band
E_g	Band gap
pH_{zpc}	pH of zero point charge

List of Contents

No.	Content	Page
	Dedication	iii
	Acknowledgment	iv
	Declaration	v
	List of Abbreviations	vi
	List of Contents	vii
	List of Tables	xi
	List of Figures	xii
	Abstract	xv
	Chapter 1: Introduction	1
1.1	Overview	2
1.2	Disinfection by Oxidation Processes	4
1.3	Disinfection Mechanisms	6
	How does Disinfection Work?	7
1.4	Microorganisms	8
1.4.1	Types of Pathogenic Microorganisms	9
1.4.2	Bacteria	9
1.4.2.1	<i>Escherichia coli (E. coli)</i>	9
1.5	Semiconductor Photocatalysis	10
1.5.1	Energy Bands of Solids	12
1.5.2	Charge Carrier Generation	14
1.5.3	Fermi Level	15
1.5.4	Photo-Effect on a Semiconductor	15
1.5.5	Semiconductor Nanoparticles	17
1.6	Zinc Oxide Semiconductor	18
1.7	Zinc Oxide Sensitization	20
1.7.1	Anthocyanin Dye	22
1.8	What is new in this work	24
1.9	Objectives	24
	Chapter 2: Materials and Methods	26
2.1	Materials	27
2.1.1	Zinc Oxide	27
2.1.2	Anthocyanin dye	27
2.1.3	Other Chemicals	27
2.1.4	Bacteria	27
2.2	Photo-Catalytic System and Irradiation Sources	28
2.2.1	Photocatalytic System	28
2.2.2	Irradiation Sources	29
2.3	Measuring Devices	30
2.3.1	UV-Visible Spectrophotometry	30

No.	Content	Page
2.3.2	Lux Meter	31
2.3.3	pH Meter	31
2.3.3	Thermometer	31
2.4	Solution Preparations	31
2.4.1	Chemical Solutions Preparation	31
2.4.2	Bacterial Cultures Preparation	32
2.5	Catalyst Preparation	33
2.5.1	Anthocyanin Dye Extraction	33
2.5.2	Zinc Oxide Powder/Anthocyanin Dye Catalyst Preparation	33
2.5.3	Nanoparticle Zinc Oxide /Anthocyanin Dye Catalyst Preparation	34
2.6	Catalyst Characterization	34
2.6.1	UV_Visible Characterization	35
2.6.2	Photoluminescence Spectra (PL)	35
2.6.3	SEM Characterization	35
2.6.4	XRD Characterization	36
2.7	Control Photo-Degradation Experiments	36
	Measuring the remaining concentration of bacteria	37
2.7.1	Dye as Catalyst	37
2.7.2	Naked ZnO as Catalyst	38
2.7.3	ZnO/Anthocyanin Catalyst	38
2.7.3.1	Time Effect	39
2.7.3.2	Temperature Effect	39
2.7.3.3	pH Effect	39
2.7.3.4	Catalyst Concentration Effect	40
2.7.3.5	Bacteria Concentration Effect	40
2.7.3.6	Nutrient broth and saline media Effect	40
2.7.4	Control Experiments	40
2.8	Catalyst Recycling	41
2.9	Disinfection by-Products Identification	41
	Chapter 3: Results	42
3.1	Introduction	43
3.2	Sensitized Commercial (micro-size) ZnO Catalyst	43
3.2.1	Catalyst Characterization	43
3.2.1.1	UV-Visible Spectra	43
	<i>Anthocyanin Dye</i>	43
	<i>ZnO/anthocyanin Catalyst</i>	45
3.2.1.2	Photoluminescence Spectra (PL)	45

No.	Content	Page
3.2.2	Solar Simulator Irradiation Experiments	46
3.2.2.1	Control Experiments	47
3.2.2.2	Photo-Catalytic Experiments	47
3.2.2.3	Factors Affecting Catalyst Efficiency	51
	<i>Photo-degradation Reaction Profile</i>	51
	<i>Effect of Temperature on Catalyst Efficiency</i>	52
	<i>Effect of pH on Catalyst Efficiency</i>	53
	<i>Effect of Catalyst Concentration on its Efficiency</i>	54
	<i>Effect of Bacteria Concentration on Catalyst Efficiency</i>	56
	Nutrient broth and saline media Effect on catalyst efficiency	57
3.2.2.4	Catalyst Recycling Experiments	59
3.2.2.5	Disinfection By-Product Identification	61
3.2.3	UV Irradiation Experiments	62
3.2.3.1	Control Experiments	62
3.2.3.2	Photo-Catalytic Experiments	62
3.3	Sensitized Nano-Particle ZnO Catalyst	64
3.3.1	Catalyst Characterization	64
3.3.1.1	UV-Visible Characterization	64
3.3.1.2	Photoluminescence Spectra (PL)	65
3.3.1.3	XRD Study	66
3.3.1.4	SEM Results	68
3.2.2	Solar-Simulator Light Photocatalytic Experiments	70
3.2.2.1	Control Experiments	70
3.2.2.2	Photo-Catalytic Experiments	70
	Chapter 4: Discussion	73
4.1	Introduction	74
4.2	The Micro-Sized ZnO	75
4.2.1	Solar Simulator Irradiation Experiments	76
4.2.1.1	Control Experiments	76
4.2.1.2	Photo-Catalytic Experiments	77
4.2.1.3	Factors Affect Photo-Degradation Reaction	79
	<i>Effect of Illumination Time on Catalyst Efficiency</i>	79
	<i>Effect of Temperature on Catalyst Efficiency</i>	79
	<i>Effect of pH on Catalyst Efficiency</i>	80
	<i>Effect of Catalyst Concentration on Efficiency</i>	81
	<i>Effect of Bacteria Concentration on Catalyst Efficiency</i>	82
	<i>Nutrient broth and saline media Effect on catalyst efficiency</i>	82
4.2.1.4	Catalyst Recycling	83

No.	Content	Page
4.2.1.5	Disinfection by-Products Identification	83
	<i>Cell Death</i>	83
4.2.2	UV Irradiation Experiments	85
4.2.2.1	Control Experiments	85
4.2.2.2	Photo-Catalytic Experiments	85
4.3	The Nano-Size ZnO	86
4.3.1	Solar Simulator Irradiation Experiments	86
4.3.1.1	Control Experiments	86
4.3.1.2	Photo-Catalytic Experiments	89
	Conclusions	89
	Suggestions for Further Work	90
	References	91
	Appendix	107
	الملخص	ب

List of Tables

No.	Table	Page
Table (1.1)	The comparison of the main disinfectants	3
Table (2.1)	UV lamp specifications	30
Table (3.1)	Degradation percents, turnover frequency and quantum yield values in the photo-catalytic and control experiment for micro ZnO	49
Table (3.2)	Degradation percents, turnover frequency and quantum yield values in cutting off UV irradiations experiment	50
Table (3.3)	Degradation percents, turnover frequency and quantum yield values in time effect experiment.	52
Table (3.4)	Degradation percents, turnover frequency and quantum yield values in temperature effect experiment	53
Table (3.5)	Degradation percents, turnover frequency and quantum yield values in pH effect experiment.	54
Table (3.6)	Degradation percents, turnover frequency and quantum yield values in catalyst concentration effect experiment.	56
Table (3.7)	Degradation percents, turnover frequency and quantum yield values for the ZnO/anthocyanin catalysts in effect of contaminant concentration study.	57
Table (3.8)	Degradation percents, turnover frequency and quantum yield values in nutrient broth medium experiment.	58
Table (3.9)	Degradation percents, turnover frequency and quantum yield values in normal saline medium experiment.	59
Table (3.10)	Degradation percents, turnover frequency and quantum yield values in Reuse experiment.	60
Table (3.11)	Degradation percents, turnover frequency and quantum yield values in Re-dying the used catalyst experiment.	61
Table (3.12)	Degradation percent, turnover frequency and quantum yield values for catalysts under UV irradiation	63
Table (3.13)	Degradation percents, turnover frequency and quantum yield values in catalyst effect and control experiment for the nano ZnO.	71
Table (3.14)	Degradation percents, turnover frequency and quantum yield values in cutting off UV irradiations experiment in nano ZnO catalyst.	72

List of Figures

No.	Figure	Page
Fig. (1.1)	Inactivation of a bacterial cell.	8
Fig. (1.2)	Schematic diagram of the energy levels of an (a) n-type semiconductor and (b) a p-type semiconductor.	14
Fig. (1.3)	Schematic diagram of the energy levels of an intrinsic semiconductor.	14
Fig. (1.4)	Fermi level in a semiconductor.	15
Fig. (1.5)	How Semiconductor Photocatalyst Functions.	16
Fig. (1.6)	Schematic Mechanism of sensitizing ZnO by dye.	21
Fig. (1.7)	Basic chemical structures of most abundant anthocyanins.	23
Fig. (2.1)	Spectrograms for the sun, mercury vapor and halogen lamps.	30
Fig. (3.1)	Electronic absorption spectra in the UV-Visible region for the prepared anthocyanin dye in ethanol.	44
Fig. (3.2)	Literature electronic absorption spectra for anthocyanin dye extracted from Hibiscus Tea.	44
Fig. (3.3)	Solid-state electronic absorption spectra in the UV-Visible region for ZnO/anthocyanin catalyst suspension.	45
Fig. (3.4)	Photoluminescence Spectra measured for the prepared ZnO/anthocyanin catalyst (a) and naked ZnO (b).	46
Fig. (3.5)	Bacteria degradation percent under control conditions compared to that when ZnO/anthocyanin catalyst was used under solar simulator (a) light irradiation effect and b) catalyst effect in absence of light.	48
Fig. (3.6)	Comparison between sensitized and naked ZnO catalytic efficiencies in bacteria degradation under solar simulator.	48
Fig. (3.7)	Effect of ZnO/anthocyanin catalyst on bacteria photo-degradation compared to naked ZnO and control conditions.	49
Fig. (3.8)	ZnO/anthocyanin and ZnO catalysts under solar simulator radiation in the presence and absence of UV light.	50
Fig. (3.9)	Time effect on bacteria inactivation reaction.	51

No.	Figure	Page
Fig. (3.10)	Temperature effect on bacteria photo-degradation reaction.	53
Fig. (3.11)	Medium pH effect on bacteria inactivation reaction.	54
Fig. (3.12)	Effect of ZnO/ anthocyanin catalyst concentration on bacteria inactivation reaction.	55
Fig. (3.13)	Bacteria concentration effect on bacteria photo-degradation reaction.	57
Fig. (3.14)	Effect of nutrient broth medium on ZnO/anthocyanin catalytic efficiency in bacteria photo-degradation reaction.	58
Fig. (3.15)	Effect of saline medium on ZnO/anthocyanin catalytic efficiency in bacteria photo-degradation reaction.	59
Fig. (3.16)	Bacteria photo-degradation reaction profiles for fresh and recovered ZnO\anthocyanin catalyst showing its catalytic activity with 1 st and 2 nd reuse compared to the fresh catalyst.	60
Fig. (3.17)	Effect of Re-dyeing the used catalyst on its catalytic efficiency compared to a fresh catalyst in bacteria photo-degradation reaction.	61
Fig. (3.18)	Effect of ZnO/anthocyanin catalyst on bacteria photo-degradation reaction compared to naked ZnO and control conditions under UV irradiation.	64
Fig. (3.19)	Solid-state electronic absorption spectra ZnO catalyst nanoparticles suspension.	65
Fig. (3.20)	Photoluminescence spectra measured for ZnO Nanoparticles.	65
Fig. (3.21)	Literature X-ray diffraction patterns of nano zinc oxide (ZnO) particles.	67
Fig. (3.22)	X-ray diffraction patterns for ZnO (nanoparticles) /anthocyanin dye (a) and ZnO nanoparticles (b).	67
Fig. (3.23)	SEM images for the prepared ZnO nanoparticles (a, b and c).	69
Fig. (3.24)	Effect of ZnO/anthocyanin (nano-particles) catalyst on bacteria photo-degradation compared to naked nano-ZnO and control conditions.	71
Fig. (3.25)	ZnO/anthocyanin and ZnO (nano-particles) catalysts under solar simulator radiation in the presence and absence of UV light (using cut-off filter).	72

No.	Figure	Page
Fig. (4.1)	Sensitization of ZnO photo-catalyst by dye molecules to the visible light.	78
Fig. (4.2)	Comparison between micro and nano sized sensitized and naked ZnO catalysts under light and dark conditions.	88

**Water Disinfection by Photo-Degradation of Microorganisms Using
Natural Dye-Sensitized ZnO Catalyst**

By

Sondos Othman Abed-Alhadi Ateeq

Supervisors

Prof. Hikmat Hilal

Dr. Majdi Dweikat

Abstract

Several procedures are commonly used for water disinfection from bacteria. Unfortunately each procedure has its shortcomings. The most important shortcoming is the formation of disinfection by-products. Photo-degradation of microorganisms using photocatalysts (such as ZnO) could be a good alternative. However, ZnO is a wide band gap (3.2 eV) semiconductor, and demands UV irradiations for excitation. Therefore, sensitization of ZnO is necessary here to make use of the solar light for the photo-catalyst excitation.

In this work, ZnO semiconductor particles, combined with safe low cost sensitizer (the natural dye anthocyanin) were used to disinfect water from bacteria by photodegrading it with solar simulator light. Both nano- and micro-sized ZnO particles were investigated here. The natural dye can sensitize ZnO to the visible light, as the dye has smaller band gap and absorbs in the visible region. More than 90% degradation percent was achieved in 90 minutes under solar simulator, with improvement ~10% than the naked ZnO.

Control experiments that were conducted in absence of catalyst or light showed only small loss in bacteria concentration. Sensitized ZnO

catalyst worked well under purely visible light. Using a cut-off filter (eliminating 400 nm and shorter wavelengths) confirmed that. The sensitized catalyst activity was almost not affected by eliminating UV from the solar simulator light. ZnO nano-particles (with average size 20 nm) were prepared and used for water disinfection. They were characterized using UV-Visible absorption spectrophotometry, photoluminescence spectrometry, XRD and SEM techniques. Sensitized ZnO nano-particles showed higher catalytic activity than the sensitized ZnO with large particle size (micro-size). Complete degradation was achieved with nano-particles under the same conditions. Some factors affecting photo-degradation reaction and catalyst efficiency, such as illumination time, temperature, pH, catalyst concentration, contaminant concentration and dissolved organic and inorganic impurities, were studied.

Changing temperature didn't significantly affect the catalyst efficiency. The amphoteric nature of ZnO decreased the effect of changing pH value for the reaction medium on the catalyst efficiency. The nominal amount of the used catalyst affected the degradation, and there was an optimum weight that should be used for maximum benefit. Increasing the initial concentration of contaminants enhanced the catalyst activity. The presence of impurities (organic and inorganic) affected the catalyst activity in different manners. Catalyst recovery after reaction completion was achieved by simple means, and the recovered catalyst showed good sound activity on reuse. Re-dyeing the re-used catalyst restored its efficiency under solar simulator.

Chapter 1

Introduction

Chapter 1

Introduction

1.1 Overview

Clean and pure water is urgently needed by all humans in our world, but due to development and high-density population, with insufficient sanitation and water treatment systems, surface water became highly polluted with human waste. Even urban tap water is becoming increasingly contaminated. Primarily humans, but also animals, are the source of microorganisms that contaminate water sources and cause intestinal infections [1].

To get water that can be used in daily life without fearing of diseases, it must be purified and disinfected before being used. Water disinfection means the removal, deactivation or killing of pathogenic microorganisms. Microorganisms are destroyed or deactivated, resulting in termination of growth and reproduction. Sterilization is a process related to disinfection. However, during the sterilization process all present microorganisms are killed, both harmful and harmless microorganisms. Disinfection can be chemical or physical. For physical disinfection of water several disinfectants can be used such as: Ultraviolet light (UV), Electronic radiation, Gamma rays and Heat. For chemical disinfection of water several disinfectants can be used such as: Chlorine dioxide (ClO_2), hypochlorite (OCl), ozone (O_3), halogens including chlorine (Cl_2), bromine (Br_2) and iodine (I_2), metal ions such as copper (Cu^{2+}) and silver (Ag^+), potassium permanganate (KMnO_4), alcohols, soaps, detergents, quarternary

ammonium salts, hydrogen peroxide, in addition to different acids and bases [2]. Table (1.1) summarizes advantages and disadvantages of common disinfecting compounds.

Table (1.1): The comparison of the main disinfectants [3]

		Advantages		Limitations	
Chlorination	Chlorine (Cl ₂)	Very effective for removing almost all microbial pathogens	Well-established technology; more cost-effective than either UV radiation or ozone disinfection; chlorine residual can prolong disinfection; reliable and effective against a wide spectrum of pathogenic organisms; effective in oxidizing certain organic and inorganic compounds; flexible dosing control; eliminate certain noxious odors	Chlorine is a dangerous gas that is lethal at concentrations as low as 0.1 percent air by volume.	All forms of chlorine are highly corrosive and toxic; create hazardous compounds - disinfection by-products (e.g., trihalomethanes (THMs))
	Chlorine dioxide (ClO ₂)	Very effective even in low concentration; broad-spectrum; quick and long time disinfection; does not generate chlorinated phenols and THMs		Pungent odor; should be stored in a dark area.	
	Sodium hypochlorite solution	Easier to handle; no disinfection by products		Very corrosive; decompose and should not be stored for more than one month; stored in a cool, dark, dry area.	
	Solid calcium hypochlorite	When packaged, calcium hypochlorite is very stable, allowing long time storage.		A corrosive material with a strong odor that requires proper handling; should be kept away from organic materials; readily absorbs moisture, forming chlorine gas.	
	Chloramine	An effective bactericide; produces fewer disinfection by-products; generated onsite; Chloramine-forming reactions are 99 percent complete within a few minutes.		A weak disinfectant, much less effective against viruses or protozoa than free chlorine; appropriate for use as a secondary disinfectant; detrimental reaction - produce nitrogen trichloride	
Ozonation		Requiring shorter contact time and dosage than chlorine; more effective than chlorine in destroying viruses and bacteria;		Ozone gas is unstable and must be generated onsite; does not maintain an adequate residual in water; requiring complicated equipment and efficient	

	does not directly produce halogenated organic materials unless a bromide ion is present; fewer safety problems associated with shipping and handling	contacting systems; very reactive and corrosive; Ozone is extremely irritating and possibly toxic.
Ultraviolet Light (UV)	Readily available; produces no known toxic residuals; requires short contact times, and the equipment is easy to operate and maintain; user-friendly for operators; equipment requires less space.	May not inactivate <i>Giardia lamblia</i> or <i>Cryptosporidium</i> cysts, and should be used only by groundwater systems not directly influenced by surface water; unsuitable for water with high levels of suspended solids, turbidity, color, or soluble organic matter, which can react with or absorb the UV radiation.

1.2 Disinfection by Oxidation Processes

Advanced Oxidation Processes (AOP) are among the newer chemical techniques used for water purification. They can be divided into two types depending on the techniques used, namely: abiotic degradation (such as thermal degradation/combustion, molten salt processes, wet oxidation, chemical oxidation or acid-base hydrolysis) and photo-degradation (by $\text{H}_2\text{O}_2/\text{UV}$, O_3/UV or $\text{O}_3/\text{H}_2\text{O}_2/\text{UV}$ processes, solar photolysis, processes in vacuum ultraviolet or photo-catalysis) [4-5].

Other water disinfection procedures involve formation of disinfecting by-products (DBPs). Important examples are the trihalomethanes (THMs). Such processes have limited use due to their carcinogenic and mutagenic nature [6]. They result from chlorination of groundwater with high total organic carbon (TOC) content. To decrease DBPs formation, it will be better to decompose organic compounds prior to chlorine addition. Solar disinfection by photo-catalysis has the advantage of destroying the bacterial population and DBPs as well.

Standard water treatment techniques are often too expensive both in capital costs, operating costs and maintenance costs. In this respect, the use

of solar energy as an alternative could prove to be an economic technology especially in countries with high sunlight exposure.

In recent years, applications to environmental cleanup have been one of the most active areas in heterogeneous photo-catalysis. Semiconductors are used to degrade organic pollutants in water to harmless inorganic materials. Titanium dioxide and zinc oxide were used in photo-catalytic degradation of textile dyeing wastewater under ultraviolet irradiation. A maximum color removal of 96% was achieved after irradiation time of 2.5 hours when titanium dioxide was used at 303°K, while 82% color reduction was observed when zinc oxide was used for the same period at same temperature [7]. Pare et al used zinc oxide suspension for photocatalytic degradation of lissamine fast yellow dye using artificial light [8]. Photocatalytic decolorization of azo-dye Orange II in water has been examined in an external UV light irradiation slurry photoreactor using zinc oxide (ZnO) as a semiconductor photocatalyst [9]. ZnO and activated carbon-supported ZnO were used in photo-degradation of methyl orange and phenazopyridine with direct solar light in aqueous solutions, both naked ZnO and AC/ZnO were highly efficient in mineralizing phenazopyridine, reaching complete removal in about 50 minutes, with AC/ZnO having the higher edge, the photo-degradation reaction was induced by the UV tail of the solar light [10-11]. Also nano-ZnO has been applied in wastewater treatment by photocatalytic oxidation [12]. Furthermore, ZnO has been used to eliminate hazardous organic compounds, such as phenol, from wastewaters [13].

There have been numerous studies carried out across the world focus on metal oxides and zinc oxide using as photo-catalyst in order to photodegrade organic pollutants and microorganisms in water. Shang and his colleagues used palladium oxide nanoparticles that are well dispersed on a nitrogen-doped titanium oxide matrix photocatalyst for water disinfection [14]. TiO₂ [15-16] silver modified titania photocatalyst [17] and ZnO nanorods [18] were used in bacteria inactivation for drinking-water disinfection. Belapurkar *et al* used TiO₂ supported on a glass tube and a stainless steel plate, and evaluated them for their bactericidal effect using water primed with *Escherichia coli*, in a quartz reactor using 350 nm light and solar light. The study indicates that the technique can be used for disinfection up to ~ 20 L water daily using solar light [19].

Solar photocatalytic disinfection of a group of bacteria and fungi aqueous suspensions was carried out with TiO₂, ZnO and Sahara desert dust by researchers [20]. Liu and Yang used ZnO and TiO₂ for Photocatalytic inactivation of *Escherichia coli* and *Lactobacillus helveticus* with ultraviolet light, both TiO₂ and ZnO with 365 nm ultraviolet (UV) light was studied in a batch reactor. Almost all the initial *E. coli* cells (10⁸ CFU/ml) were inactivated in 40 min in the presence of 2 g ZnO /L [21].

1.3 Disinfection Mechanisms

Chemical inactivation of microbiological contamination in natural or untreated water is usually on the final steps to reduce pathogenic microorganisms in drinking water. Combinations of water purification

steps (oxidation, coagulation, settling, disinfection and filtration) make drinking water safer [2].

How does Disinfection Work?

Disinfection commonly takes place by: destroying cell wall of microorganisms, inhibiting proteins or nucleic acids synthesis, changing cell membrane permittivity and antagonizing enzymes action (structural change in enzymes).

These disturbances in cell activity cause microorganisms to no longer be able to multiply. This causes the microorganisms to die out. Oxidizing disinfectants also demolish organic matter in the water, causing a lack of nutrients [22].

In 1988 Matsunaga et al. suggested that the hole in the semiconductor valence band (VB) received an electron from coenzyme A (CoA) as the donor forming dimeric CoA. Dimerization of CoA inhibits respiration and causes death of the cells [23]. In 1999 Maness et al. reported that in the presence of TiO_2 the lipid peroxidation reaction takes place. Consequently, the normal functions associated with an intact membrane, such as respiratory activity, are lost [24]. The same authors investigated the mechanisms of cell death with a focus on the features of cell wall and cytoplasmic membrane damages caused by the photocatalytic reactions [25]. Figure (1.1) shows a sketch for the photo-catalytic inactivation of a bacterial cell process.

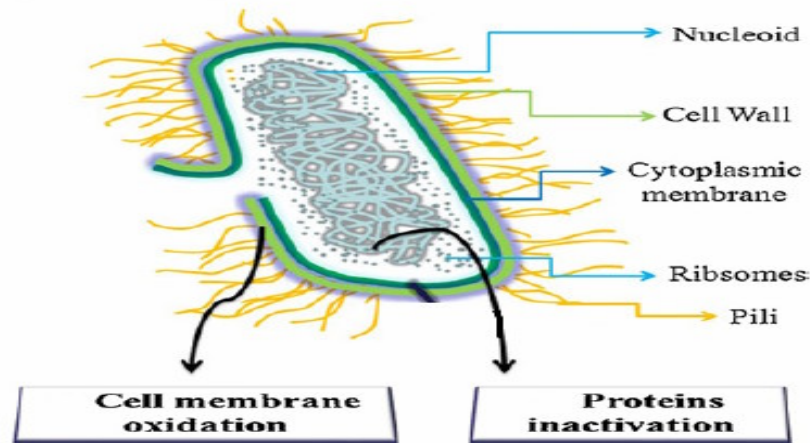


Figure (1.1): Inactivation of a bacterial cell [17].

1.4 Microorganisms

Microorganisms can be found commonly in nature, they are invisible to bare eyes and present in soil, air, food and water [26]. Through consumption of food and air we are exposed to microorganisms. Most microorganisms are harmless and will contribute to a number of vital processes in the human body, such as the metabolism. However, there are also microorganisms which can cause disease or which are harmful to people with low resistance to disease.

Pathogenic microorganisms in the water can be distinguished from chemical contaminants. Microorganisms are living organisms and are not dissolved in water, but they will coagulate or attach to colloids and solids in water.

1.4.1 Types of Pathogenic Microorganisms

Pathogenic microorganisms in drinking water can be divided up into three types: bacteria, viruses and parasitic protozoa. Bacteria and viruses can exist in both surface water and groundwater, whereas parasitic protozoa can be found mainly in surface water.

1.4.2 Bacteria

Bacteria are the most abundant life-form on earth. They are single-cell organisms, they can be founded in different shapes; a sphere, a spiral or a rod. Their presence as individual bacteria or in bacterial chains, bundles or pairs. Their length normally between 0.40 and 14 μm and the width is about 0.20 to 12 μm . Consequentially they can only be viewed under a microscope. They can reproduce by means of DNA replication, causing a bacterium to split into two independent cells. The replication process takes about 15 to 30 minutes in ideal circumstances [27]. Bacteria are enclosed in cell walls that are largely composed of a carbohydrate and protein complex called *peptidoglycan* [28]. Bacteria generally reproduce by dividing into two equal cells (*binary fission*)., Most bacteria use organic chemicals for nutrition, which can be obtained from either dead or living organisms. Some bacteria can manufacture their own food by photosynthesis, and some can derive nutrition from inorganic substances [29].

1.4.2.1 *Escherichia Coli* (*E. Coli*)

The bacterial species *Escherichia coli* is one of the most common inhabitants of the human intestinal tract and is probably the most familiar

organism in microbiology. Optimal growth of *E. coli* occurs at 37°C [30], and the optimum pH growing in a culture at 37°C is 6.0-7.0. It has a minimum pH level of 4.4 and a maximum level of 9.0 required for growth [31]. It is a Facultative anaerobes organism that can grow in either the presence or absence of oxygen. It is used frequently as biological indicator of disinfection efficiency in water systems. They are a large and diverse group of bacteria. Although most strains of *E. coli* are harmless, others can cause some diseases; some kinds of *E. coli* can cause diarrhea, while others cause urinary tract infections, respiratory illness and pneumonia and other illnesses. Still other kinds of *E. coli* are used as markers for water contamination [32]; they are an indicator of fecal contamination. This was based on the premise that *E. coli* is abundant in human and animal feces. The presence of *E. coli* in recreational waters is used to indicate fecal contamination and the possible presence of other more pathogenic microorganisms such as *Salmonella*, *Shigella*, *Campylobacter*, *Giardia*, *Cryptosporidium* or *Norovirus* [33].

1.5 Semiconductor Photocatalysis

Semiconductors have numerous important applications in daily life. They are promising materials for future applications in solar light investment aspects. For example light to electricity conversion and as photocatalyst in water, soil and air purification and disinfection from microorganisms, pesticides, herbicides, drugs and other chemical pollutants.

A semiconductor is a material that has an electrical conductivity between a conductor and an insulator. In semiconductors, the highest occupied energy band that is the valence band (VB) which is completely filled with electrons and the empty next band is conduction band (CB). The resistivities of the semiconductor can be altered by up to 10 orders of magnitude [34]. Their conductivities can be controlled by introduction of an electric or magnetic field, by exposure to light or heat or by doping.

Photocatalysis has attracted attention since the discovery of the Fujishima and Honda in the early 1970's [35], (they discovered that photolysis of water could occur using photocatalysts). This discovery suggested a large number of potential applications, such as photovoltaic cells, degradation of pollutants and photolysis of water. Since then, photocatalysis has been a subject of serious research.

Some attempts were made in the past to define the term “photocatalysis”. Indeed, one of the IUPAC Commissions defined *photocatalysis* as “*a catalytic reaction involving light absorption by a catalyst or a substrate*” [36].

The aim of semiconductor photocatalysis is to effectively detoxify noxious organic pollutants. UV or visible light is used to create electron-hole pairs in the semiconductor, then the electrons react with oxygen in the sample to form $O_2^{\bullet-}$ and holes react with surface hydroxyl groups to form OH \cdot radicals. The radical species then attack the organic molecule which is eventually oxidized to CO_2 , H_2O and other mineral acids [37].

Heterogeneous photo-catalysis performed with irradiated semiconductor dispersions is one of the more interesting advanced oxidation process treatments and it is able, in most cases, to completely mineralize the organic harmful species [38]. Hence, one of the major advantages of photocatalytic processes over the existing technologies is that there is no further need for secondary treatments. The process can be summarized as follows:



There are many semiconductors known and used such as TiO_2 , ZnO , ZrO_2 , V_2O_5 , WO_3 , Fe_2O_3 , SnO_2 , CdSe , GaAs , GaP and metal sulphides (CdS and ZnS). TiO_2 and ZnO are the most important and widely used photocatalysts as they have the advantages of being cheap (viz. 10 g Titanium dioxide only costs two cents), efficient, safe and eco-friendly [39].

1.5.1 Energy Bands of Solids

Semiconductors differ from metals in their electrical properties. In metals, there are always a large number of electrons associated with valence bands which have sufficient energy to become conduction electrons. Another way of saying this is that the valence band of electron energy levels overlaps with the conduction band. In semiconductors, there is a large energy gap between the top of the valence band and the bottom of the conduction band. This results in a relatively low electronic conductivity since the number of electrons which have enough thermal energy to bridge

the gap and provide current carriers is relatively low. There are two types of current carriers in semiconductors; conduction band electrons (electrons free to move through the crystal lattice) and valence band holes (electrons missing from covalent bonds). Each electron that bridges the energy gap produces one hole and one electron current carrier. The product of the concentrations of holes and electrons is a constant at a given temperature [40].

The relative concentrations of holes and electrons in semiconductors are controlled by doping with small amounts of impurities. If such dopants provide energy levels lying close to the valence band they may then accept electrons from the semiconductor and form p-type semiconducting material. On the other hand, if such dopants are close to the conduction band they will then donate electrons to the semiconductor and make it n-type semiconductor.

The terminology n- and p-type refers to the polarity of the major current carrier in the semiconductor, n is used for negative charges (electrons) and p is for positive charges (holes) [41]. Figure (1.2) shows the energy levels of an n-type semiconductor and a p-type semiconductor.

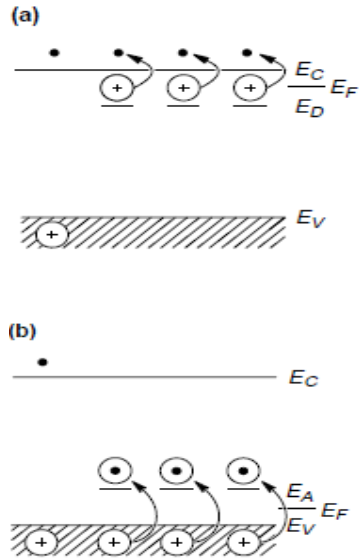


Figure (1.2): Schematic diagram of the energy levels of an (a) n-type semiconductor and (b) a p-type semiconductor [42].

1.5.2 Charge Carrier Generation

Semiconductor electrodes absorb photons with suitable energy when it is exposed to light illumination source and produce excited electrons in the conduction and holes in the valence bands as shown in Figure (1.3) below. Photo-excited electrons and holes in semiconductors are relatively stable compared to photoelectrons in metals, so that the photo-effect on electrode reactions is more distinctly with semiconductor electrodes than with metal electrodes [43].

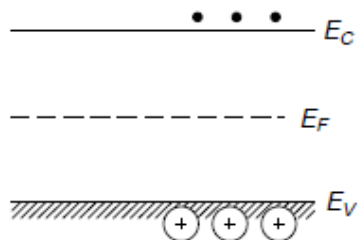


Figure (1.3): Schematic diagram of the energy levels of an intrinsic semiconductor [42].

1.5.3 Fermi Level

In metals, the Fermi Level (E_F) is defined as the highest occupied molecular orbital in the valence band at 0°K , so that there are many states available to accept electrons, if the case were a metal. But that this is not the case in insulators and semiconductors since the valence and conduction bands are separated. In semiconductors, the Fermi level is located in the band gap. It can be seen in Figure (1.4) below. We can consider the probability of finding electrons at E_F to be $\frac{1}{2}$.

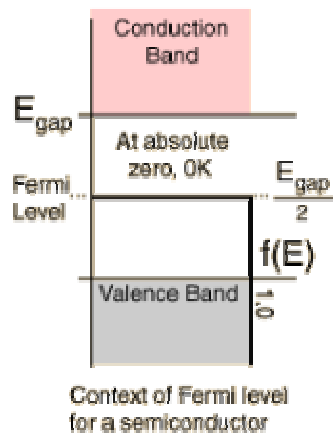


Figure (1.4): Fermi level in a semiconductor [44].

The Fermi level changes its place depending on number of doping density, in either n- or p-types. In p-type semiconductors, the Fermi level lies closer to the valence band. If it is n-type then it will correspondingly be closer to the conduction band.

1.5.4 Photo-Effect on a Semiconductor

The irradiation of ZnO particle with photons of energy equal or greater than its band-gap (3.2 eV) results in the transition of electrons from

the valence band (VB) to the conduction band (CB). The result of this process is region of positive charge termed a hole (h^+) in the VB, and a free electron (e^-) in the CB [45].

At the ZnO particle surface, the holes react with surface hydroxyl groups (OH^-) and adsorbed H_2O molecules to form OH^\bullet radicals. In the absence of electron acceptors the electron-hole recombination is possible. The presence of oxygen prevents this recombination by trapping electrons and forms superoxide ions. The final product of the reduction may also be OH^\bullet radical and the hydroperoxy radical HO_2^\bullet . The presence of other more powerful electron acceptors than O_2 , for example the hydrogen peroxide, increases the efficiency of the oxidative reaction. Hydroxyl radicals have the power to oxidize the organic compounds adsorbed onto the semiconductor surface and inactivate microorganisms [46]. These processes are summarized in Figure (1.5).

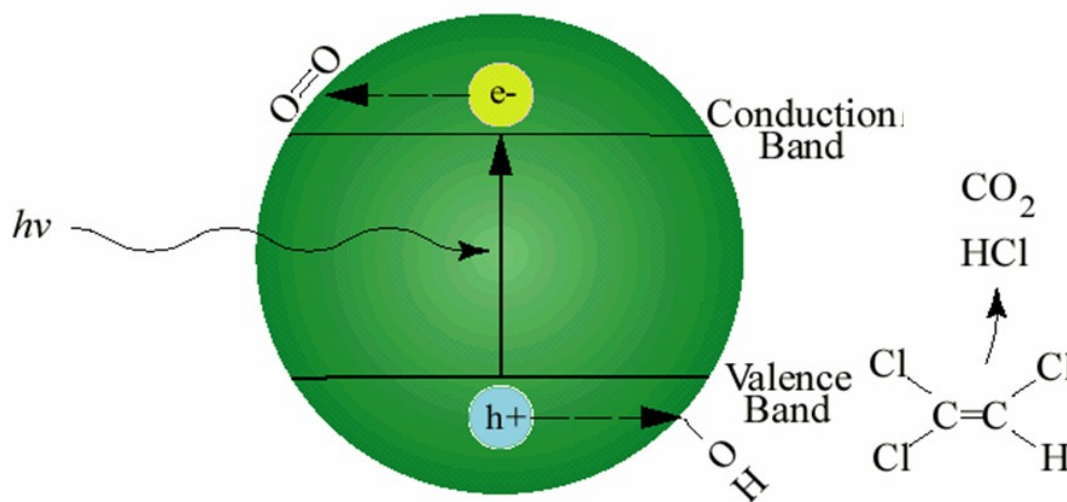
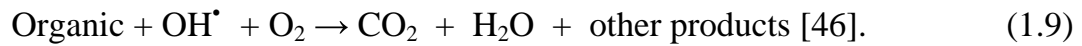


Figure (1.5): How semiconductor photocatalyst functions [37].

The basic reactions of above-mentioned process are as follows:



And the termination reactions are:



1.5.5 Semiconductor Nanoparticles

Recently nanomaterials have become a major area of research interest. They have the potential for wide-range industrial, biomedical, and electronic applications. Surface and interfaces are very important phenomena in nanomaterials. This is because relatively large fractions of atoms are considered to be surface atoms. In bulk materials, relatively small percentage of atoms will be at or near a surface or interface. As surface atoms (coordinatively unsaturated) are less stable and more active than bulk counterparts (coordinatively saturated), the idea of nanomaterials becomes relevant to our work. When the size of semiconductor materials

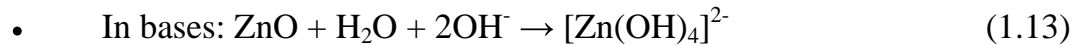
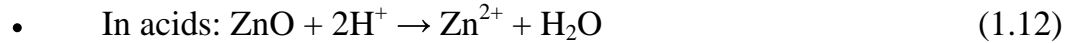
reduces to nanoscale, their physical and chemical properties change, resulting in unique properties due to their large surface area or quantum size effect [47].

1.6 Zinc Oxide Semiconductor

Oxide semiconductors were known long before elemental semiconductors. However, the oxide materials are not nearly as well understood. Their semiconducting properties stem largely from structural defects in oxides that would be insulators if the crystals were defect-free. These oxides are of considerable practical significance. For example, many battery electrodes and corrosion films are composed of semiconducting oxides [48].

Zinc oxide (ZnO) is a white inorganic powder. It is nearly insoluble in water but soluble in acids or alkalies. It is widely used in industries including medical, electronic and chemical industries. It is used as additive material in plastics, ceramics, glass, cement, lubricants, paints, adhesives, sealants, pigments, foods (source of Zn nutrient), batteries, ferrites, fire retardants, first aid tapes and others. Zinc white used as a pigment in paints is less opaque than lithopone, and remains white when exposed to hydrogen sulfide or ultraviolet light. It is also used as filler for rubber goods and in coatings for paper. Chinese white is a special grade of zinc white used in artists' pigments. Because it absorbs ultraviolet light, zinc oxide can be used in ointments, creams, and lotions to protect against sunburn. Crystalline zinc oxide is light sensitive.

ZnO is considered as amphoteric oxide, its reaction depends on the pH of the media, as it reacts as base in acidic solutions and as acid in basic solutions.



In materials science, ZnO is often called a II-VI semiconductor because zinc and oxygen belong to the 2nd and 6th groups of the periodic table, respectively. This semiconductor has several favorable features such as: good transparency, high electron mobility, wide band-gap, strong room-temperature luminescence, etc. [49]. Those features are already used in emerging applications for transparent electrodes in liquid crystal displays and in energy-saving or heat-protecting windows. ZnO is one of the potential semiconductor materials in dye sensitized solar cells (DSSCs) due to its stability against photocorrosion and photochemical properties similar to TiO_2 [50]. TiO_2 and ZnO photocatalysts have been examined for inactivation of *Escherichia coli* and some other types of bacteria by photodegradation. But ZnO has attracted attention as an interesting alternative to TiO_2 in dye sensitized solar cells. Both TiO_2 and ZnO have similar band gaps (3.2 eV) and similar electron injection efficiencies from excited dyes [51]. Moreover ZnO has improved performance with cheap organic dyes because it is more sensitive to UV fraction of solar light than TiO_2 [52].

1.7 Zinc Oxide Sensitization

ZnO has a wide band gap (3.2 eV), with limited photo-catalytic applications to shorter wavelengths (it demands UV light). But only about 4% of the solar spectrum falls in the UV region, so ZnO semiconductor performance under solar light must be improved. Using small band gap semiconductors instead is not an alternative, because they are unstable [53]. In order to improve zinc oxide properties as semiconductor and photocatalyst under solar light; studies have been made to sensitize ZnO by adding another element or compound to.

CdS sensitized ZnO was used in electrodes in photoelectrochemical cells [54] and in photocatalytic degradation of organic contaminants [52]. Silver-loaded zinc oxide (Ag/ZnO) photocatalyst was fabricated by chemical deposition [55]. Enhancement of cyanide photocatalytic degradation was done using sol-gel ZnO sensitized with cobalt phthalocyanine [56]. ZnO was sensitized by phthalocyanine and/or porphyrin molecules attached by electrochemical self-assembly [57]. ZnO was also sensitized with acriflavine in photoelectrochemical cells [58]. G-doped ZnO transparent conducting films and well-aligned ZnO nanotips were sequentially grown on a glass substrate and used in DSSCs [59]. The sensitization of the conductivity and the discharge both of ZnO single crystals and zinc oxide-resin layers with rhodamin B, eosin, and methylene blue have been studied [60]. An attempt was made for the photocatalytic degradation of polyvinyl chloride (PVC) using ZnO as semi-conductor

catalyst in the form of PVC-ZnO composite film sensitized with Eosin Y dye [61].

But many sensitizers are environmentally hazardous, such as CdS which leaches Cd^{2+} ions [10]. So there are some suggestions to use natural dyes as sensitizers in solar cells due to their safe, cheap and eco-friendly nature.

The dye has a small band gap and absorbs light wavelengths in the visible region. This leads to electron-hole generation in the dye molecule, by exciting the electrons from dye HOMO to LUMO. Charge transfer from dye LUMO to ZnO conduction band occurs, and then generation of hydroxyl radicals. Then oxidation of bacterial cells by ZnO occurs. The dye has a small band gap and can't itself oxidize the bacterial cells.

Figure (1.6) shows the sensitization of ZnO by the dye.

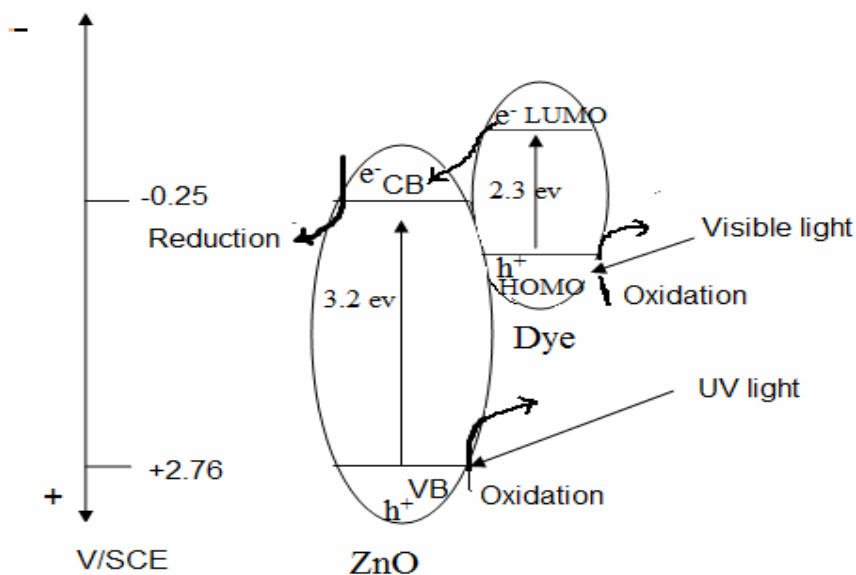


Figure (1.6): Sensitizing of ZnO by the anthocyanin dye.

1.7.1 Anthocyanin Dye

The low cost of materials and high demand for renewable energy sources have increased the use of dye sensitized solar cells. Numerous efforts have been done by several research groups all over the world to utilize natural dyes as sensitizers in dye-sensitized solar cells. A photoelectrochemical cell utilizing flavonoid anthocyanin dyes extracted from blackberries, along with colloidal TiO_2 powder, was reported to convert sunlight to electrical power at an efficiency of 0.56% under full sun [62]. Hetero-structures formed by quantum-sized ZnO nanocrystals and photosynthetic pigments were prepared by adsorbing either chlorophyll a, carotenoids or their mixture onto a film of organic-capped ZnO nanoparticles and studied in photoelectrochemical processes. The photoconversion process was found to be greatly enhanced at the nanocrystalline electrodes upon sensitization with a dye mixture [63]. Natural carotenoids were also used as photosensitizers for dye-sensitized solar cells [64]. Tennakone et al used the flower pigment cyaniding as sensitizer with nanoporous TiO_2 , as a film deposited on conducting glass [65]. The cell generates high photocurrents of good stability. Chlorophyll derivatives and related natural porphyrins were used in photosensitization of titania solar cells [66]. Zinc oxide semiconductor was coated with extracts of natural pigments, chlorophyll or anthocyanin and used for the photobleaching of rose bengal dye [67]. Sensitized TiO_2 was used in water purification in order to photodegrade organic pollutants such as Methyl Orange and Phenazpyridine [68].

Anthocyanins are water-soluble vacuolar pigments. Their color (red, purple or blue) changes with pH. They belong to a parent class of molecules called flavonoids. Anthocyanins occur in all tissues of higher plants, including leaves, stems, roots, flowers, and fruits. Their functions in flowers, with bright red and purple colors, are adaptive for attracting pollinators. In fruits, the colorful skins also attract the attention of animals, which may eat the fruits and disperse the seeds. In photosynthetic tissues (such as leaves and sometimes stems), anthocyanins have been shown to act as a "sunscreen", protecting cells from high-light damage by absorbing blue-green and UV light, thereby protecting the tissues from photoinhibition, or high-light stress [69]. Figure (1.7) shows some possible structural formulas for different anthocyanins.

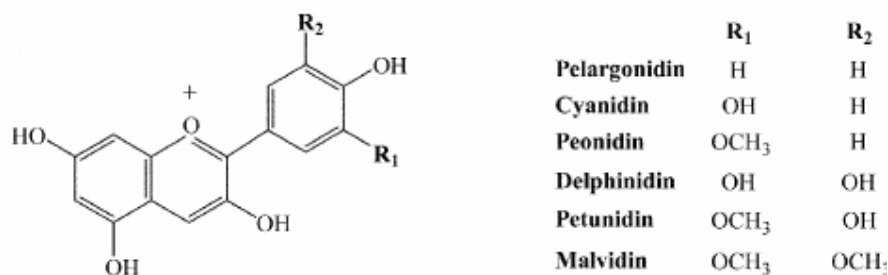


Figure (1.7): Basic chemical structures of most abundant anthocyanins [70]

Anthocyanins available in many fruits such as blueberry, cranberry, black raspberry, red raspberry and blackberry, blackcurrant, cherry, eggplant peel, black rice, concord grape and muscadine grape and red cabbage. In most flowers anthocyanins give attractive colors. For example the dark red color of Hibiscus tea (karkade), which is used in this work, is due to anthocyanins.

Anthocyanin dye has been used as sensitizer for photocatalysts due to different reasons: it is a natural dye that is environment-friendly. So there is no fear of additional contamination or poisoning when using it with ZnO. Anthocyanin has small band gap (~2.3 eV) and absorbs in the visible region. Thus it sensitizes ZnO catalyst to the visible light. It is a low cost dye, available, easy to extract and applicable without additional purifications. Moreover it has several carbonyls and hydroxyl groups that make it easy to anchor to the semiconductor surface [68]. All these reasons make anthocyanin vital alternative for synthetic dyes and most of other natural dyes.

1.8 What is new in this work

Naked ZnO has been used by researchers as antibacterial agent depending on its ability to accumulate in the cell membrane and cause its disruption. Also it was studied by others as photo-catalyst under UV radiations and solar light [18, 20-21]. Sensitized ZnO was applied in photo-electrochemical processes and degradation of organic pollutants.

To our knowledge this is the first work that investigates anthocyanin sensitized ZnO catalyst in water disinfection from bacteria.

1.9 Objectives

The main objective of this work is to disinfect water from bacteria by photo-degradation using solar light and a safe and low cost semiconducting material (ZnO) in its powder and nanoparticles forms,

combined with safe, low cost and available sensitizer (a natural dye called anthocyanin). Evaluation of the process in terms of efficiency, cost, environmental and economic points of view will also be investigated. Reuse of the sensitized catalysts will also be investigated. Other technical objectives include:

- 1) Preparation of new dye-sensitized semiconducting nano-sized powder (ZnO/anthocyanine) which use solar light for microorganism photodegradation and water disinfection.
- 2) Characterization of the ZnO/anthocyanin system using XRD, SEM, UV/Visible spectra, and other techniques.
- 3) Using the dye-sensitized semiconductor and naked ZnO in photo-degradation of microorganisms (*E Coli* bacteria as a model organism) in water with UV, Visible, and direct solar light.
- 4) Studying effects of pH, contaminant concentration, catalyst concentration, temperature, time and presence of organic and inorganic species on photocatalyst activity and photo-degradation process efficiency.
- 5) Studying the possibility of multiple use of the catalyst (recovering and reusing the photocatalyst for multiple times in photo-degradation process).

Chapter 2

Materials and Methods

Chapter 2

Materials and Methods

2.1. Materials

2.1.1. Zinc Oxide

Commercial ZnO powder (catalog no. 205532 with particle size of 5 μ m) was purchased from Sigma Co. and used as the photo-catalyst for water disinfection. ZnCl₂ that was purchased from Sigma Co. and NaOH from Frutarom Co. were used for ZnO nanoparticle synthesis that was used as naked ZnO and as dye sensitized ZnO photocatalysts.

2.1.2 Anthocyanin Dye

Anthocyanin dye was extracted from Karkade plants flowers (Hibiscus tea) in ethanol and supported onto ZnO particles to form the dye-sensitized photo-catalyst. Karkade was purchased from local markets.

2.1.3 Other Chemicals

Barium Chloride, nitric acid, sulphuric acid, ethanol, sodium hydroxide and hydrochloric acid were all purchased from either Aldrich-Sigma Co. or Frutarom Co. as analytical grade, and were used as received without further purifications.

2.1.4 Bacteria

Escherichia coli bacteria were used as model organisms for the inactivation studies. This bacterial species is one of the most common

inhabitants of the human intestinal tract and is probably the most familiar organism in microbiology. It is facultative anaerobic, Gram-negative, straight, rod-shaped bacteria, and is commonly found in the human intestinal tract and feces. Its presence in water or food is an indication of fecal contamination [32].

E coli was chosen as the test species because it is easily grown [71]. Its disinfection mechanisms are well reported. This enables validation of the experimental approaches (including culturing the bacteria and knowing its growing characteristics) and comparison of results in this study with published articles.

This bacterium was isolated from clinical specimens (from patient with urinary tract infection), the isolated bacteria were obtained from medical laboratory sciences department in An_Najah National University. The isolates were identified according to standard diagnostic methods.

2.2 Photo-catalytic System and Irradiation Sources

2.2.1 Photocatalytic System

The photo-degradation reaction was carried out in a 100 ml beaker containing the water sample contaminated with bacteria and the catalyst. The beaker was placed in a thermostated water-bath to prevent sample temperature changes. Temperature was measured through reaction time and adjusted by manipulating the water bath when needed. The reactor walls were covered with aluminum foil to prevent light scattering from the water

sample inside the reactor. The reactor was stirred magnetically and throughout reaction time to make good distribution of the catalyst through the sample. Light source was adjusted above the reactor, ~ 2 cm in case of visible light lamps and ~25 cm in case of UV light lamp. The default temperature was 25 C temperature and the default pH was 7.5.

2.2.2 Irradiation Sources

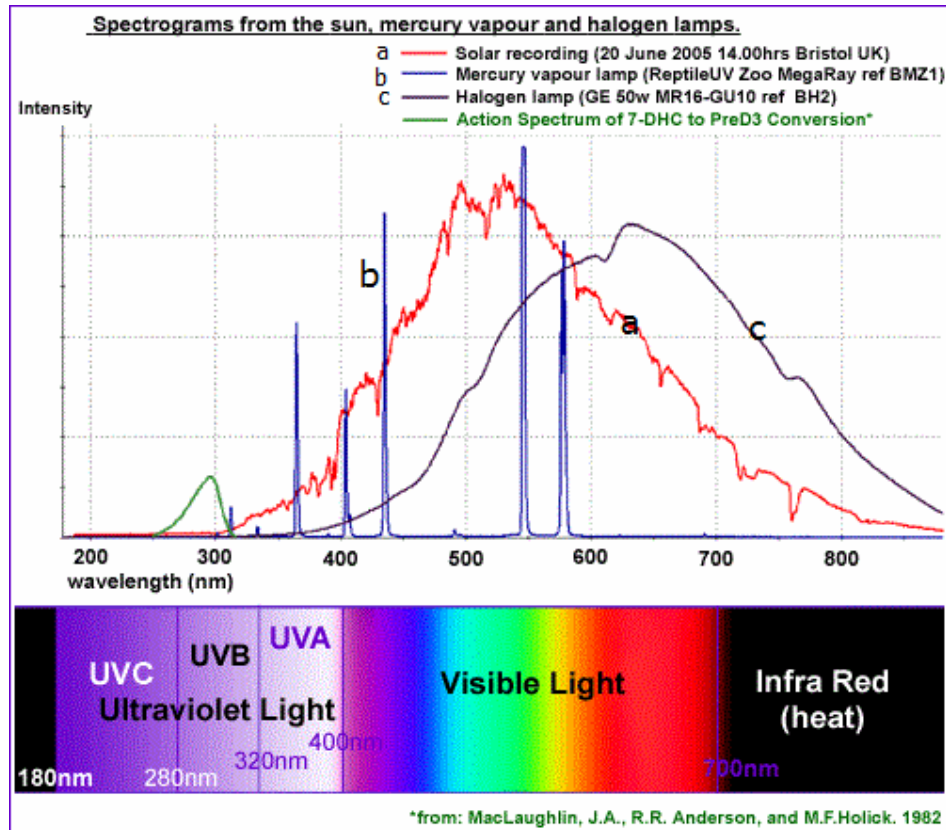
In the photocatalytic experiments, a 50 W, 230V halogen spot lamp solar simulator (LUXTEN) was used as the visible light irradiation source. The fluorescent luminance (70000 Lux, 0.010248902 W/cm²) was monitored using a luxmeter through the experiments.

The light source was assembled above the sample, and the light intensity was controlled using a lux-meter, the reaction mixture was thermostated at the desired temperature. The lamps have a high stability and an intense coverage of wide spectral range, from about 450 to 800 nm and a UV tail. The measured solar light intensity in June month at noon time in Nablus city was 90000 lux (0.01317716 W/cm²) which is nearly as the intensity that used from the solar simulator lamp.

Illumination in the UV range was carried out using an 300 W/ 230V mercury tungsten (Osram Ultra-Vitalux) lamp housed in a protection box with luminance (4400 lux, 0.000644217 W/cm²). Table (2.1) summarizes the features of the used UV lamp. Its spectrum, are shown in Figure (2.1) in comparison with solar light and halogen spot lamp spectra.

Table (2.1): UV lamp specifications [72].

Model	Lifespan (hours)	Rated Wattage (W)	Lamp Voltage (V)	Light Technical Data
003313	1000	300	230	UVA radiated power 315...400 nm, 13.6 W UVB radiated power 280...315 nm, 3.0 W

**Figure (2.1): Spectrograms for the sun, mercury vapor and halogen lamps [73]**

2.3 Measuring Devices

2.3.1 UV-Visible Spectrophotometry

A LaboMed, Inc. spectrophotometer was used to quantitatively determine bacterial concentration using turbidometric methods, and adjust suspensions to 0.5 McFarland standard turbidity.

2.3.2 Lux Meter

A lux meter (Lx-102 light meter) was used to adjust light intensity that reaches the water sample in the photo-catalytic disinfection experiments. The recorded value using the halogen lamp was 70000 lux ($0.010248902\text{W}/\text{cm}^2$) compared to the solar light intensity was 90000 lux ($0.01317716\text{W}/\text{cm}^2$).

2.3.3 pH Meter

Controlling reaction pH was necessary for two reasons. Firstly, bacteria growth is affected by pH value. Secondly, effect of pH on catalyst efficiency was studied. A pH meter was used to adjust the reaction mixture pH as desired.

2.3.4 Thermometer

A mercury thermometer was used to measure temperature.

2.4 Solution Preparations

2.4.1 Chemical Solutions Preparation

A 0.50 M McFarland standard was prepared from original 1.18% w/v $\text{BaCl}_2 \cdot 2\text{H}_2\text{O}$ and 1.00% v/v H_2SO_4 solutions. 9.95 ml of H_2SO_4 solution were pipeted using 1.00-5.00 ml and 100.00-1000.00 μl micropipettes and 0.05 ml of $\text{BaCl}_2 \cdot 2\text{H}_2\text{O}$ solution using 1.00-50.00 μl micropipette, they were mixed together. The solution absorbance was measured spectrophotometrically at 625 nm, showing its typical

absorptivity in the range 0.08-0.10. This standard is commonly used as a reference to adjust the turbidity of bacterial suspensions so that the number of bacteria will be within a given range [74]. At this standard concentration the bacteria concentration is known to be about 1.50×10^8 cfu/ml. The bacterial solution absorbance is then measured and diluted to achieve the same absorbance as the McFarland standard.

NaOH and HNO₃ solutions were prepared and used to adjust the pH as desired. NaOH (0.025 M) was prepared by dissolving 1.000 g solid NaOH in 100.00 ml distilled water in a 100.00 ml volumetric flask and HNO₃ (0.08 M) was prepared by diluting 0.50 ml of concentrated HNO₃ in 100.00 ml distilled water in a 100.00 ml volumetric flask .

2.4.2 Bacterial Cultures Preparation

Nutrient agar was used as growth medium for measuring the remaining concentration of bacteria after the photo-degradation process by plate counting method. The nutrient agar media was prepared by dissolving 28.00 g in 1.00 L distilled water and poured in Petri dishes after being autoclaved. The inoculum of microorganisms was prepared using 4 h cultured nutrient broth at 37°C. The broth was prepared by dissolving 13.00 g in 1.00 L distilled water. Saline solution (0.9%) was prepared by dissolving 9.00 g NaCl in 1.00 L distilled water. The solutions were then used to prepare suitable dilutions for the remaining bacteria in the contaminated water samples after reaction stoppage. After dilution, the

remaining bacteria were cultured on nutrient agar to achieve accountable number of colonies on the plates.

Prior to use in bacterial contamination and disinfection experiments, each water sample, was prepared by pouring 50.0 ml of distilled water in a 100 ml beaker. Each beaker was then charged with a magnetic stirrer and tightly stoppered with aluminum foil to prevent external contamination.

All solutions were autoclaved at 121°C under 1.5 atm, and all work with microorganisms was done under sterile conditions.

2.5 Catalyst Preparation

2.5.1 Anthocyanin Dye Extraction

20.000 g of dry karkade plants flowers were cut into small pieces and finely crushed in a mixer, soaked in 50.00 ml ethanol with continuous magnetic stirring for 30 min, and the extracted dye was then filtered. Few drops of concentrated HCl were added to the filtrate, so that the solution became deep red in colour with $\text{pH} < 1$, and more stable [75]. The extracted dye was stored in a dark-color glass flask for further use.

2.5.2 Zinc Oxide Powder/Anthocyanin Dye Catalyst Preparation

10.000 g of commercially ZnO powder were mixed with the extracted amount of anthocyanin dye and stirred magnetically for 30 min. in a 100 ml beaker at room temperature. The mixture was then covered and

left in the dark overnight to precipitate the resulting solid. The solid was then filtered and dried in air away from light for further application.

2.5.3 Nanoparticle Zinc Oxide /Anthocyanin Dye Catalyst Preparation

ZnO nanoparticles were first prepared by precipitation at room temperature as follows: 0.45 M aqueous solution of zinc chloride (ZnCl_2) was prepared by dissolving 15.231g in 200.00 ml distilled water. The solution was then diluted to 250.00 ml in a 250.00 ml volumetric flask. Aqueous 0.90 M solution of sodium hydroxide (NaOH) was prepared by dissolving 9.000 g NaOH in 200.00 ml distilled water, and the solution was then diluted to 250.00 ml in a volumetric flask. The NaOH solution was then poured into a 500 ml beaker and heated at to ~55 C. The ZnCl_2 solution was added slowly drop-wise (in about 40 minutes) to the heated NaOH solution under high speed stirring (magnetically). The beaker was then sealed at this condition for 2 hours. The white fine ZnO nano-particles precipitate was cleaned with deionized water and ethanol successively, then dried in air atmosphere at about 60 C [76]. The nano-particle ZnO was then treated with anthocyanin as described for commercial ZnO above.

2.6 Catalyst Characterization

UV-Visible absorption spectrophotometry, photoluminescence spectrometry, XRD and SEM techniques were all used for the characterization.

2.6.1 UV_Visible Characterization

Solid state UV-Visible electron absorption spectra were measured for the extracted anthocyanin, ZnO and ZnO/anthocyanin systems. A Shimadzu UV-1601 spectrophotometer, equipped with a thermal printer Model DPU-411-040, type 20BE, was used. The spectra were scanned on a small amount of fine solid catalyst suspension. The suspension spectra were measured in a quartz cell.

2.6.2 Photoluminescence Spectra (PL)

The prepared ZnO systems were characterized using fluorescence spectra. A Perkin-Elmer LS50 Luminescence Spectrophotometer was used to measure the emission fluorescence spectra. Small amounts of suspensions of the solid materials were placed in a quartz cell, and the samples were excited by a suitable wavelength (325 nm). Emission spectra were used to calculate semiconductor catalyst band gaps which were compared with literature values. The spectra were studied for naked ZnO systems, the prepared nanoparticles and the commercial ones. The spectra were also measured for different ZnO/anthocyanin systems.

2.6.3 SEM Characterization

Field emission scanning electron microscopy was measured on a Jeol microscope, Model JSM-6700F, using the energy dispersive spectroscopic FE-SEM/EDS technique. SEM shows the surface morphology and an estimated size of the prepared ZnO particles.

2.6.4 XRD Characterization

ZnO X-ray diffraction (XRD) patterns were measured at ICMCB laboratories at the University of Bordeaux using a Philips XRD XPERT PRO diffractometer with Cu K α radiation ($\lambda = 1.5418$) as a source. Particle size was calculated from XRD diffraction pattern measured for ZnO particles using Scherrer equation [77]:

$$d = K\lambda / (B \cos\theta)$$

where K is the shape factor that has a typical value of about 0.9, λ is the x-ray wavelength, B is the line broadening at half the maximum intensity (FWHM) in radians, and θ is the Bragg angle; d is the mean size (averaged dimension of crystallites in nm) of the ordered (crystalline) domains [78], which may vary for different particles.

2.7 Control Photo-Degradation Experiments

ZnO/anthocyanin dye and naked ZnO in both micro and nano scales were used as photo-catalysts for bacteria inactivation experiments. The catalyst (0.100) g was added to 50.00 ml distilled water pre-contaminated with *E coli* bacteria ($\sim 5 \times 10^5$ cfu/ml) in magnetically stirred 100 ml glass beaker. The beaker walls were covered with aluminum foil and exposed from above to the light source for 90 minutes at room temperature.

Anthocyanin dye was used in dark to know if it affects *E coli* bacteria growth. A sample was also exposed to light without addition of catalyst or dye to examine light effect on bacteria.

Measuring the remaining concentration of bacteria

After 90 minutes (end of the selected time) 1.00 ml of the treated sample was withdrawn using a micropipette and diluted in a series of saline solution tubes with different dilutions, 10^{-1} , 10^{-2} and 10^{-3} dilutions. Aliquot of 100.00 μl was pipeted from each tube, cultured onto nutrient agar media plates and incubated at 37°C for 24 hours. After that the remaining concentration of bacteria was calculated using plate count method, normalized to per ml water, reported, and compared with the initial concentration in the control sample that was prepared using the same concentration of bacteria in the same volume of water but without adding anything to or exposing to any type of light. When counts are > 300 or < 30 CFUs/plate due to inappropriate dilution, data are not reliable according to microbiology practices [79] and hence such data were ignored. The degradation percent was calculated as follows: $(\text{bacteria initial concentration} - \text{bacteria final concentration}) \div \text{bacteria initial concentration}$. Where the initial concentration is known from the control samples, and the final concentration by the plate count of the bacterial remaining concentration.

2.7.1 Dye as Catalyst

To investigate if the used dye itself has antibacterial activity toward the examined bacteria, a control experiment was conducted. Few drops of anthocyanin dye that was extracted in distilled water were added to a 50 ml contaminated water sample in a 100 ml beaker, under continued magnetic

stirring. The beaker walls were covered with aluminum foil to prevent the reaction media from light. Then the sample was treated as described above.

2.7.2 Naked ZnO as Catalyst

Zinc oxide powder was used as catalyst for bacteria photodegradation in some experiments, ZnO is a well known semiconductor that has been used in solar cells. Here it was used without sensitizing under solar simulator light to study the role of the used dye in sensitization. An experiment was conducted to study ZnO photocatalytic activity in absence of UV light and compare it with the sensitized one using cut-off filter that cuts off wavelength 400 nm and shorter. An experiment was conducted under UV irradiation and 1.00 ml was withdrawn at 30 and 90 minutes and treated for bacteria culturing.

ZnO in nano size was used also in presence and absence of solar simulator light to study its activity as photo-catalyst and antibacterial properties without light effect.

2.7.3 ZnO/Anthocyanin Catalyst

The prepared ZnO/anthocyanin catalysts were applied to contaminated water samples with bacteria to investigate their efficiency under solar simulator, using the cut-off filter, this was intended to confirm sensitization by the dye, and UV light. The contaminated samples were treated as described above and the results were reported.

Effect of different parameters on the photo-catalyst efficiency and photo-degradation process was studied, and are shown herein.

2.7.3.1 Time Effect

Aliquots were pipeted out of the reactor at different reaction times (0, 30, 60 and 90 minutes) and the concentration of the contaminants was measured.

2.7.3.2 Temperature Effect

Different experiments were conducted at different temperatures using 20, 27 or 37 °C. The remaining bacteria concentrations were compared with control samples at the same corresponding temperature.

2.7.3.3 pH Effect

Photo-degradation experiments were conducted on pre-contaminated water samples under different pH values. Acidic (pH 5), almost neutral (pH 7.5) and basic media (pH 8.7) were all used. Control experiments were also conducted at these pH values to see if pH itself affects bacterial growth in the contaminated samples. One drop of 0.08 M HNO₃ solution was added to the first sample to make it acidic, the pH of the second sample was measured without any addition, and the third sample was made basic by adding a drop of 0.025 M NaOH solution. The pH values of the three samples were checked several times during reaction interval.

2.7.3.4 Catalyst Concentration Effect

The added amount of the catalyst to the contaminated water sample under solar simulator was varied. Catalyst weights of 0.000, 0.050, 0.100, 0.200 and 0.400 g were added to 5 water samples with same volumes of same bacterial concentrations under similar conditions.

2.7.3.5 Bacteria Concentration Effect

Different concentrations of bacteria were used to study the effect of contaminant concentration. The concentration that was used in most experiments was 5.00×10^5 cfu/ml, this concentration was chosen because it's generally used for measuring the ability of antimicrobial agents to kill bacteria [80]. The concentrations that were used to study the effect of changing initial bacteria concentration are: 2.67×10^5 , 3.70×10^5 , 4.93×10^5 , 7.37×10^5 , 10.40×10^5 , 13.25×10^5 and 13.9×10^5 cfu/ml. Control samples were made for each used concentration to calculate the degradation percent.

2.7.3.6 Nutrient broth and saline media Effect

The catalyst activity against bacteria was studied in different media. Nutrient broth solution was studied as an example of organic medium and normal saline solution as inorganic medium. The results were compared with that of distilled water media.

2.7.4 Control Experiments

Control experiments were conducted under solar simulator light without adding catalyst to study effect of light on the presented bacterial

concentration. Other experiments were conducted in presence of catalyst in the dark. In each conducted experiment, a control experiment was made without catalyst or without light to know the exact initial concentration of the added bacteria.

2.8 Catalyst Recycling

After the end of the photo-degradation reaction, and after measuring the remaining concentration of bacteria, the treated solutions were autoclaved and filtered then the catalyst was collected and reused for another time as a fresh catalyst, following the same procedure. Second and third reuse experiments were also similarly conducted. In another experiment the filtered catalyst was re-dyed and used as a fresh one in attempt to restore its efficiency as photo-catalyst under solar simulator.

2.9 Disinfection By-Products Identification

A Perkin Elmer Clarus 500 GC/MS (2010) was used to study water disinfection by-products using SPME-GC/MS technique. It was supported with auto injector and capillary column with 30 m length and 0.25 mm I.D. (available from Perkin Elmer). Analysis conditions were as follows: initial temperature 50 °C for the first 10 minutes, then (with rate of 2 °C/min.) was raised to 100 °C, at which it was kept for other 20 minutes. The examined sample was a 50.00 ml contaminated water with $\sim 5 \times 10^5$ cfu/ml *E coli* bacteria treated with ZnO/anthocyanin catalyst under solar simulator. And another sample treated with ZnO nanoparticles in absence of light.

Chapter 3

Results

Chapter 3

Results

3.1 Introduction

In this work, ZnO semiconductor in micro and nano size combined with safe low cost sensitizer, the natural dye anthocyanin, was used to disinfect water from bacteria by photo-degradation with solar simulator radiation. The anthocyanin dye was extracted from Karkade plant flowers as described earlier. UV irradiation was used in some experiments for comparison purposes. Effect of different parameters on reaction progress was studied. Evaluation of the process in terms of efficiency, cost, environmental and economic points of view were investigated. Reuse of the sensitized catalysts was also investigated.

3.2 Sensitized Commercial (micro-size) ZnO Catalyst

3.2.1 Catalyst Characterization

UV-Visible absorption spectrophotometry and photoluminescence spectrometry techniques were used for catalyst characterization.

3.2.1.1 UV-Visible Spectra

The extracted anthocyanin dye and ZnO/anthocyanin catalyst were characterized by UV-Visible spectrophotometry.

Anthocyanin Dye

Anthocyanin dye spectrum was measured and compared with literature. Anthocyanin molecules absorb strongly from around 530 - 560

nm. This corresponds to green (520-570 nm) [81]. The dye extracted from Karkade (Hibiscus Tea) here showed a characteristic absorption band at $\lambda_{\text{max}} = 540 \text{ nm}$ with absorptivity about 1.4 as shown in Figure (3.1). The results are consistent with literature spectrum of anthocyanin (Figure 3.2).

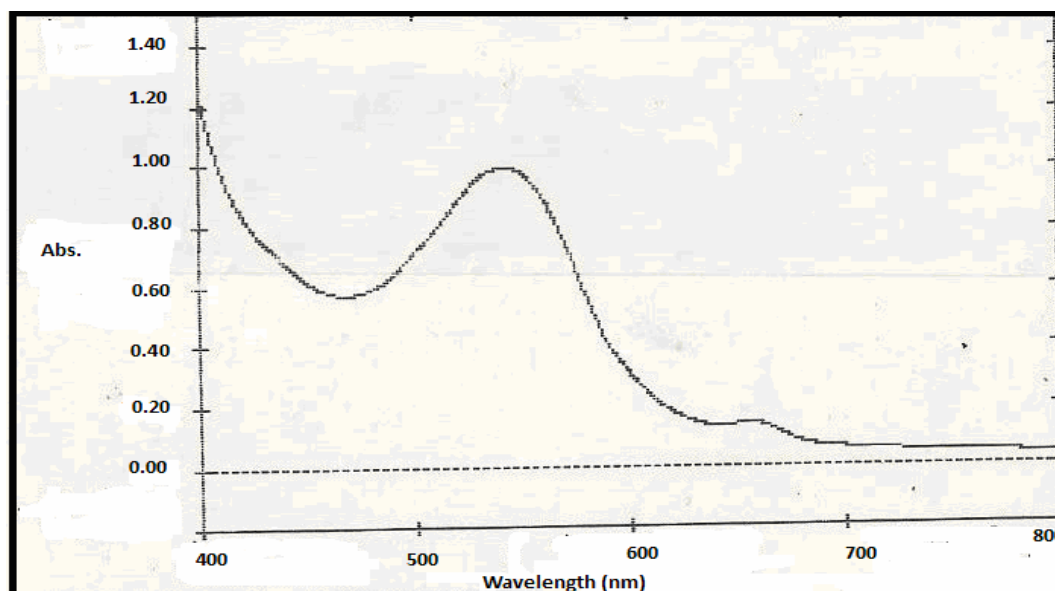


Figure (3.1): Electronic absorption spectra in the UV-Visible region for the prepared anthocyanin dye in ethanol.

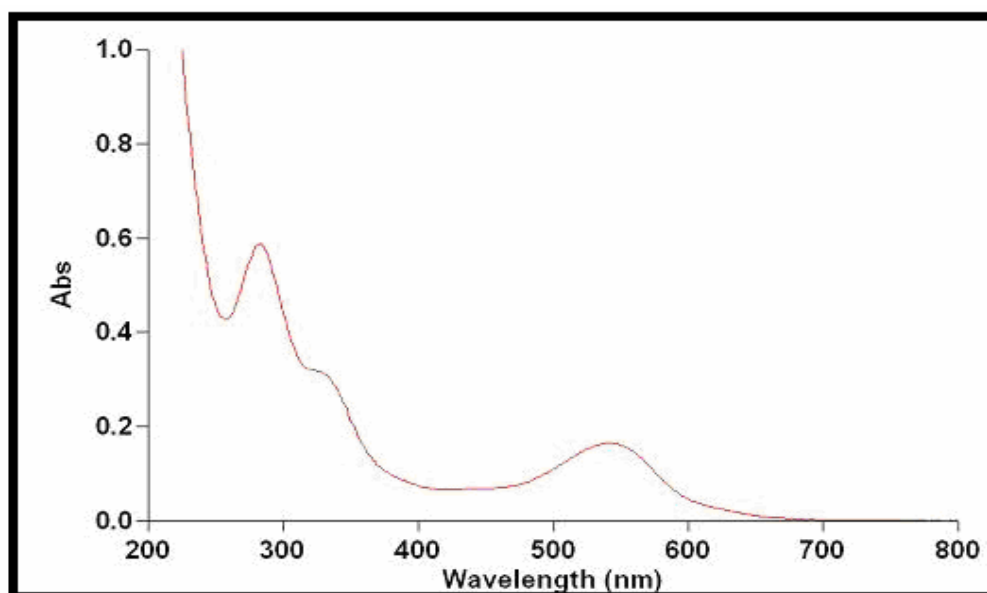


Figure (3.2): Literature electronic absorption spectra for anthocyanin dye extracted from Hibiscus Tea, (peaks at 283 nm and 542 nm with absorbancies at 0.59 and 0.165) [81].

ZnO/anthocyanin Catalyst

Electronic absorption spectrum was measured for ZnO/anthocyanin catalyst suspension. Figure (3.3) shows absorption bands at $\lambda_{\max} = 600$ nm and at ~ 280 nm for anthocyanin dye and at $\lambda_{\max} = 390$ nm for ZnO. The spectra indicate the fixation of anthocyanin dye molecules on ZnO particles and forming the supported catalyst.

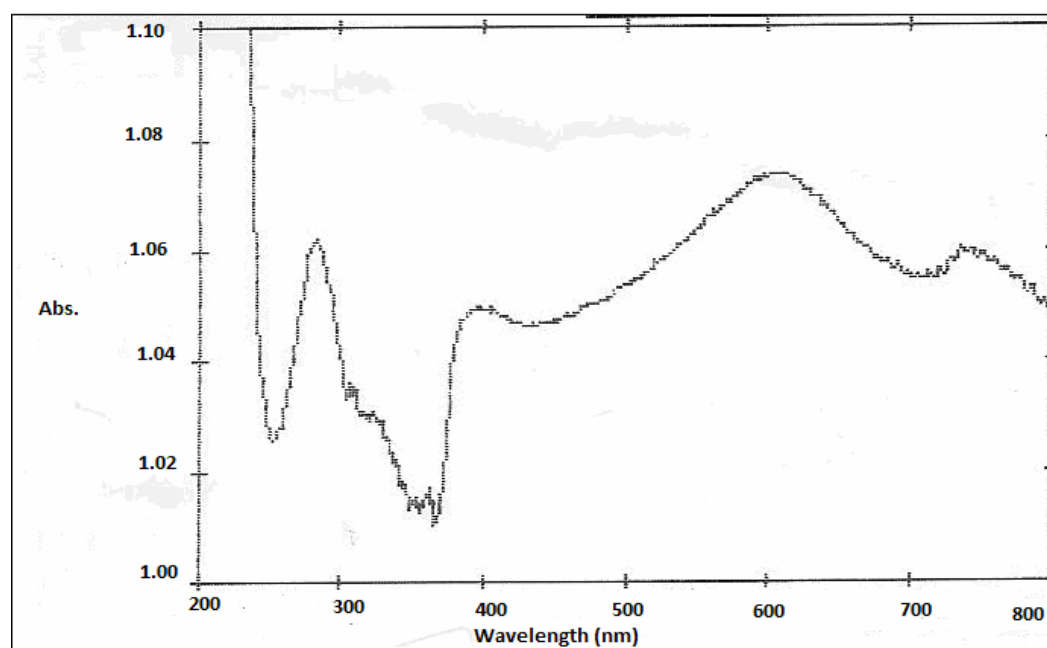


Figure (3.3): Electronic absorption spectra in the UV-Visible region for ZnO/anthocyanin catalyst suspension.

3.2.1.2 Photoluminescence Spectra (PL)

Photoluminescence emission spectrum was studied for the prepared ZnO/anthocyanin catalyst. Emission spectrum was used to calculate ZnO catalyst band gap which was compared with literature value. Figure (3.4) shows photoluminescence emission spectrum for the naked and sensitized ZnO.

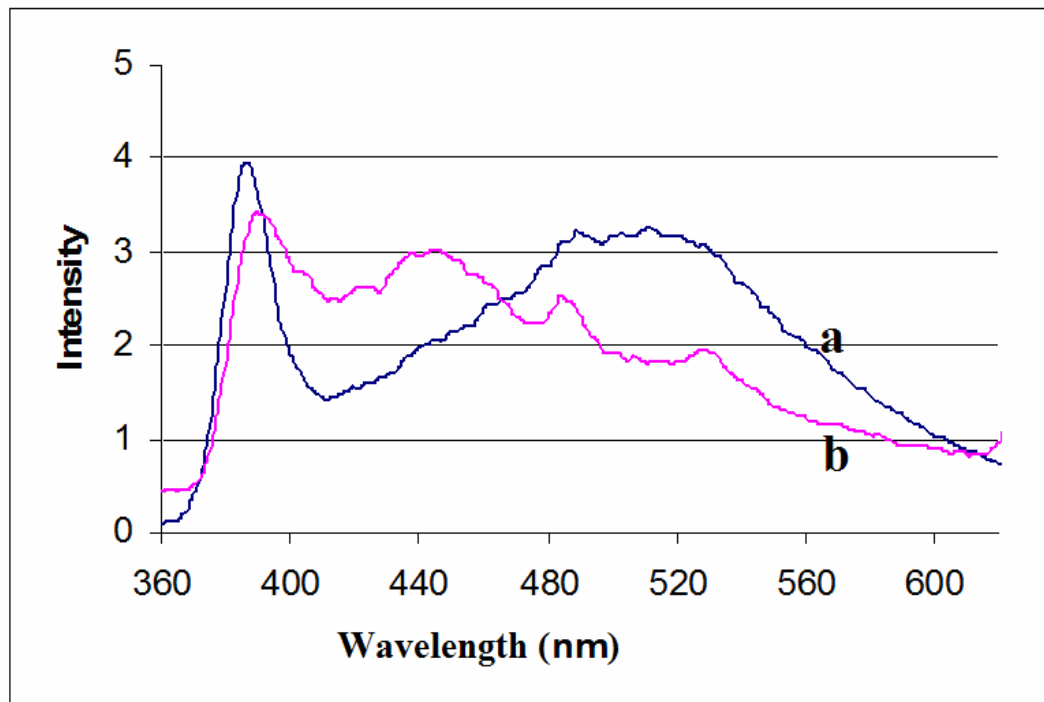


Figure (3.4): Photoluminescence Spectra measured for the prepared ZnO/anthocyanin catalyst (a) and naked ZnO (b).

The excitation wavelength was 325 nm. An intense emission peak was found, for ZnO, at ~ 390 nm (3.18) eV as calculated from the relation E_g (eV) = $1240/\lambda_{\max}$ (nm), consistent with reported values [82-83]. And at $\lambda_{\max} = \sim 500$ nm for anthocyanin dye.

3.2.2 Solar Simulator Irradiation Experiments

ZnO and ZnO/anthocyanin catalysts systems were used in bacteria photo-degradation under solar simulator radiations. Efficiencies of both catalysts were measured and compared together depending on degradation percent, turnover frequency and quantum yield (the number of molecules, or bacterial colonies here, being decomposed per photon absorbed). In order to study and evaluate the feasibility of the dye as sensitizer.

3.2.2.1 Control Experiments

Control experiments were conducted in the absence of catalyst, absence of light, or absence of both. Bacteria were affected with photolysis, in the absence of any catalyst, showing 30% loss in concentration, (Figure 3.5 A). In dark control experiment, which was conducted using sensitized or naked ZnO in absence of light, there was some decline in bacteria concentration (~27%), (Figure 3.5 B). Anthocyanin dye alone was also used; the dye itself didn't show effect on *E coli* bacteria. This coincides with previous report [84]. The same result was achieved when comparing sensitized and naked ZnO under dark conditions, with no noticed difference in their bactericidal activity. This emphasizes the role of the dye as sensitizer under solar light, as shown later.

3.2.2.2 Photo-Catalytic Experiments

Up to 90% degradation percent was achieved by the ZnO/anthocyanin catalyst system under solar simulator light. Generally the achieved degradation percent was in the range 85-95%. Experiments were repeated 3-4 times to make our data documented, the consistent results were reported and the odd ones were ignored. Sensitized ZnO was used under solar simulator and compared with naked ZnO. ZnO/anthocyanin system showed better catalytic efficiency under solar simulator light (~10%) than the naked ZnO. Figure (3.6) shows improvement in ZnO efficiency by using anthocyanin dye as sensitizer. This can be noticed by comparing percent of the photo-degraded bacteria in case of naked and

sensitized ZnO catalyst. Also values of turnover frequency and quantum yield shows that.

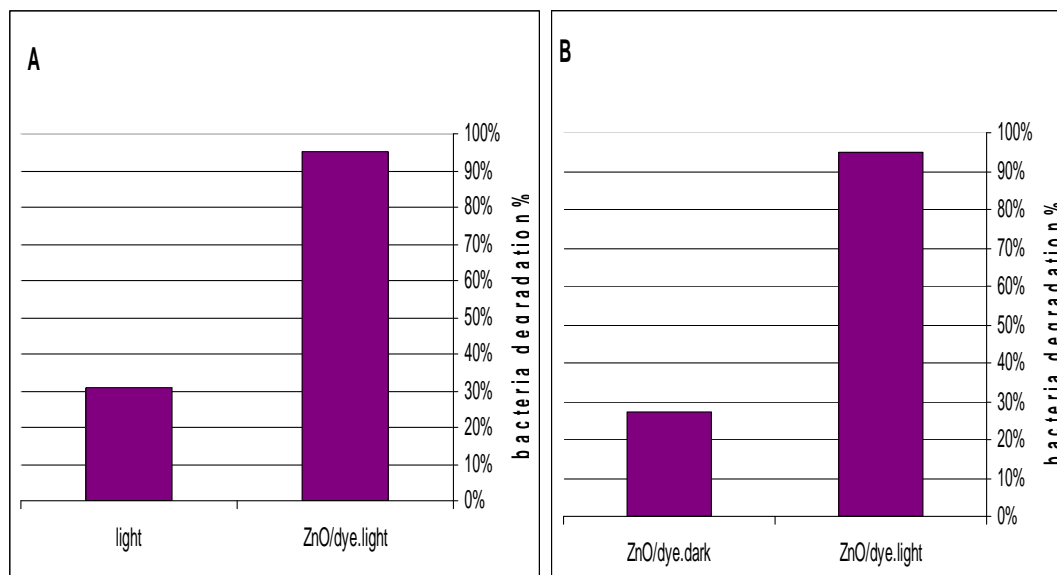


Figure (3.5): Bacteria degradation percent under control conditions compared to that when ZnO/anthocyanin catalyst was used under solar simulator (0.0102 W/cm^2). (50.00 ml neutral suspension, 3.0×10^5 cfu/ml *E coli* bacteria) with 0.100 g catalyst, at room temperature for 90 min. a) light irradiation effect and b) catalyst effect in absence of light.

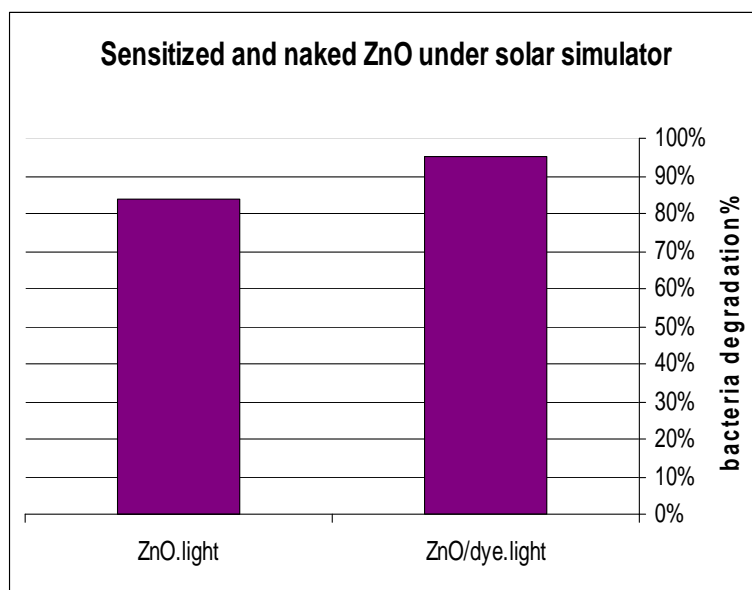


Figure (3.6): Comparison between sensitized and naked ZnO catalytic efficiencies in bacteria degradation under solar simulator (0.0102 W/cm^2), (50.00 ml neutral suspension, 3.0×10^5 cfu/ml *E coli* bacteria) with 0.100 g catalyst, at room temperature for 90 min.

Photo-catalytic and control experiment results are summarized in Figure (3.7), and are shown in Table (3.1).

Table (3.1): Degradation percents, turnover frequency and quantum yield values in the photo-catalytic and control experiment.

	Bacteria degradation%	Turnover frequency (min^{-1})	Quantum yield
ZnO/dye in light	95%	1.918×10^{-16}	58.07×10^{-16}
ZnO/dye in dark	27%	0.743×10^{-16}	14.318×10^{-16}
ZnO in light	84%	1.703×10^{-16}	51.545×10^{-16}
Light	30%		20.457×10^{-16}
Anthocyanin dye in dark	2%		

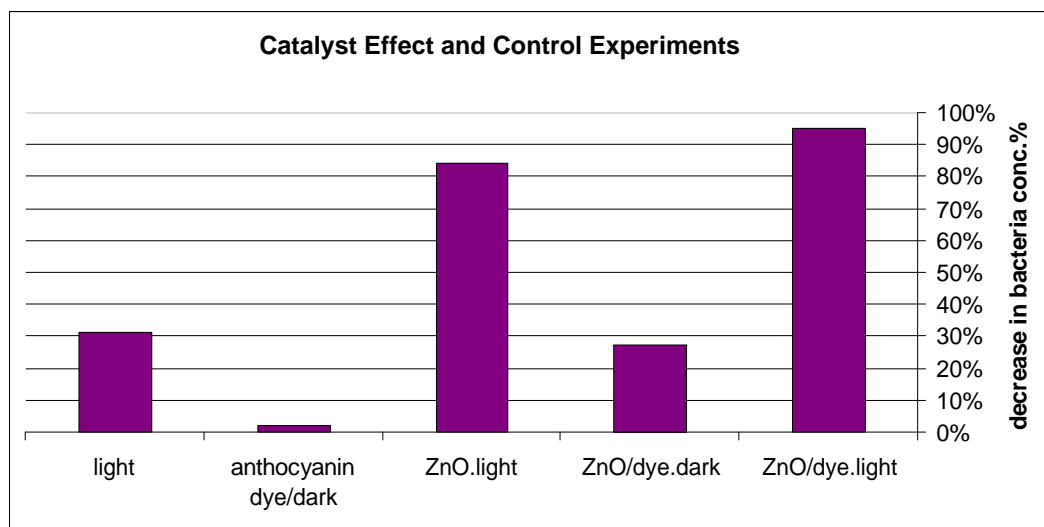


Figure (3.7): Effect of ZnO/anthocyanin catalyst on bacteria photo-degradation compared to naked ZnO and control conditions, (50.00 ml neutral suspension, 3.00×10^5 cfu/ml *E coli* bacteria) with 0.100 g catalyst, under solar simulator radiation (0.0102 W/cm^2) at room temperature for 90 min.

A cut-off filter (eliminating 400 nm and shorter wavelengths) was placed between the solar simulator and the reactor in case of both naked and sensitized ZnO catalysts. This was to study the role of dye in sensitizing ZnO to the visible light. Naked ZnO showed a significant decrease in catalytic activity (about 40%) with cutting off UV light (Figure

3.8). But in case of ZnO/anthocyanin system the catalyst was almost not affected by cutting off UV light. The catalyst worked under visible light radiation with high percent of bacteria degradation, as can be indicated from Figure (3.8).

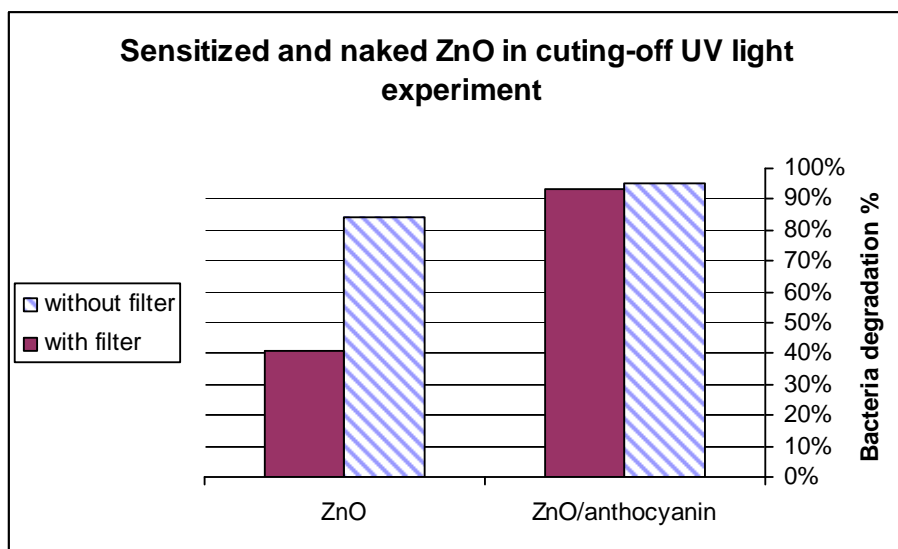


Figure (3.8): ZnO/anthocyanin and ZnO catalysts under solar simulator radiation (0.0102 W/cm^2) in the presence and absence of UV light (using cut-off filter), (50.00 ml neutral suspension, 3.00×10^5 cfu/ml *E coli* bacteria) with 0.100 g catalyst, at room temperature for 90 min.

Table (3.2) shows values of turnover frequency and quantum yield for the previous reactions.

Table (3.2): Degradation percents, turnover frequency and quantum yield values in cutting off UV irradiations experiment.

	Bacteria degradation%	Turnover frequency (min^{-1})	Quantum yield
ZnO/anthocyanin without using filter	95%	1.918×10^{-16}	58.07×10^{-16}
ZnO/anthocyanin with filter using	93%	1.885×10^{-16}	57.075×10^{-16}
ZnO without using filter	84%	1.703×10^{-16}	51.545×10^{-16}
ZnO with filter using	40%	0.831×10^{-16}	25.162×10^{-16}

3.2.2.3 Factors Affecting Catalyst Efficiency

Effect of different parameters on the photo-catalyst efficiency and photo-degradation process was studied. In general all these experiments were conducted under solar simulator (0.0102 W/cm^2) using 50.00 ml neutral suspension, $\sim 5 \times 10^5$ cfu/ml bacteria with 0.100 g ZnO/anthocyanin catalyst, at room temperature for 90 min. However, a number of parameters were changed to study their effect, such as:

Photo-Degradation Reaction Profile

Bacteria photo-degradation with time was studied in some experiments, as shown in Figure (3.9) and Table (3.3). The results show that as time proceeded, bacteria concentration decreased. Values of turn over frequency and quantum yield were higher at the beginning of the reaction. This is not unexpected results. The Figure shows that more than 90% bacteria loss occurred within 90 min.

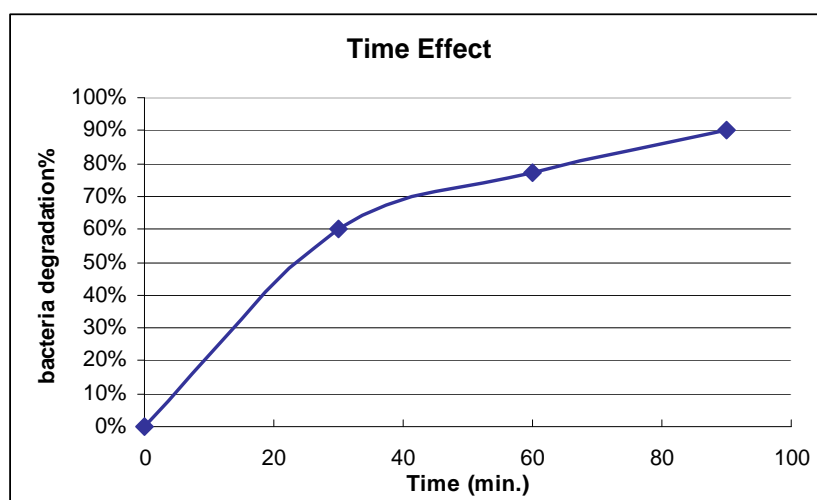


Figure (3.9): Time effect on bacteria inactivation reaction using ZnO/anthocyanin catalyst (0.100 g) for 90 minutes under solar simulator (0.0102 W/cm^2) at room temperature. (50.00 ml neutral suspension, 3.00×10^5 cfu/ml *E coli* bacteria).

Table (3.3): Degradation percents, turnover frequency and quantum yield values in time effect experiment.

Time (min)	Bacteria degradation%	Turnover frequency (min^{-1})	Quantum yield
0	0	0	0
30	60%	3.189×10^{-16}	128.571×10^{-16}
60	77%	2.046×10^{-16}	77×10^{-16}
90	90%	1.595×10^{-16}	61.363×10^{-16}

Effect of Temperature on Catalyst Efficiency:

Photo-degradation of bacteria, using ZnO/anthocyanin catalyst, under solar simulator, was studied at different temperatures, within only a narrow range of temperatures (20-37°C). This range is known to be suitable for bacteria living and growth, and thus it was chosen here. Catalytic reaction was almost insensitive to temperature within the used range. Values of turn over frequency and quantum yield showed small increase with temperature gain within the studied range. The remained concentration of bacteria inside reaction media at each temperature was compared to that of a thermo-stated control sample (no catalyst or light) at the corresponding temperature. Figure (3.10) shows a correlation between bacteria degradation percent and used temperature under photo-degradation experiments. Also Table (3.4) shows the degradation percents and the turnover frequency and quantum yield values.

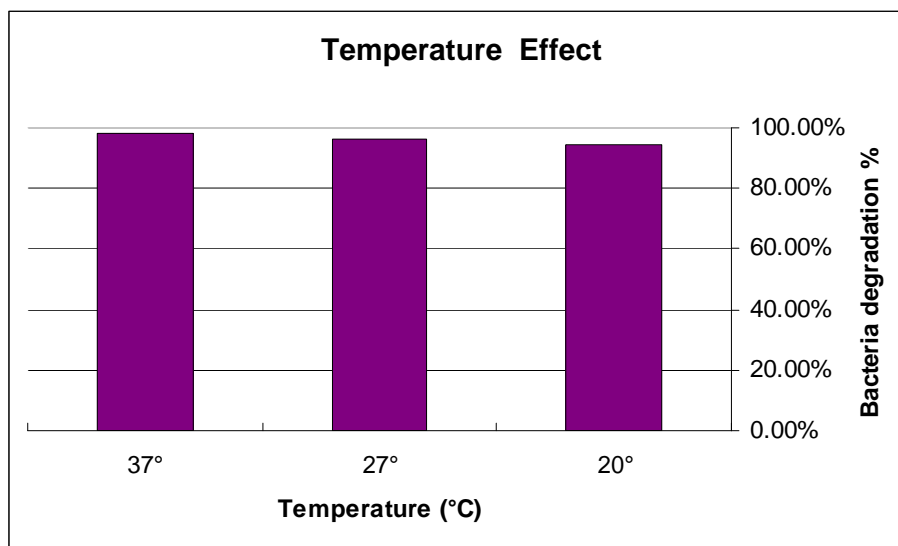


Figure (3.10): Temperature effect on bacteria photo-degradation reaction using ZnO/anthocyanin catalyst (0.100 g) in neutral 50.00 ml suspension, 4.70×10^5 cfu/ml *E coli* bacteria), for 90 minutes under solar simulator (0.0102 W/cm^2).

Table (3.4): Degradation percents, turnover frequency and quantum yield values in temperature effect experiment.

Temperature (°C)	Bacteria degradation%	Turnover frequency (min^{-1})	Quantum yield
20	94%	2.741×10^{-16}	100.741×10^{-16}
27	96%	3.413×10^{-16}	102.558×10^{-16}
37	98%	4.083×10^{-16}	104.694×10^{-16}

Effect of pH on Catalyst Efficiency:

Effect of pH on catalyst efficiency in bacteria photo-degradation was investigated, using ZnO/anthocyanin, under solar simulator at room temperature. The photo-degradation reaction was studied using three different pH values, almost neutral (7.5), acidic (5.0) and basic (8.7) media. These pH values are suitable for bacteria life and don't affect their growth. This was also confirmed from control experiments using no catalyst or light, at these three different pH values. The pH values for the three samples were measured at reaction start and after 30 minutes. Despite the

used pH nominal value, the reaction mixture became nearly neutral after 30 min, with pH values in the range 7.3-7.6. Moreover, the reaction was not much affected with changing nominal pH value. The degradation results were almost the same in the three media, with only a slight preference for basic medium, and the least preferred is the acidic media. Results for pH effect are presented in Figure (3.11) and Table (3.5).

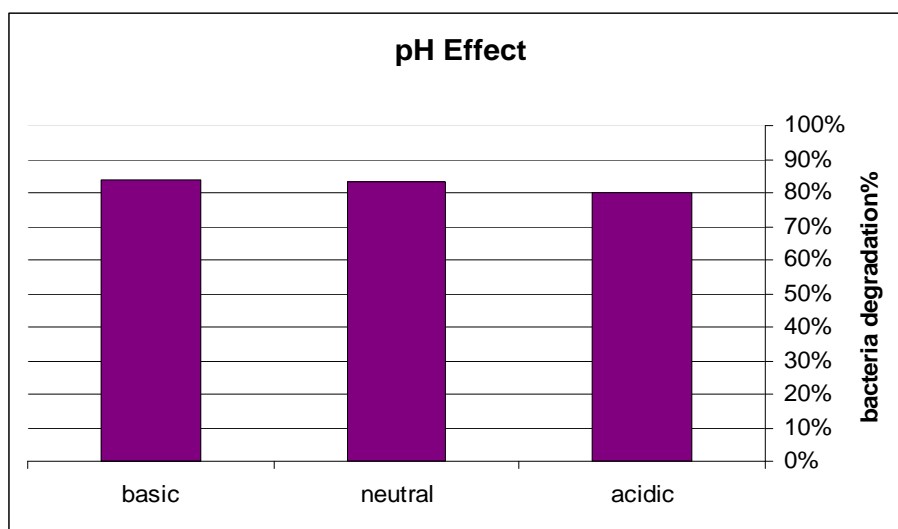


Figure (3.11): Medium pH effect on bacteria inactivation reaction using ZnO/anthocyanin catalyst (0.100 g) in 50.00 ml suspension with 5.00×10^5 cfu/ml *E coli* bacteria under solar simulator (0.0102 W/cm^2) at room temperature for 90 minutes.

Table (3.5): Degradation percents, turnover frequency and quantum yield values in pH effect experiment.

pH value	Bacteria degradation%	Turnover frequency (min^{-1})	Quantum yield
5.0	80%	3.005×10^{-16}	90.988×10^{-16}
7.5	83%	3.134×10^{-16}	94.895×10^{-16}
8.7	84%	3.168×10^{-16}	95.921

Effect of Catalyst Concentration on its Efficiency:

Increasing the added weight of ZnO/anthocyanin catalyst, to reaction suspension under solar simulator radiation, increased bacteria degradation

percentage. This trend continued to occur until a maximum efficiency was observed at a given catalyst weight. Then increasing the added weight of catalyst didn't show any improvement in the photo-degradation reaction. In fact, there was some decline in catalyst activity when its concentration was higher (depending on turnover frequency and quantum yield values). The optimum amount of catalyst was found to be 0.100-0.200 g for the treated volume of water in this work. Figure (3.12) shows this relation.

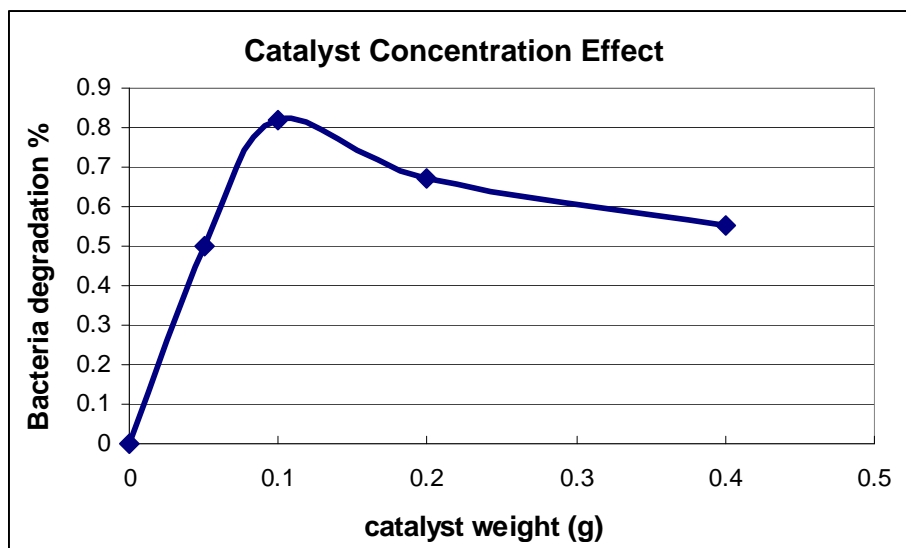


Figure (3.12): Effect of ZnO/anthocyanin catalyst concentration on bacteria inactivation reaction under solar simulator (0.0102 W/cm^2), neutral 50.00 ml suspension, $4.00 \times 10^5 \text{ cfu/ml}$ *E coli* bacteria, for 90 minutes at room temperature.

Degradation percents, turnover frequency and quantum yield values are presented in Table (3.6).

Table (3.6): Degradation percents, turnover frequency and quantum yield values in catalyst concentration effect experiment.

Catalyst weight (g)	Bacteria degradation%	Turnover frequency (min⁻¹)	Quantum yield
0.050	50%	1.415X10 ⁻¹⁶	42.846X10 ⁻¹⁶
0.100	82%	2.303X10 ⁻¹⁶	69.713X10 ⁻¹⁶
0.200	67%	1.899X10 ⁻¹⁶	57.507X10 ⁻¹⁶
0.400	55%	1.554X10 ⁻¹⁶	47.051X10 ⁻¹⁶

Effect of Bacteria Concentration on Catalyst Efficiency:

Effect of bacteria concentration on degradation under solar simulator radiation, using ZnO/anthocyanin catalyst, was studied. Initial concentration of bacteria affected photo-degradation percentage and catalyst efficiency. At initial bacteria concentrations, increasing the concentration increased the degradation percent, but there was decline in degradation percent at higher concentrations. However, increasing the initial bacterial concentration increased values of turn over frequency and quantum yield, over the used range ($\sim 2-14 \times 10^5$ cfu/ml). Figure (3.13) shows the relation between the initial concentration and the degraded percent of bacteria. From this Figure it is obvious that the catalyst degradation percent is highest in the range $5.0-10.0 \times 10^5$ cfu/ml. Turnover frequency and quantum yield values are presented in Table (3.7).

Table (3.7): Turnover frequency and quantum yield values for the ZnO/anthocyanin catalysts in effect of contaminant concentration study:

Bacteria concentration (cfu/ml)	Bacteria degradation%	Turnover frequency (min^{-1})	Quantum yield
2.67×10^5	72%	1.445×10^{-16}	43.755×10^{-16}
3.7×10^5	73%	2.02×10^{-16}	61.144×10^{-16}
4.93×10^5	82%	3.048×10^{-16}	92.283×10^{-16}
7.37×10^5	87%	4.794×10^{-16}	145.072×10^{-16}
10.4×10^5	85%	6.644×10^{-16}	200.933×10^{-16}
13.25×10^5	82%	8.168×10^{-16}	246.961×10^{-16}
13.9×10^5	80%	8.316×10^{-16}	252.727×10^{-16}

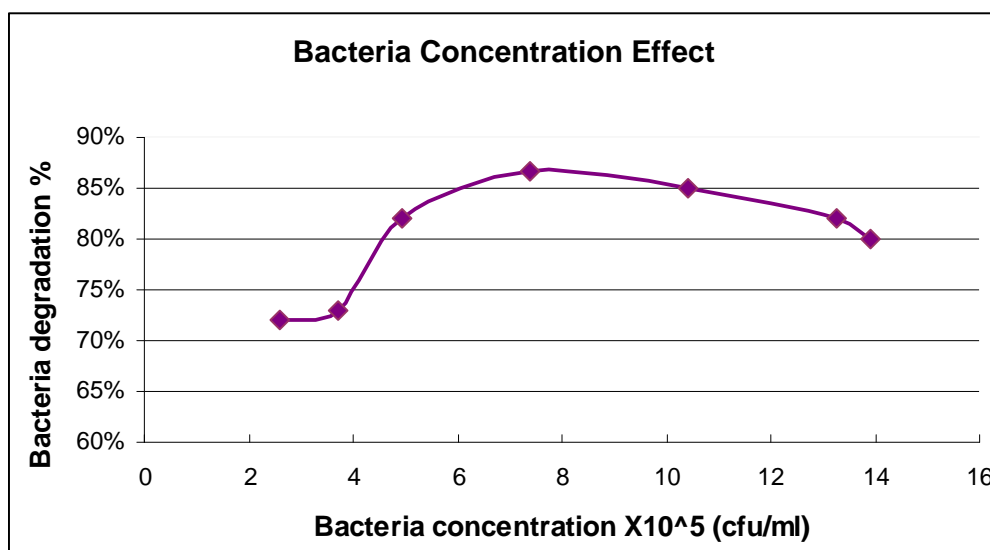


Figure (3.13): Bacteria concentration effect on the photo-degradation reaction using ZnO/anthocyanin catalyst (0.100 g) for 90 minutes under solar simulator (0.0102 W/cm^2) at room temperature, in neutral 50.00 ml suspension. Bacteria concentrations were: 2.67×10^5 , 3.70×10^5 , 4.93×10^5 , 7.37×10^5 , 10.40×10^5 , 13.25×10^5 and 13.90×10^5 cfu/ml.

Nutrient Broth and Saline Media Effect

Media type may affect bacteria photo-degradation in water. In the nutrient broth medium degradation percent was 74% compared to 96% in distilled water, (Figure 3.14). This was repeated several times in nutrient

broth medium, showing maximum degradation percentage of no more than 80%. This indicated a decline in catalyst activity in this media, compared to distilled water medium. Normal saline solution (0.9% NaCl) was used also as a living medium for bacteria. It showed negligible effect on degradation percentage (~87%) compared to distilled water media (~91%), as shown in Figure (3.15).

Degradation percent, turnover frequency and quantum yield values are presented in Tables (3.8) and (3.9).

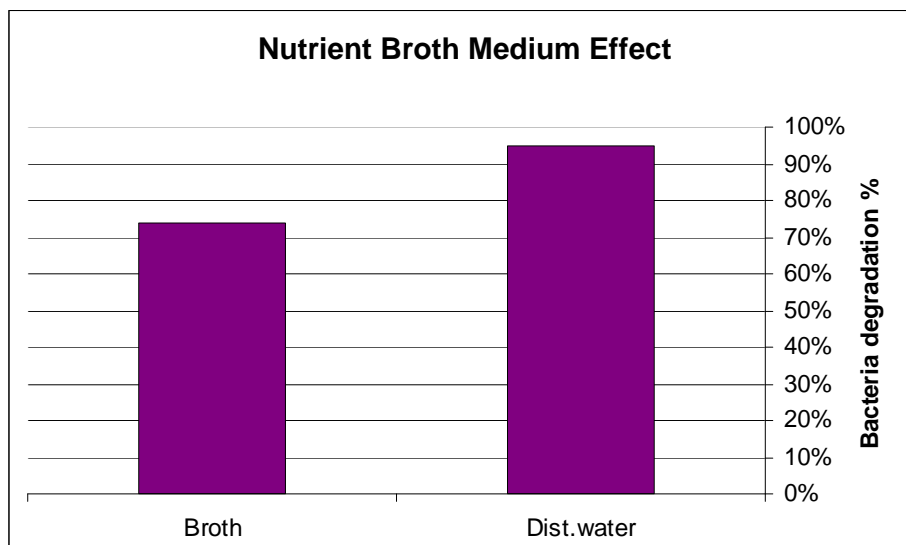


Figure (3.14): Effect of nutrient broth ZnO/anthocyanin (0.100 g) catalytic efficiency in bacteria photo-degradation reaction in neutral $\sim 3 \times 10^5$ *E coli* suspension under solar simulator (0.0102 W/cm^2) at room temperature for 90 minutes.

Table (3.8): Degradation percents, turnover frequency and quantum yield values in nutrient broth medium experiment.

Medium	Bacteria degradation%	Turnover frequency (min^{-1})	Quantum yield
Distilled water	95%	2.08×10^{-16}	65.462×10^{-16}
Nutrient broth	74%	1.907×10^{-16}	50.461×10^{-16}

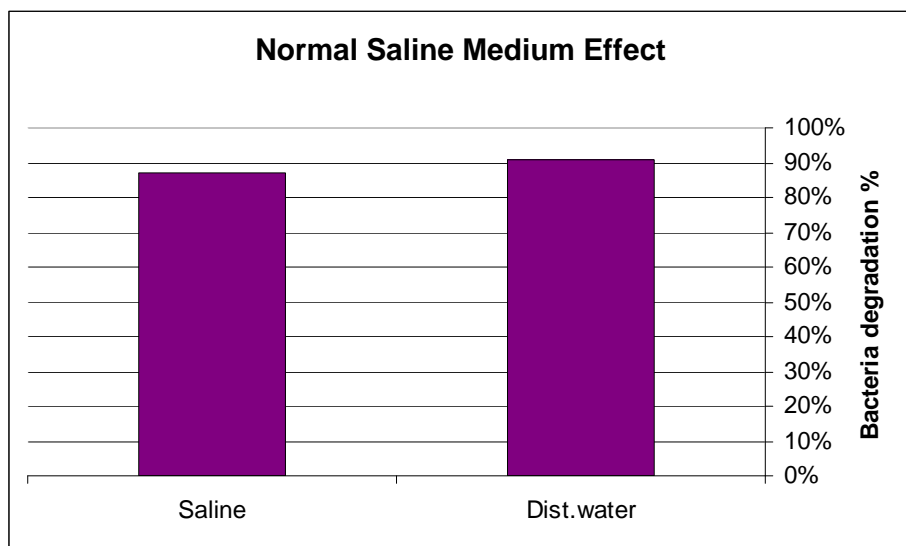


Figure (3.15): Effect of normal saline on ZnO/anthocyanin (0.100 g) catalytic efficiency in bacteria photo-degradation reaction in neutral $\sim 5 \times 10^5$ *E coli* suspension under solar simulator (0.0102 W/cm^2) at room temperature for 90 minutes. Turnover frequency (and quantum yield) values are: $3.424 \times 10^{-16} \text{ min}^{-1}$ (103.422×10^{-16}) in distilled water medium, and $3.213 \times 10^{-16} \text{ min}^{-1}$ (98.876×10^{-16}) in saline medium.

Table (3.9): Degradation percents, turnover frequency and quantum yield values in normal saline medium experiment.

Medium	Bacteria degradation%	Turnover frequency (min^{-1})	Quantum yield
Distilled water	91%	3.424×10^{-16}	103.422×10^{-16}
Normal saline	87%	3.213×10^{-16}	98.876×10^{-16}

3.2.2.4 Catalyst Recycling Experiments

The ZnO/anthocyanin catalyst samples, used in photo-degradation experiments, were recovered from bacteria degradation reaction mixtures and reused in fresh experiments, just like fresh catalyst samples. This was to study catalyst ability to be used several times and its efficiency and stability under multi-use. This is an important objective from economical and environmental viewpoint. The catalyst showed good but decreased efficiency on successive usage ($\sim 10\%$ efficiency loss in each run), (Figure

3.16). Re-dyeing the used catalyst was found to restore its efficiency, it gave high degradation percent as the fresh catalyst, (Figure 3.17).

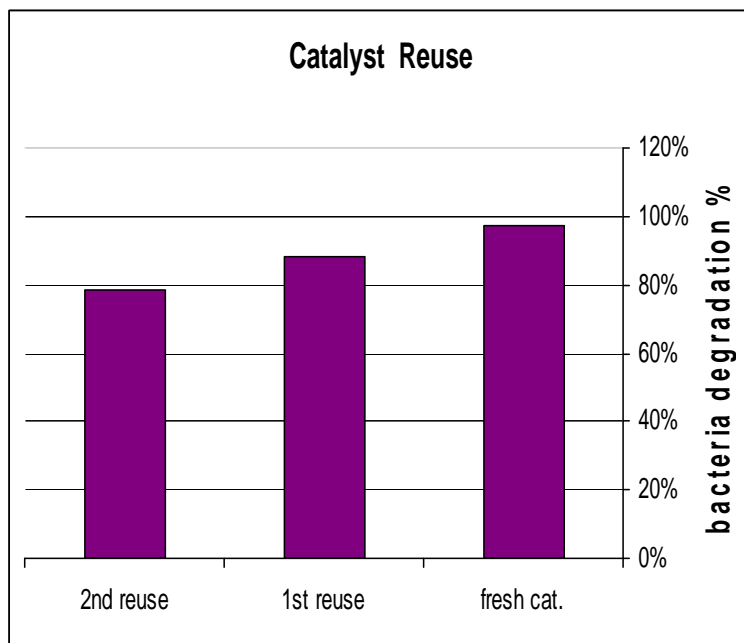


Figure (3.16): Bacteria photo-degradation reaction profiles for fresh and recovered ZnO\anthocyanin catalyst showing its catalytic activity with 1st and 2nd reuse compared to the fresh catalyst. (50.00 ml neutral suspension, 5.00×10^5 cfu/ml *E coli* bacteria) with 0.100 g catalyst, under solar simulator radiation (0.0102 W/cm^2) at room temperature for 90 min.

Degradation percent, turnover frequency and quantum yield values are shown in Tables (3.10) and (3.11).

Table (3.10): Degradation percents, turnover frequency and quantum yield values in Reuse experiment.

	Bacteria degradation%	Turnover frequency (min^{-1})	Quantum yield
Fresh catalyst	97%	3.494×10^{-16}	110.241×10^{-16}
1 st reuse	88%	3.146×10^{-16}	100.239×10^{-16}
2 nd reuse	79%	2.808×10^{-16}	89.443×10^{-16}

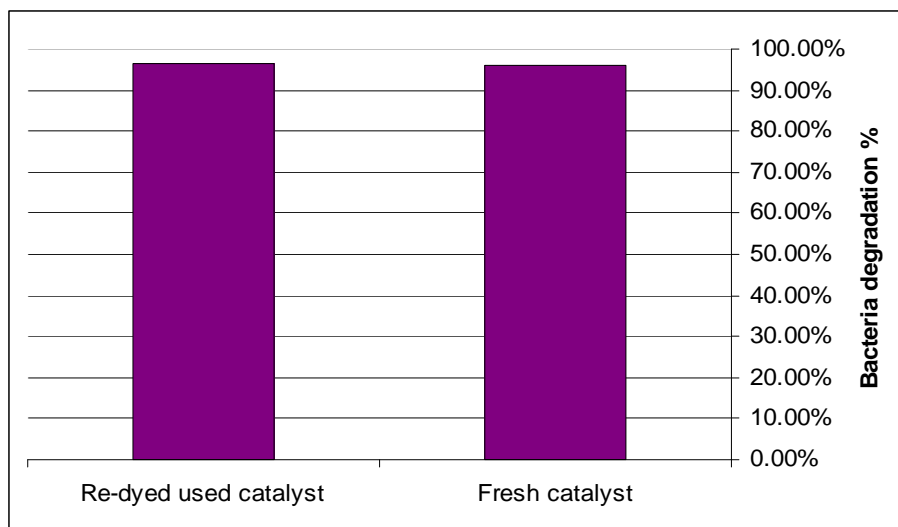


Figure (3.17): Effect of Re-dying the used catalyst on its catalytic efficiency compared to a fresh catalyst in bacteria photo-degradation reaction, (50.00 ml neutral suspension, 10.0×10^5 cfu/ml *E coli* bacteria) with 0.100 g catalyst, under solar simulator radiation (0.0102 W/cm^2) at room temperature for 90 min.

Table (3.11): Degradation percents, turnover frequency and quantum yield values in Re-dying the used catalyst experiment.

	Bacteria degradation%	Turnover frequency (min^{-1})	Quantum yield
Fresh catalyst	96%	7.2×10^{-16}	217.955×10^{-16}
re-dyed used catalyst	97%	7.23×10^{-16}	218.864×10^{-16}

3.2.2.5 Disinfection By-Product Identification

ZnO/anthocyanin catalyst was used to disinfect water from bacteria by photo-degradation, in 50 ml pre-contaminated neutral water with *E coli* bacteria under solar simulator at room temperature for 90 min. Bacteria counting was carried for the sample that was treated with the catalyst and the control sample (without adding catalyst or exposing to light), and the concentrations were compared, there was decline in bacteria concentration.

Bacteria degradation to smaller organic molecules, and then to simple inorganic molecules (complete mineralization), can be assumed

depending on earlier reports [5, 24, 85-86]. After reaction stoppage, the remained bacteria were filtered and a GC-MS analysis was carried for the reaction mixture. The analysis indicated appearance of organic compounds containing nitrogen (which is a vital component of bacterial cell) [87] were detected. Presence of these organic compounds indicated the degradation of bacterial cells, and their presence in small concentrations indicated that these compounds may be oxidized to CO₂, H₂O and other simple molecules, which can not be detected by GC-MS.

3.2.3 UV Irradiation Experiments

Effect of UV light on bacteria photo-degradation, in the presence of both ZnO and ZnO/anthocyanin was studied. This was for comparison purposes with solar simulator studies. Control experiments were also conducted.

3.2.3.1 Control Experiments

Control experiments were conducted here to compare the results with those in photo-catalytic experiments. Photolysis experiments showed that UV light may degrade bacteria, with and without catalyst, to different extents.

3.2.3.2 Photo-Catalytic Experiments

Naked and sensitized ZnO catalysts were used under UV irradiation for water disinfection from bacteria. Experiments were conducted in similar conditions to those in solar simulator studies. Both naked and

sensitized ZnO catalysts showed high degradation rate, reaching complete degradation within 90 minutes. A comparative study was conducted with the both catalysts to study the effect of anthocyanin dye, by withdrawing aliquots after 30 minutes from reaction start showed higher efficiency for naked ZnO under UV irradiation than ZnO/anthocyanin catalyst. Results for photo-catalytic and control experiments are shown in Figure (3.18). Degradation percent, turnover frequency and quantum yield values for catalysts are shown in Table (3.12):

Table (3.12): Degradation percent, turnover frequency and quantum yield values for catalysts under UV irradiation:

	Turn over frequency (min ⁻¹)		Quantum yield		Bacteria degradation %	
	30 min.	90 min.	30 min.	90 min.	30 min.	90 min.
ZnO/dye under light	17.771X10 ⁻¹⁶	7.567X10 ⁻¹⁶	14.9 X10 ⁻¹⁶	6.604X10 ⁻¹⁶	89%	100%
ZnO Under light	22.366X10 ⁻¹⁶	7.577X10 ⁻¹⁶	16.833X10 ⁻¹⁶	6.611X10 ⁻¹⁶	98%	100%
UV light			8.117X10 ⁻¹⁶	5.817X10 ⁻¹⁶	49%	88%

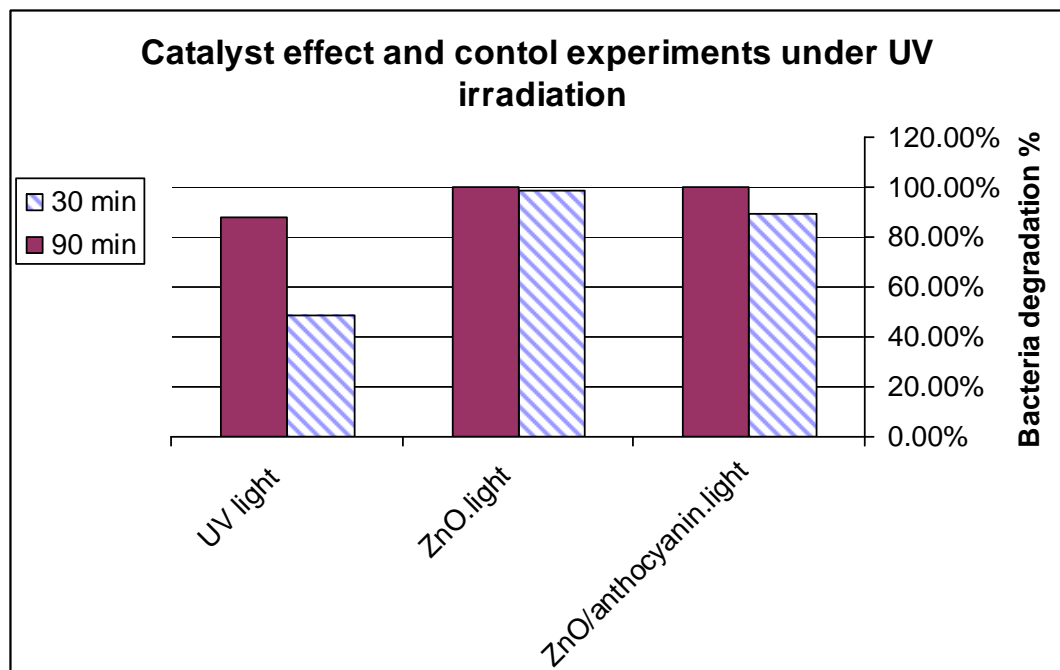


Figure (3.18): Effect of ZnO/anthocyanin catalyst on bacteria photo-degradation reaction compared to naked ZnO and control conditions, (50.00 ml neutral suspension, 9.00×10^5 cfu/ml *E coli* bacteria) with 0.100 g catalyst, under UV irradiation (0.00064 W/cm^2) at room temperature for 90 min.

3.3 Sensitized Nano-Particle ZnO Catalyst

3.3.1 Catalyst Characterization

The prepared ZnO nanoparticles were characterized using UV-Visible absorption spectrophotometry, photoluminescence spectrometry, XRD and SEM techniques.

3.3.1.1 UV-Visible Characterization

Electronic absorption spectrum in the UV-Visible region was measured for the prepared ZnO nanoparticles. Figure (3.19) shows absorption bands at $\lambda_{\text{max}} = \sim 380 \text{ nm}$ for ZnO.

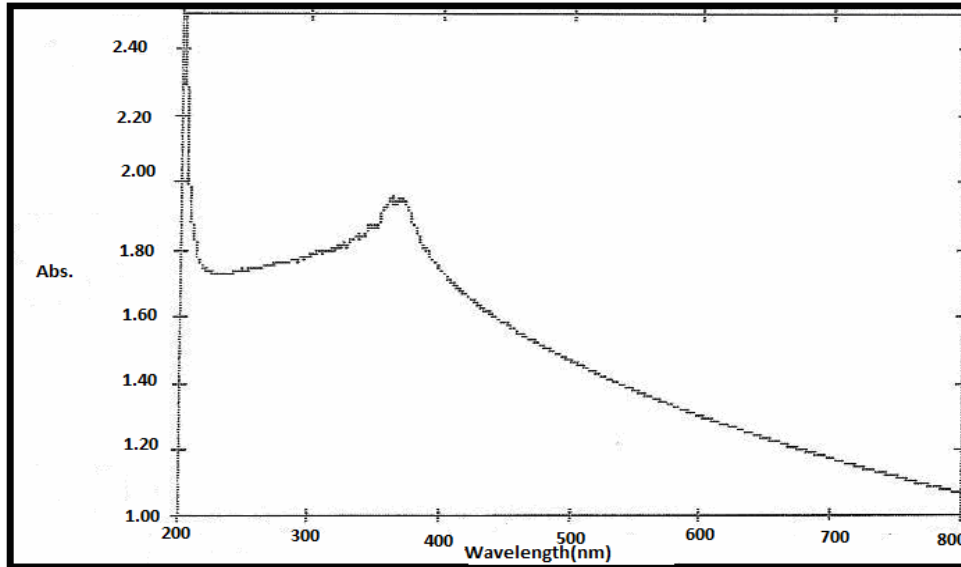


Figure (3.19): Electronic absorption spectra for ZnO catalyst nanoparticles suspension.

3.3.1.2 Photoluminescence Spectra (PL)

Photoluminescence emission spectrum was studied for the prepared ZnO nanoparticles, as shown in Figure (3.20). Emission peak at ~380 nm is due to ZnO band gap (E_g), which is in good agreement with reported values [82-83]. Value of E_g calculated from the photoluminescence spectra for ZnO was 3.26 eV.

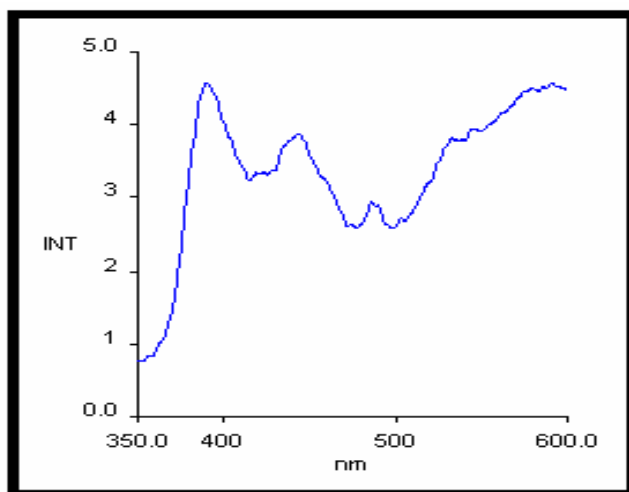


Figure (3.20): Photoluminescence spectra measured for ZnO nanoparticles.

3.3.1.3 XRD Study

ZnO nanoparticles were characterized using XRD technique. Particle size was calculated from XRD diffraction pattern measured for ZnO particles using Scherrer equation [77]:

$$d = K\lambda / (B \cos\theta)$$

where K is the shape factor that has a typical value of about 0.9; λ is the X-ray wavelength (0.15418 nm); B is the line broadening at half the maximum intensity (FWHM) in radians, and θ is the Bragg angle; d is the mean size (averaged diameter of crystallites in nm) of the ordered (crystalline) domains [78], which may vary for different particles.

The X-ray pattern showed a hexagonal wurtzite crystal type for ZnO particles, (Figure 3.22), which coincides with literature XRD pattern for wurtzite ZnO, Figure (3.21). Based on three different XRD peaks at (102), (110) and (103) indices, the average ZnO particle diameter was 20 nm. XRD pattern for ZnO/dye showed some additional small peaks to that of ZnO, such as those at $2\theta = \sim 65$ and 78 , this may be due to dye particles aggregates.

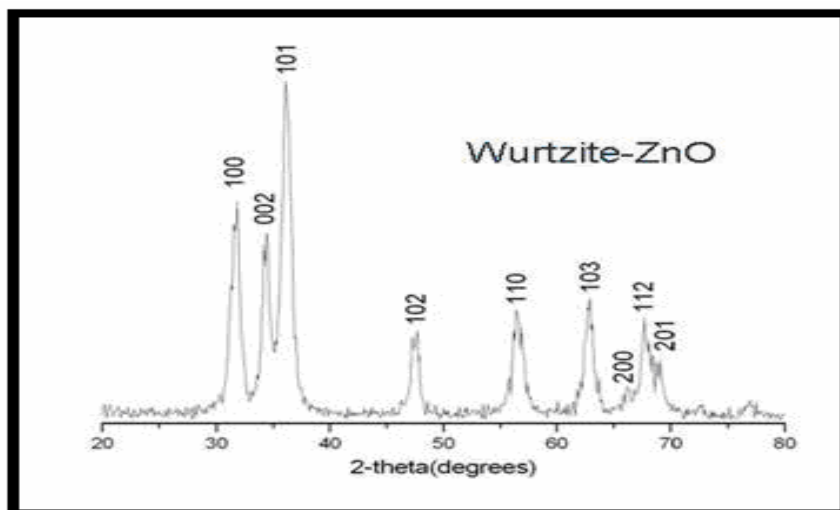


Figure (3.21): Literature X-ray diffraction patterns of nano zinc oxide (ZnO) particles [87].

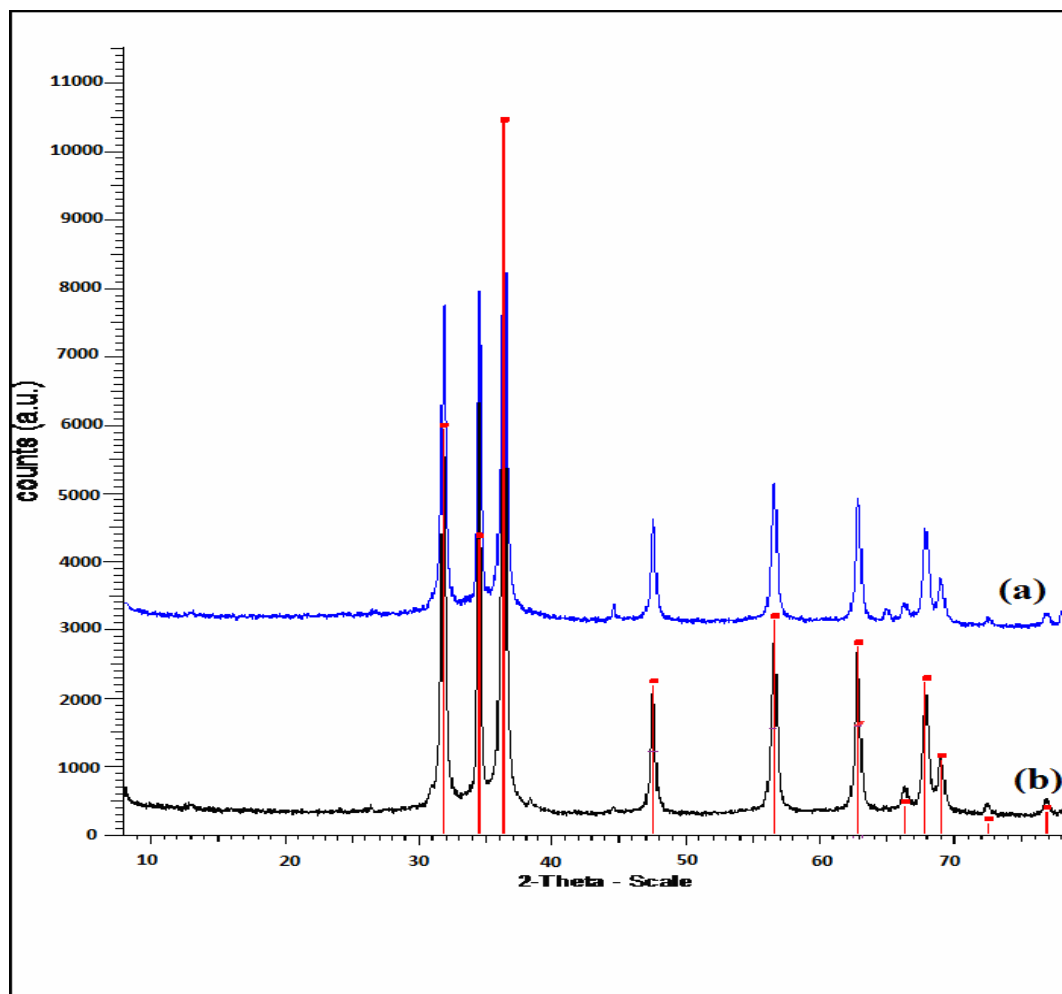
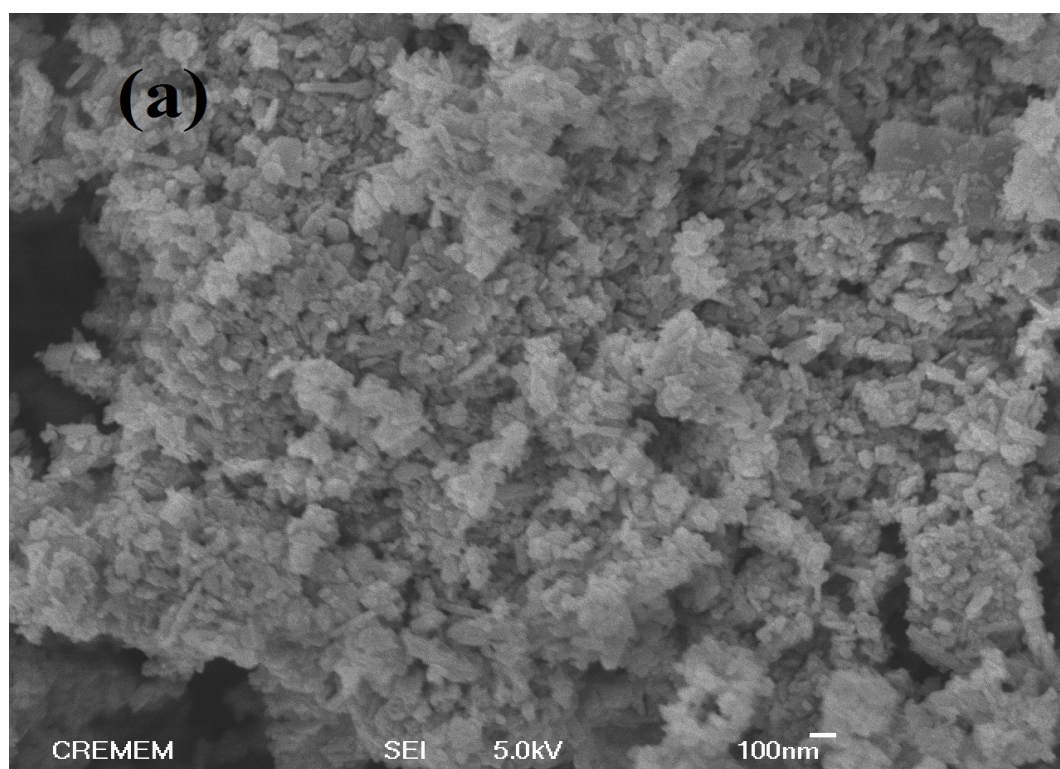


Figure (3.22): X-ray diffraction patterns for ZnO (nanoparticles)/ anthocyanin dye (a) and ZnO nanoparticles (b).

3.3.1.4 SEM Results

SEM characterization was used to show the surface morphology and estimated size of prepared ZnO particles. SEM images showed elongated nanorods (rice-shaped) ZnO particles with about 25 nm in diameter and 140 nm in length. Surface morphology of the nanoparticles is shown in Figure (3.23).



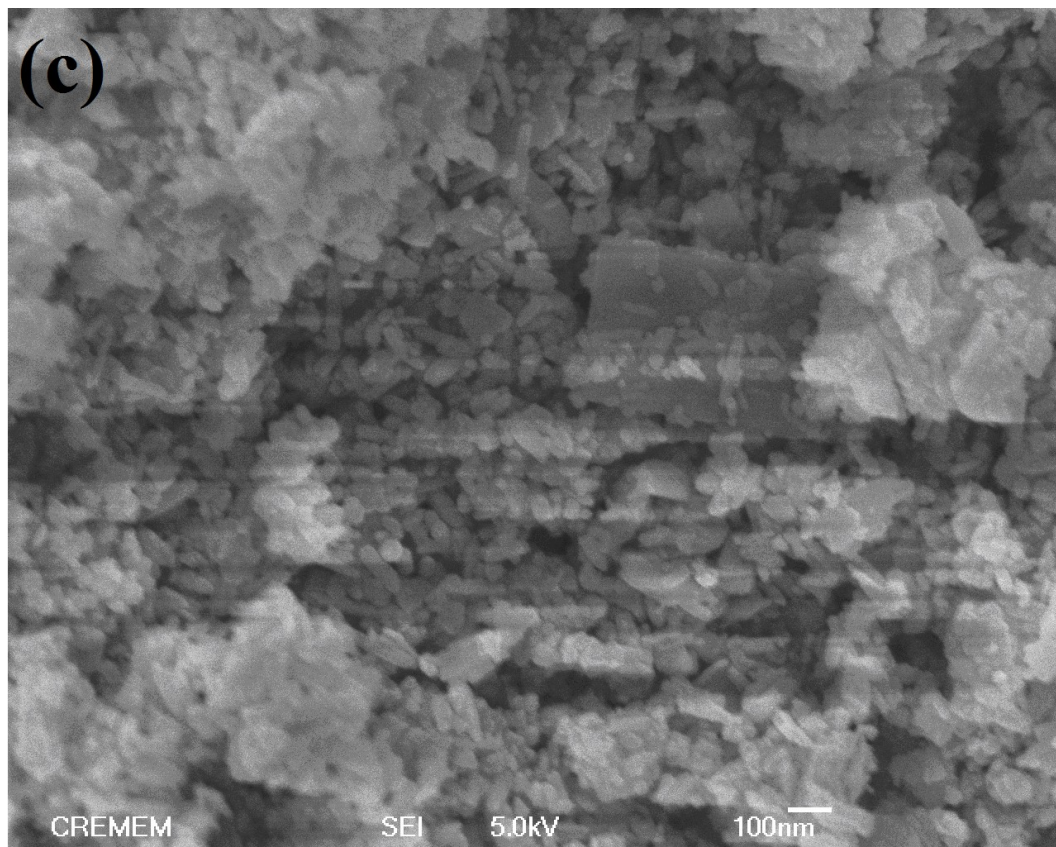
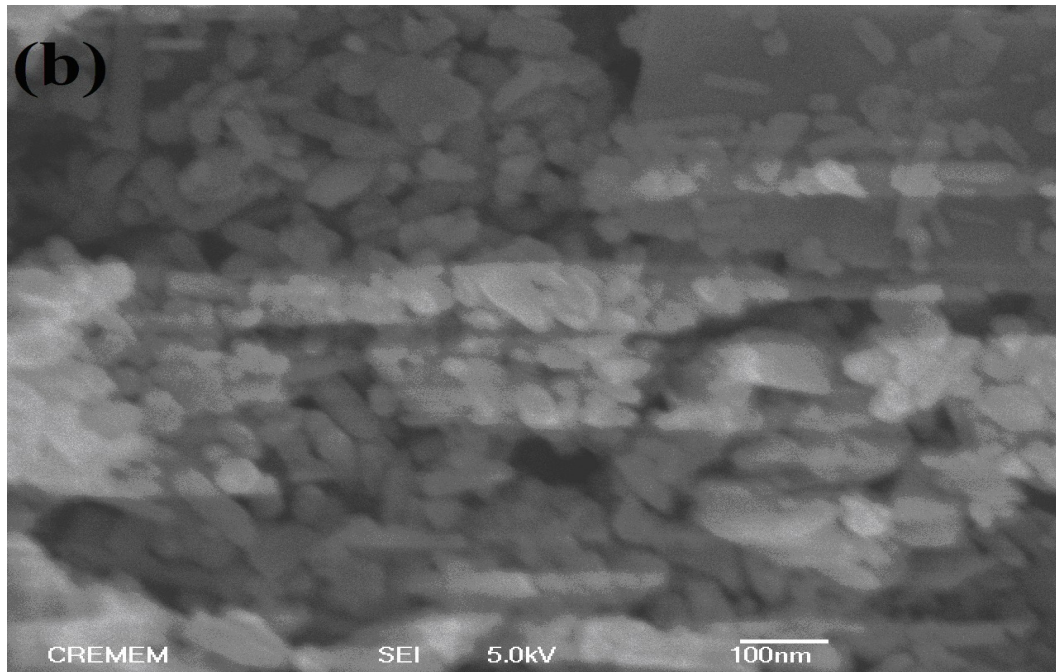


Figure (3.23): SEM images for the prepared ZnO nanoparticles (a, b and c)

3.3.2 Solar-Simulator Light Photocatalytic Experiments

Naked and sensitized ZnO nanoparticle catalysts were used under solar simulator irradiation light source for water disinfection from bacteria as described before.

3.3.2.1 Control Experiments

Control experiments were conducted in the absence of catalyst, absence of light or absence of both. A degradation percent of ~30% was obtained by photolysis. In dark control experiments, which were conducted using sensitized or naked ZnO in absence of light, there was high decline in bacteria concentration (~ 90% in 90 minutes). *E coli* bacteria were not affected by anthocyanin dye alone. The same result was achieved when comparing sensitized and naked ZnO under dark conditions, there was no noticed difference in their bactericidal activity, which emphasize the role of the dye as sensitizer under solar light.

3.3.2.2 Photo-Catalytic Experiments

Both naked and sensitized ZnO nanoparticle catalysts showed high percent of degradation. The system was more efficient than micro-sized ZnO particles. Anthocyanin dye showed ~9% enhancement on nano-sized ZnO particle catalyst efficiency under solar simulator light in 60 minutes. Results of photocatalytic and control experiments are presented in Figure (3.24) and Table (3.13).

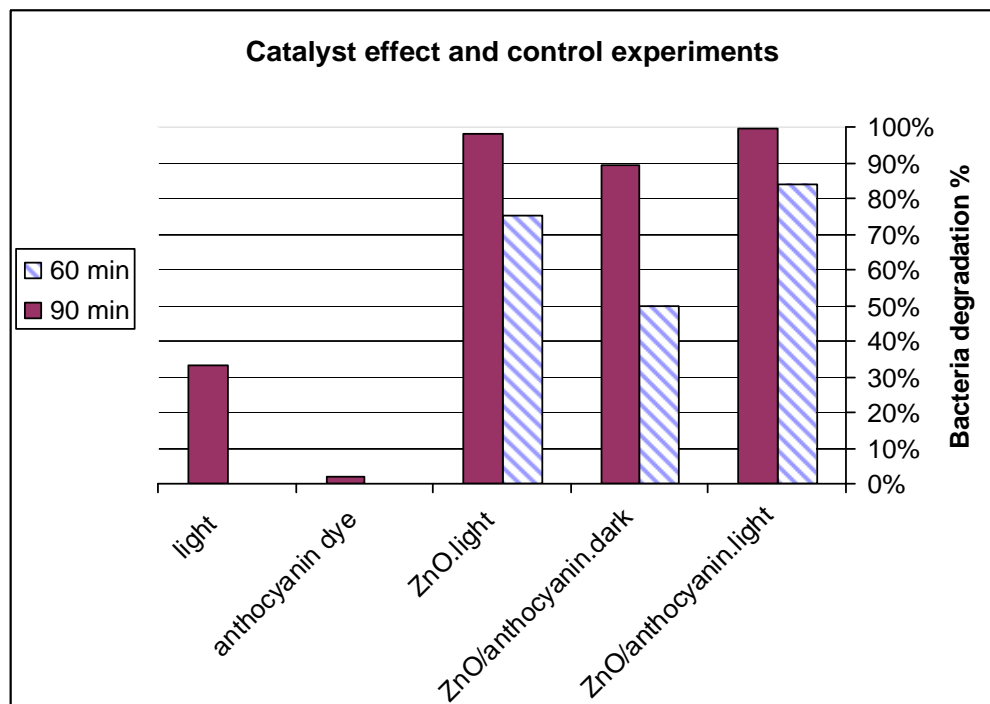


Figure (3.24): Effect of ZnO/anthocyanin (nano-particles) catalyst on bacteria photo-degradation compared to naked nano-ZnO and control conditions, (50.00 ml neutral suspension, 3.80×10^5 cfu/ml *E coli* bacteria) with 0.100 g catalyst, under solar simulator radiation (0.0102 W/cm^2) at room temperature.

Table (3.13): Degradation percents, turnover frequency and quantum yield values in catalyst effect and control experiment for the nano ZnO.

	Bacteria degradation%		Turnover frequency (min^{-1})		Quantum yield	
	60 min.	90 min.	60 min.	90 min.	60 min.	90 min.
ZnO/ dye in light	84%	100%	3.595×10^{-16}	2.806×10^{-16}	106.400×10^{-16}	86.115×10^{-16}
ZnO/ dye in dark	50%	90%	2.123×10^{-16}	2.519×10^{-16}	62.827×10^{-16}	77.304×10^{-16}
ZnO in light	75%	98%	3.210×10^{-16}	2.750×10^{-16}	95.000×10^{-16}	84.560×10^{-16}
Light		33%				20.457×10^{-16}
The dye in dark		2%				

To study the dye effect on ZnO catalytic efficiency, a light filter that cuts off wavelengths with 400 nm and shorter (UV light) was used. The

experiment was thus conducted under visible light only. ZnO/anthocyanin was not significantly affected by cutting off UV light. Naked ZnO nanoparticles showed some decline in the catalytic efficiency with cutting off UV light, (Figure 3.25). These results confirm sensitizing effect of the dye.

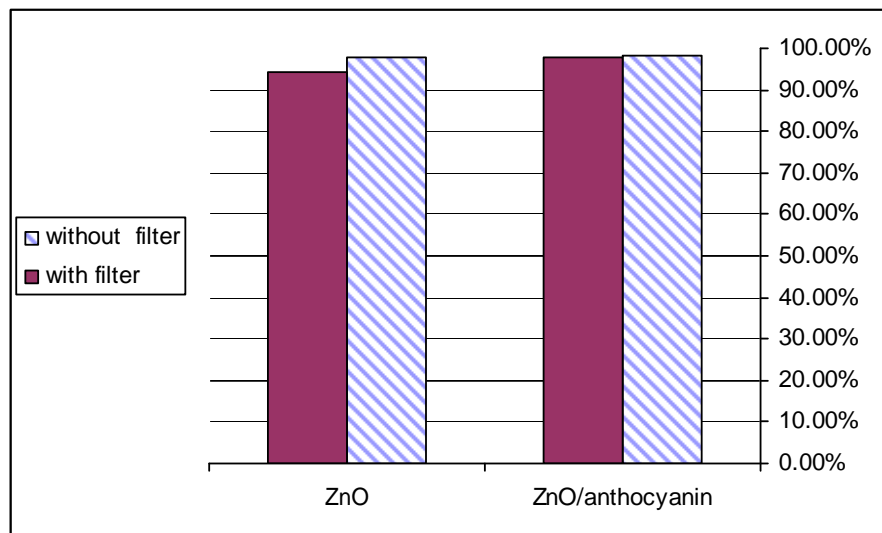


Figure (3.25): ZnO/anthocyanin and ZnO (nano-particles) catalysts under solar simulator radiation (0.0102 W/cm^2) in the presence and absence of UV light (using cut-off filter), (50.00 ml neutral suspension, 5.00×10^5 cfu/ml *E coli* bacteria) with 0.100 g catalyst, at room temperature for 90 min.

Table (3.14) shows degradation percent and values of turnover frequency and quantum yield.

Table (3.14): Degradation percents, turnover frequency and quantum yield values in cutting off UV irradiations experiment in nano ZnO catalyst.

	Bacteria degradation%	Turnover frequency (min^{-1})	Quantum yield
ZnO/anthocyanin without using filter	98%	3.393×10^{-16}	111.604×10^{-16}
ZnO/anthocyanin with filter using	97%	3.38×10^{-16}	111.263×10^{-16}
ZnO without using filter	97%	3.05×10^{-16}	89.01×10^{-16}
ZnO with filter using	94%	2.935×10^{-16}	85.647×10^{-16}

Chapter 4

Discussion

Chapter 4

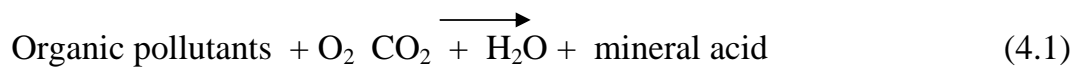
Discussion

4.1 Introduction

Both pristine and natural dye sensitized ZnO photo-catalysts were used in water disinfection from bacteria. More than 90% degradation percent was achieved in 90 minutes under solar simulator radiation. The sensitized ZnO showed higher catalytic efficiency (~10%) than the naked counterpart. Control experiments showed only small percent of degradation. The sensitized catalyst worked well under cutting off UV light (using cut off filter eliminating 400 nm and shorter wavelengths), and was almost not affected by eliminating UV from the solar simulator light. This indicates the role of the dye in sensitizing ZnO to the visible light. Sensitized ZnO nanoparticles showed higher catalytic activity than the sensitized ZnO micro-size counterparts. Complete degradation was achieved with nanoparticles under the same conditions. Some factors affecting photo-degradation reaction and catalyst efficiency, such as illumination time, temperature, pH, catalyst concentration, contaminant concentration and dissolved organic and inorganic impurities, were studied and discussed here.

It is known that photo-degradation of organic contaminants and microorganisms occur due to generation of reactive hydroxyl radicals on the surfaces of the semiconductor particles [37]. When semiconductor crystals are exposed to light with wavelengths suitable for semiconductor band gap, electrons transfer from the valance band to the conduction band

leaving holes in the valence band. Presence of electron acceptors such as O_2 molecules prevents electrons-holes recombination, by accepting the electrons and giving $O_2^{\bullet-}$. Holes oxidize hydroxyl groups (OH^-) and adsorbed H_2O molecules to form OH^{\bullet} radicals. The $O_2^{\bullet-}$ species also reacts with H^+ ions and forms hydroxyl radicals. The hydroxyl radicals have the power to oxidize and degrade organic molecules to smaller ones [46]. The photo-degradation process can be summarized as follows:



4.2 The Micro-Sized ZnO:

ZnO/anthocyanin catalyst characterization using UV-Visible spectrophotometry showed an absorption band for the anthocyanin dye at $\lambda_{\text{max}} = 600$ nm, compared to that for the free dye (in ethanol) at $\lambda_{\text{max}} = 540$. The shift of absorption peak is an evidence for the attachment of the dye on ZnO catalyst surface. The chemical adsorption of the dye takes place due to condensation of alcoholic-bound protons with the hydroxyl groups at the surface of ZnO [89]. This chemical bond affects the energy levels of the highest occupied molecular level (HOMO) and the lowest unoccupied molecular level (LUMO) of the dye and cause a shift in the absorption spectra.

There was some shift toward a smaller wavelength in the emission peak for the sensitized ZnO from that of the naked ZnO noticed from the photoluminescence spectra. This indicates an increase in the band gap for ZnO. The presence of the dye may be increased ZnO stability.

The calculated value for the band gap for the micro ZnO was 3.18 eV whereas it was higher for the nano sized ZnO (3.26 eV), this is consistent with literature [90]. This can be explained by the fact that the crystal size for the micro ZnO is larger than the crystal size of the nano, and so the micro crystal contains larger number of ZnO and higher number of energy levels inside the crystal, this make the band gap to be smaller.

4.2.1 Solar Simulator Irradiation Experiments

4.2.1.1 Control Experiments

Control experiments were conducted in the absence of catalyst, absence of light, or absence of both. Some bacteria were affected with photolysis, in the absence of any catalyst type, showing up to 30% loss due to solar simulator light. Despite the need of bacteria for light in their life and growth, it may be harmful for them. Solar light contains UV tail that affects the bacterial cell and makes mutations (changes in DNA sequence). The *E coli* bacteria are known to be especially sensitive to UV irradiation [91]. In the dark, using sensitized or naked ZnO, there was some decline in bacteria concentration (~27%), which is due to bactericidal activity of Zn²⁺ ions that could accumulate in the cell membrane and make disruption of the membrane [92-93]. Zinc penetrates through the cell membrane and inhibits nutrient uptake and interferes with proton transfer [94]. Anthocyanin dye itself didn't affect *E coli* bacteria (it is antioxidant agent [95]). This is consistent with literature [85]. Sensitized and naked ZnO systems showed similar results under dark conditions, which means that they have the same

bactericidal activity with no role for the dye in absence of light. This emphasizes the role of the dye as sensitizer under solar light.

4.2.1.2 Photo-Catalytic Experiments

More than 90% degradation percent was achieved by the ZnO/anthocyanin catalyst system under solar simulator light. ZnO is a powerful oxidizing agent, due to its wide band gap (3.2 eV). Therefore, it can oxidize organic compounds to simple molecules, when excited by suitable radiations. Excitation of electrons from the valance band to the conduction band creates holes, in valance band, which lead to hydroxyl radical formation. The radicals oxidize the bacterial cell wall together with internal contents, and consequently cause cell death and degradation. Supporting anthocyanin dye on ZnO surface makes it sensitive to visible light because the dye has small band gap and can be excited with visible light. The excited electrons then move to the conduction band of ZnO semiconductor, as shown in (Figure 4.1). The creation of more holes and hydroxyl radicals would then increase the percent of degradation compared to naked ZnO system.

The ZnO is sensitive to UV tail that exists in the solar light. Thus the ZnO absorbs the UV tail and behaves as photo-catalyst with good catalytic activity causing up to ~ 84% degradation. Sensitization showed improvement in ZnO catalytic activity under solar simulator with ~ 10% (Figure 3.6). This is because sensitized ZnO uses both UV and visible light together, and excitation occurs via two routes.

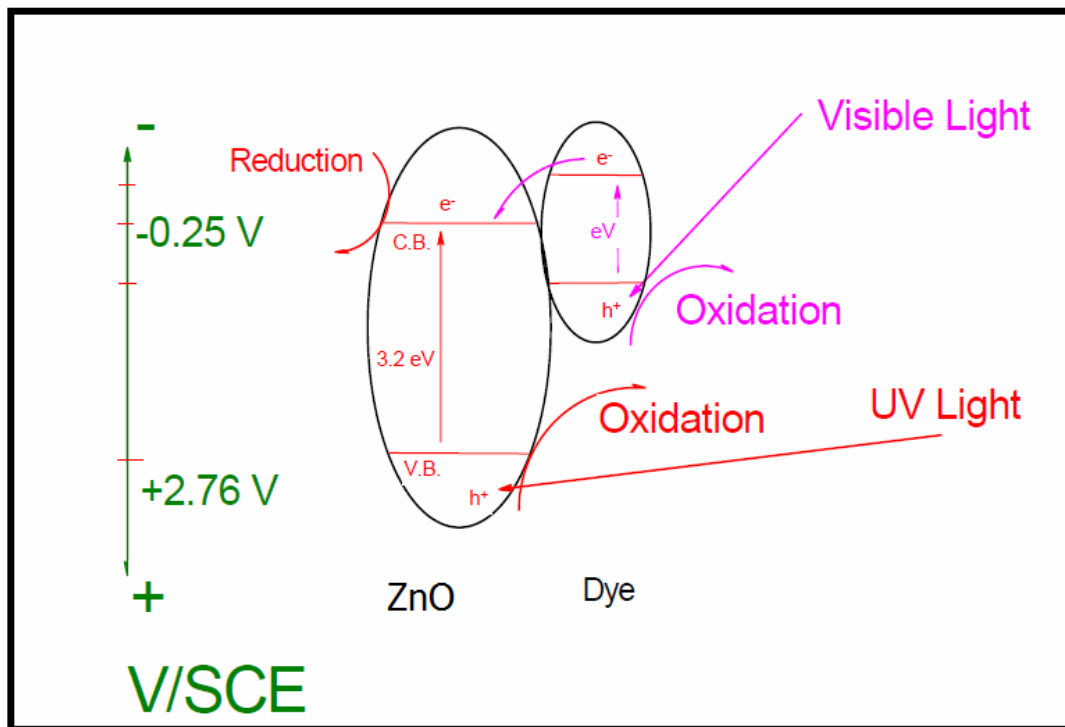


Figure (4.1): Sensitization of ZnO photo-catalyst by dye molecules to the visible light [96].

Experiments conducted using the light filter (cutting off UV light), emphasized the role of dye as sensitizer. ZnO/anthocyanin catalytic activity was almost not affected with cutting off UV light (Figure 3.8). The dye has a small band gap and absorbs light wavelengths in the visible region. This is sufficient for electron-hole generation in the dye molecule, by exciting the electrons from dye HOMO to LUMO. Charge transfer from dye LUMO to ZnO conduction band occurs. The oxidation of bacterial cells may consequently occur, as a result of visible light excitation.

In case of naked ZnO cutting UV light significantly decreased its catalytic activity (Figure 3.8). This is because ZnO depends on UV light for electrons excitation. Thus elimination of UV light lowered the degradation percent, in a similar fashion to using ZnO catalyst under dark conditions.

4.2.1.3 Factors Affect Photo-Degradation Reaction

Effect of Illumination Time on Catalyst Efficiency

The results show that as time proceeded, bacteria concentration decreased (Figure 3.9). Values of turn over frequency and quantum yield were higher at the beginning of the reaction. This is expected. At the beginning of the reaction, the bacteria concentration was higher, which promoted more degradation. As the reaction proceeded bacteria concentration was lowered which caused lowering in the degradation percent per time unit. As reaction progressed, organic molecules resulted from bacteria degradation, and the catalyst functioned to decompose both these organic molecules and the remaining bacterial cells. Another reason for lowering relative catalyst efficiency with time could be due to degradation of ZnO itself.

Effect of Temperature on Catalyst Efficiency

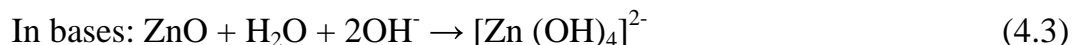
Values of turn over frequency and quantum yield showed small increase with temperature gain within the studied range. The results are consistent with previous works [11, 51, 67, 96-97]. Photo-degradation reactions may not necessarily be affected by temperature [98]. Different paradoxing factors may thus affect rate of bacterial degradation.

On one side, higher temperature may increase bacterial mobility, and its ability to reach OH[·] radicals. On the other hand increasing temperature decreases the concentration of oxygen molecules in the reaction media, and

thus. lowers catalyst efficiency. This explains the low effect of temperature on catalyst efficiency in this work. The insensitivity of the photo-catalytic reaction toward temperature is added to the advantages of the catalyst described here, as the catalyst needs no special temperatures to function effectively.

Effect of pH on Catalyst Efficiency

The degradation results were almost the same in three different media (acidic, neutral and basic), with only a slight preference for the basic medium, and the least preferred is the acidic medium (Figure 3.11). ZnO is considered as an amphoteric oxide, and its reaction depends on pH value. ZnO reacts as a base in acidic solutions, and as an acid in basic solutions, as shown in equations (4.2-3)



This behavior affects the pH value for reaction mixtures. In this work, it was found that the three media became neutral (pH ~7) after short times. So the pH affected the reaction for short time only, and a small difference between degradation percents in the three media was achieved.

The small preference for the basic medium coincided with previous works [11]. At higher pH values there is higher concentration of hydroxyl ions, which may yield more hydroxyl radicals. At lower pH values, ZnO degrades readily yielding Zn^{2+} ions [10], which lowers the catalyst

efficiency. ZnO reactions in the acidic and basic media caused degradation of the catalyst and therefore lowered the bacteria degradation percentage.



The surface charge didn't affect the adsorption of bacteria in this work. This was because the used range of pH values is 5.0-8.7. And the pH_{zpc} of ZnO is 9.0 (the surface of the catalyst is positive below pH 9.0) [99]. The bacteria are considered to have negative surface charges [100].

Effect of Catalyst Concentration on Efficiency

For economic disinfection of contaminated water, the optimum amount of catalyst necessary for efficient degradation was investigated here. Degradation percent increased with increasing the added weight of the catalyst until a maximum efficiency was observed at a given catalyst weight (0.100-0.200 g). Increasing the amount of the catalyst provides higher surface area and more active sites for the adsorption and degradation reaction and makes more utilization for the incoming light that transmitted through the reaction medium in the photo-catalytic reaction. Therefore, higher percent of degraded bacteria was achieved with more catalyst. However, increasing amount of the catalyst more than the optimum weight makes turbidity in the reaction medium, which shields off incident light. This leads to decrease in measured catalyst efficiency and bacteria degradation percentage.

Effect of Bacteria Concentration on Catalyst Efficiency

At low bacterial concentrations, increasing the concentration increased the degradation percent. At higher concentrations, increasing bacterial concentration lowered degradation percentage, as shown in Figure (3.13). However, increasing the initial bacterial concentration increased values of turn over frequency and quantum yield, over the whole range ($\sim 2-14 \times 10^5$ cfu/ml) (Table 3.1). When bacteria concentration increases more bacterial cells are adsorbed on the catalyst surface and so more bacterial cells are degraded. This gives higher percent of degradation till reaching a limited concentration, and higher values for the turnover frequency and quantum yield over all concentrations that were studied here.

Nutrient broth and saline media Effect on catalyst efficiency

The photodegradation reaction conducted in saline medium was found not to be affected by this medium. The catalyst still worked as it was in distilled water with little difference ($\sim 4\%$) in degradation percent. This coincides with previous works [19, 93]. The small decrease in zinc toxicity with increasing concentrations of NaCl is probably due to the decrease in the levels of Zn^{2+} ions due to the formation of Zn-Cl species, which is less toxic than Zn^{2+} ions [93]. In presence nutrient broth medium there was a decrease in the catalytic efficiency with $\sim 20\%$. This can be attributed to degradation competition between the organic molecules from nutrient broth media and bacteria cells. The hydroxyl radical is a non-selective oxidizing

species. Also the colored medium may absorb part of incident light and decrease the light intensity that reaches surfaces of the catalyst particles.

4.2.1.4 Catalyst Recycling

The ability of the catalyst to be recovered and reused in photocatalytic reactions is an important characteristic and receives considerable attention. This can contribute significantly to lowering the operational cost of the water purification and disinfection processes.

The recovered catalyst used here showed good but decreased efficiency, (~10%) loss in each run, on successive usage after recovery from the reaction mixture, (Figure 3.16). Exposure of the sensitized catalyst/dye to light may degrade the dye itself throughout the reaction time. This decreases the catalyst efficiency and gives lower percentage for bacteria degradation. It was reported that increasing pH, temperature or exposure to light is able to spoil the anthocyanin molecule [101]. Bacteria accumulation on the surface of the catalyst particles decreases the sites available for degradation reaction to occur and so decreases in the catalytic efficiency. Re-dyeing the used catalyst was found to restore its efficiency. This supports the first explanation.

4.2.1.5 Disinfection By-Products Identification

Cell death

Many mechanisms were proposed and examined by researchers for cell death in photodegradation processes using photocatalysts. The first

mechanism proposed was that by Matsunaga and coworkers, who believed that direct photochemical oxidation of intracellular coenzyme A to its dimeric form was the root cause of decreases in respiratory activities that led to cell death [23, 102].

Lipid peroxidation reaction was proposed as underlying mechanism of death of *Escherichia coli* K-12 cells by irradiation with UV in the presence of the TiO₂ photocatalyst. Using production of malondialdehyde (MDA) as an index to assess cell membrane damage by lipid peroxidation, an exponential increase in the production of MDA was observed [24]. The TiO₂ photochemical reaction was reported to cause disruption of the cell membrane and the cell wall of *Streptococcus sobrinus* AHT, as shown by leakage of intracellular K⁺ ions that paralleled cell death [103]. Leakage of intracellular Ca²⁺ ions has also been observed with cancer cells [104-105]. Under photocatalytic conditions when TiO₂ was applied to *E. coli*, it was found that the endotoxin, an integral component of the outer membrane, was destroyed. This is a more direct evidence that outer membrane damage occurs [106]. Sunada *et al.* attribute cell death to the combination of cell membrane damage and further oxidative attack of internal cellular components [107]. It was reported that treatment of *E. coli* with TiO₂ and near-UV light resulted in an immediate increase in permeability to small molecules, and the leakage of large molecules such as β-D-galactosidase. Also cell wall was shown to be damaged in less than 20 min, followed by a progressive damage of cytoplasmic membrane and intracellular components [25].

According to literature complete oxidation of organic compounds and *Escherichia coli* cells to carbon dioxide can be achieved using photocatalysts [5, 84- 85]. In this work, GC-MS analysis showed the presence of organic compounds that contain nitrogen in the disinfection medium. This emphasizes the degradation of bacterial cells to smaller organic molecules and may be gases such as CO₂, H₂O and other simple molecules, using our solar simulator light experiments.

4.2.2 UV Irradiation Experiments

4.2.2.1 Control Experiments

Photolysis experiments showed that UV light can degrade bacteria, with and without catalyst, to different extents. DNA molecules inside the bacterial cell absorb UV photons. This absorption damages the DNA by altering nucleotide base pairing, and creating new linkages between adjacent nucleotides on the same DNA strand. If this damage is unrepaired, DNA replication is blocked. This inhibits proteins synthesis for important jobs, growth and healing, and leads to cell death [108]. UV irradiation is one of the known methods that can be used in water disinfection despite its disadvantages, as discussed in Chapter one.

4.2.2.2 Photo-Catalytic Experiments

ZnO is a powerful oxidizing agent with a wide band gap that needs UV irradiation to be excited. Results of bacteria degradation were higher than those under solar simulator light, using same conditions. However,

using UV light instead of solar light is not preferred due to the high cost for application. The usage of UV irradiations has some rescues on human health and the environment.

Naked ZnO catalyst showed higher efficiency than ZnO/anthocyanin catalyst under UV irradiation. In case of ZnO/anthocyanin catalyst, the dye screened away the incident light from the active sites on ZnO surface therefore lowered its catalytic efficiency under UV irradiations compared to the naked ZnO. This indicates the dye role as sensitizer to visible light under solar simulator, it enhanced ZnO efficiency under solar simulator, but under UV light it has no role. In the contrary, its presence decreased the reached light to ZnO surface.

4.3 The Nano-Size ZnO

4.3.1 Solar Simulator Irradiation Experiments

4.3.1.1 Control Experiments

A degradation percent of 30% was obtained by photolysis with no catalysis. That is because the solar light contains a fraction of UV radiation that is harmful to the bacterial cells. In dark control experiments, using nano-ZnO system, there was high decline in bacteria concentration (~90%), Zn²⁺ ions have a bactericidal activity. Many benign materials develop toxicity when reduced to the nanoscale size [109-110]. The presence of nanoparticles causes the increase of membrane permeability leading to accumulation of ZnO nanoparticles in the bacterial membrane. GC-MS

analysis for the sample that was treated with ZnO nanoparticles at dark have not showed degradation products, which indicates that the cell death is not due to cell components degradation as it was found when the reaction was conducted under light. Free anthocyanin dye solutions didn't affect bacteria growth. Similar result was achieved when comparing sensitized and naked ZnO activities under dark conditions, with no noticeable difference in their bactericidal activity. Thus, the dye has no role in absence of light. This emphasizes the role of the dye as sensitizer under solar simulator light.

4.3.1.2 Photo-Catalytic Experiments

Both naked and sensitized ZnO nanoparticle catalysts showed high percent of degradation. The system was more efficient than micro-sized ZnO particles. Degradation percent of 84% was achieved using nano-ZnO/anthocyanin catalyst, compared to 77% using the micro sizes in 60 minutes. This behavior was noticed in both naked and sensitized ZnO catalysts even in dark. Figure (4.2) shows more results. Many reports emphasized parallel behaviors [94, 111-113]. Nano sized ZnO particles have higher surface area and more active sites. More bacterial cells adsorbed on the catalyst surface and more percent of bacteria degradation is achieved. The amount of the dispersion particles, per volume in the reaction medium, increases with decreasing ZnO particle size. This enhances photon absorbance and H₂O adsorption on the surface.

Enhancement of ~ 9% was achieved using anthocyanin dye with nano-sized ZnO under solar simulator light in 60 minutes.

Despite the better catalytic efficiency for the nano ZnO catalyst, the micro ZnO catalyst is still superior to it in terms of catalyst separation and recycling at the end of the reaction. Micro ZnO is easier to separate from reaction medium. It can be done simply by filtration or decantation. This makes it more applicable in water disinfection.

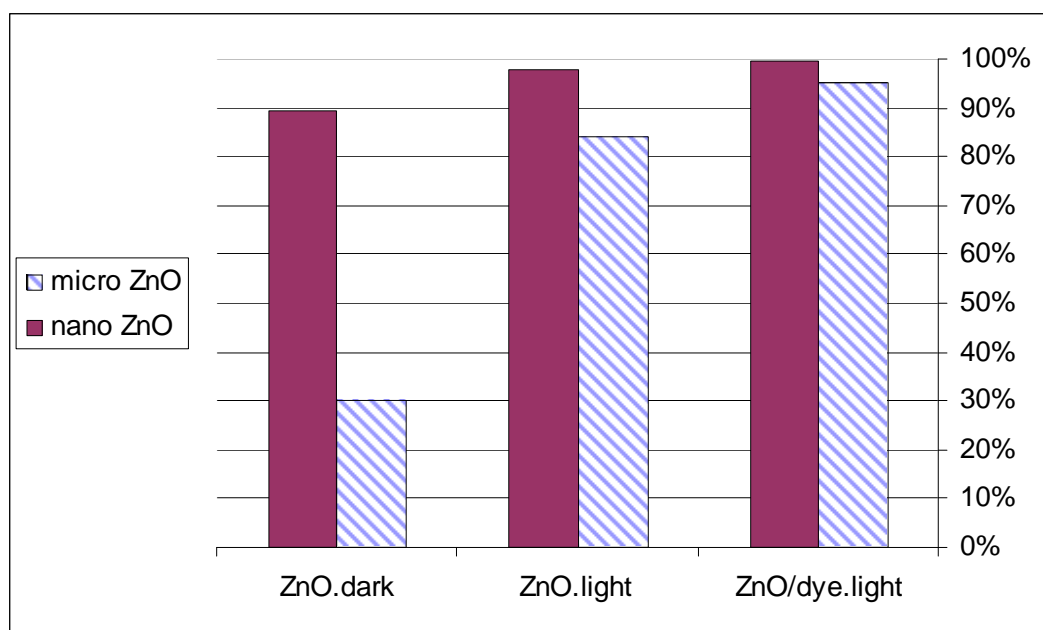


Figure (4.2): Comparison between micro and nano sized sensitized and naked ZnO catalysts under light and dark conditions. Using 50.00 ml distilled water pre-contaminated with $\sim 4 \times 10^5$ cfu/ml *E coli* bacteria, and 0.100 g catalyst under solar simulator (0.0102 W/cm^2), at room temperature for 90 min.

Conclusions

1. Sensitized and naked ZnO catalysts showed good activity against the examined bacteria under a solar simulator, with improvement ~10% in the catalytic efficiency when using anthocyanin dye as sensitizer for ZnO.
2. ZnO/anthocyanin functioned efficiently in presence and absence of UV light under solar simulator, this because of sensitizing effect of the anthocyanin dye.
3. Sensitized and naked ZnO catalyst nanoparticles showed higher catalytic activity than their micro-sized counterparts. Particle size played an important role in enhancement of the catalysts activity against bacteria.
4. The activity of the naked ZnO catalyst under UV irradiations was higher than that of ZnO/anthocyanin catalyst, as the dye screened away the radiations from the catalyst surface.
5. Changing temperature didn't significantly affect the catalyst efficiency.
6. Changing the pH value showed only little effect on the catalyst efficiency.
7. The catalyst amount affected the degradation, and there was an optimum weight that should be used to obtain an efficient disinfection process.
8. Increasing the initial concentration of bacteria enhanced the catalyst activity.

9. The presence of impurities (organic and inorganic) affects the catalyst activity in different manners.
10. Catalyst recovery can readily be achieved simply. This makes it applicable for water disinfection purposes.

Suggestion for Further Work:

1. Using anthocyanin dye from sources other than Karkade, and other natural dyes from different natural sources with different colors, as sensitizers for ZnO catalyst.
2. Applying the ZnO/anthocyanin catalyst against other types of bacteria (e.g gram positive bacteria) and other microorganisms.
3. Applying the ZnO/anthocyanin catalyst on different chemical pollutants, such as fertilizers, pesticides, drugs and other water pollutants.
4. Supporting the catalyst on different supports, such as activated carbon and sand.
5. Using other methods for ZnO nanoparticles preparation to achieve smaller particle size and studying the efficiency.
6. Studying the catalytic activity against bacteria on longer time intervals.
7. Studying the effect of presence of Ca^{2+} and Mg^{2+} ions in water on the catalytic efficiency in water disinfection.
8. Studying the effect of presence of organic contaminant such as halocarbons and humic acid on the catalytic efficiency in water disinfection.

References

1. <http://wwwnc.cdc.gov/travel/yellowbook/2012/chapter-2-the-pre-travel-consultation/water-disinfection-for-travelers.htm>,(accessed Sep. 9th 2011).
2. What is water disinfection? Water treatment solutions. Available at: <http://www.lenntech.com/processes/disinfection/what-is/what-is-water-disinfection.htm>. (Accessed 21 Jun 2011).
3. National drinking water clearinghouse. Disinfection- A national drinking water clearinghouse fact sheet. Tech Brief. (1996). Available at: http://www.nesc.wvu.edu/ndwc/pdf/ot/tb/tb1_disinfection.pdf . (Accessed July 20th 2011) .
4. D.G. Crosby: Environmental Toxicology and Chemistry. New York: Oxford University Press; 1998.
5. O. Legrinin, E. Olivros and A.M. Braun. “Photochemical Processes for Water Treatment”, *Chem. Rev*, **93** (1993) 671–698.
6. S.D. Richardson, A.D. Thruston, T.W. Collette, K.S. Patterson, B.W. Lykins and J.C. Ireland, “Identification of TiO₂/UV disinfection byproducts in drinking water”, *Environ. Sci. Technol.* **30** (1996) 3327-3334.
7. A. J. Attia, S. H. Kadhim and F. H. Hussien, “Photocatalytic Degradation of Textile Dyeing Wastewater Using Titanium Dioxide and Zinc Oxide”, *E-J. Chem.*, **5** (2008) 219-223.

8. B. Pare, P. Singh and S. P. Jonnalagadda, “Artificial light assisted photocatalytic degradation of lissamine fast yellow dye in ZnO suspension in a slurry batch reactor”, *Indian J. Chem., Sect A*, **48A** (2009) 1364-1369.
9. J. Nishio, M. Tokumura , H.T. Znad and Y. Kawase , “Photocatalytic decolorization of azo-dye with zinc oxide powder in an external UV light irradiation slurry photoreactor”, *J Hazard Mater.* **138** (2006) 106-115.
10. H. S. Hilal, G. Y. M. Al-Nour , A. Zyoud, M. H. Helal and I. Saadeddin, “Pristine and supported ZnO catalysts for phenazopyridine degradation with direct solar light”, *Solid State Sci.*, **12** (2010) 578–586.
11. H. S. Hilal, G.Y. M. Nour and A. Zyoud , “Photo-degradation of metheyl orange with direct solar light using ZnO and activated carbon-supported ZnO”, Chapter 6 in *Water Purification*, Eds. Nikolaj Gertsen and Linus S nderby, Novascience Publ., NY, (2009), 227-246, **ISBN:** 978-1-60741-599-2.
12. M. Zhao and Z. Juan, “Wastewater treatment by photocatalytic oxidation of Nano-ZnO”, *Global Environmental Policy in Japan*, No.12 (April, 2008) Internet Version,1-9.
13. A .Fortuny, C .Bengoa, J .Font and A .Fabregat. “Bimetallic catalysts for continuous catalytic wet air oxidation of phenol”, *J Hazard Mater B.* **64** (1999) 181–193.

14. Q. Li, Y. Wai Li, Z. Liu, R. Xie and J. Ku Shang, “Memory antibacterial effect from photoelectron transfer between nanoparticles and visible light photocatalyst”, *J. Mater. Chem.* **20** (2010) 1068-1072.
15. A. Sobczyński and A. Dobosz, “Water Purification by Photocatalysis on Semiconductors”, *Pol. J. Environ. Stud.* **10** (2001) 195-205.
16. F. Saleh. Sensitization of Semiconducting Nano powder Catalysts in photodegradation of medical Drugs and Microorganisms in Water. M.Sc. Thesis, An-Najah National University, Palestine, (2011).
17. X. Pan, I. Medina-Ramirez, R. Mernaugh and J. Liu, “Nanocharacterization and bactericidal performance of silver modified titania photocatalyst”, *Colloids Surf, B* , **77** (2010) 82–89.
18. A. Sapkota, S. Baruah, O. Shipin and J. Dutta, 2009. the 3rd Thailand nanotechnology conference 2009, “ Photocatalytic inactivation of bacteria with ZnO nanorods”, 2009 dec 21-22, Asian Institute of Technology, KlongLuang, Pathumthani 12120, Thailand, 2p.
19. A. D. Belapurkar, P. Sherkhane and S. P. Kale, “Disinfection of drinking water using photocatalytic technique”, *Curr. Sci.*, **91** (2006).
20. O. Seven, B. Dindar, S. Aydemir, D. Metin, M.A. Ozinel and S. Icli, “Solar photocatalytic disinfection of a group of bacteria and fungi aqueous suspensions with TiO₂, ZnO and Sahara desert dust”, *J. Photochem. Photobiol. A.* **165** (2004) 103–107.

21. H. L. Liu and Th. C. K. Yang, "Photocatalytic inactivation of *Escherichia coli* and *Lactobacillus helveticus* by ZnO and TiO₂ activated with ultraviolet light", *Process Biochem.* **39** (2003) 475_481.
22. http://water.me.vccs.edu/courses/env211/lesson14_3.htm . 9 (Accessed 20 July 2011) .
23. T. Matsunaga, T. Tomoda, T. Nakajima, N. Nakamura and T. Komine, "Continuous-sterilization system that uses photoconductor powders", *Appl. Environ. Microbiol.* **54** (1988) 1330.
24. P. C. Maness, S. Smolinski, D.M. Blake, Z.H.E.J. Wolfrum and W.A. Jacoby, "Bactericidal Activity of Photocatalytic TiO₂ Reaction: toward an Understanding of Its Killing Mechanism", *Appl. Environ. Microbiol.* **65** (1999) 4094.
25. Z. Huang, P. Maness, D.M. Blake and E.J. Wolfrum, "Bactericidal mode of titanium dioxide photocatalysis". *J. Photochem. Photobiol. A*, **130** (2000) 163.
26. P. Burke: Preventing Waterborne Disease. Environmental Protection Agency, United States: 1993, p2.
27. <http://www.lenntech.com/processes/disinfection/necessity/necessity-drinking-water-disinfection.htm>. (Accessed 21 Jun 2011).
28. D. J. Petit, J.C. Liébart, J. A. Ayala and R. D'Ari, "Unstable *Escherichia coli* L Forms Revisited: Growth Requires Peptidoglycan Synthesis", *J. Bacteriol.* **189** (2007) 6512-6520.

- 29** G. J. Tortora, B. R. Funke and C. L. Case. *Microbiology An Introduction*: San Francisco, USA: Pearson Education, Inc., 2010, p4.
- 30.** Enterohaemorrhagic *Escherichia coli* (EHEC), (2005) WHO Fact sheet N°125, Available at: <
<http://www.who.int/mediacentre/factsheets/fs125/en/> > (Accessed 18 July 2011) .
- 31.** Free Essay Sample on: Growth Dynamics of E coli in Varying Media , available at: <http://www.essayssample.com/essay/001193.html>. (Accessed 18 July 2011).
- 32.** Reference 29, p310.
- 33.** R.W. Sampson, S. A. Swiatnicki, V. L. Osinga, J. L. Supita, C. M. McDermott and G. T. Kleinheinz, “Effects of temperature and sand on E. coli survival in a northern lake water microcosm”, *J Water Health*, (2006) 389-393.
- 34.** <http://www.eecs.umich.edu/~singh/bk7intro.pdf>. (Accessed 29 JAN 2012)
- 35.** A. Fujishima, K. Honda, “Electrochemical Photolysis of Water at a Semiconductor Electrode”, *Nature*. **238** (1972) 37 – 38.
- 36.V.** Parmon, A.V. Emeline, and N. Serpone, “glossary of terms in photocatalysis and radiocatalysis”, *Int. J. Photoenergy*, **4** (2002) 91-131.

37. <http://www.chem.purdue.edu/raftery/research/photocat.pdf>, (Accessed 2011 July 10).
38. T. Pandiyan, O. Martinez Rivas, J. Martinez, G. Amezcua and M. Martinez-Carrillo, "Comparison of methods for the photochemical degradation of chlorophenols", *J. Photochem. Photobiol. A Chem.* **146** (2002) 149-155.
39. http://books.mcgrawhill.com/EST10/site/spotlight/green/articles/McGraw-Hill_Evil_Genius_Project.pdf. (Accessed 2011 July 20).
40. D.R. Turner, "Electrochemical Reactions at Semiconductor Electrodes", Bell Telephone Laboratories, Inc.~ Whippany, New Jersey. http://www.anl.gov/PCS/acsfuel/preprint%20archive/Files/11_1_MIAMI_04-67_0019.pdf, (accessed 2011 July 17).
41. W. Paul, A. J. Lewis, G. A. N. Connell and T. D. Moustakas, "Doping, Schottky barrier and p-n junction formation in amorphous germanium and silicon by rf sputtering", *Solid State Commun.* **20** (1976) 969-972.
42. A. W. Bot, "Electrochemistry of Semiconductors", *Curr. Sep.* **3** (1998) 87-91.
43. N. Sato: *Electrochemistry at Metal and Semiconductor Electrodes*. Elsevier B.V; 1998. p325.
44. <http://hyperphysics.phy-astr.gsu.edu/hbase/solids/fermi.html>, (Accessed 18 July 2011).

45. M. Alhamed, W. Abdullah, “Structural and optical properties of ZnO:Al films prepared by the sol–gel method”, *JED* , **7** (2010) 246-252.
46. A. G. Rinc n, C. Pulgarin, N.Adler and P. Peringer, “Interaction between *E. coli* inactivation and DBP-precursors dihydroxybenzene isomers in the photocatalytic process of drinking-water disinfection with TiO₂”, *J. Photochem Photobiol A*. **139** (2001) 233–241.
47. N.L. Pickett and P. O’Brien, “synthesis of semiconductor nanoparticles using single-molecular precursors”. *Chemical Record*, **1** (2001) 467-479.
48. L.S. Mende and Judith L. M. Driscoll, “ZnO – nanostructures, defects, and devices”, *Mater. Today* , **10** (2007) 40-48.
49. Koushik Biswas and Mao-Hua Du, “AX centers in II-VI semiconductors: Hybrid functional calculations”, *Appl. Phys. Lett.* **98** (2011) 3pp.
50. Z. Chen, Y. Tang , L.a Zhang and L. Luo, “Electrodeposited nanoporous ZnO films exhibiting enhanced performance in dye-sensitized solar cells”, *Electrochim. Acta*, **51** (2006) 5870–5875.
51. L. Ke, S. Bin Dolmanan, L. Shen, P. K. Pallathadk, Z. Zhang, D. M. Y. Lai and H. Liu, “Degradation mechanism of ZnO-based dye-sensitized solar cells”, *Sol. Energ. Mat. Sol. Cells.* **94** (2010) 323–326.

- 52.** Al-Nour, Ghazi, "Photocatalytic degradation of organic contaminants in the presence of graphite supported and unsupported ZnO modified with CdS particles ", M.Sc. Thesis, An-Najah National University, Palestine, 2009.
- 53.** J. Portier, H.S. Hilal, I. Saadeddin, S. J. Hwang, M.A. Subramanian and G. Campet, "Thermodynamic correlations and band gap calculations in metal oxides". *Prog. Solid State Chem.* **32** (2004) 207–217.
- 54.** T. C. Dang, D. L. Pham, H. L. Nguyen and V. H. Pham. "CdS sensitized ZnO electrodes in photoelectrochemical cells", *Adv. Nat. Sci.: Nanosci. Nanotechnol.* **1** (2010) 6pp.
- 55.** Sh.Seki, T. Sekizawa, K. Haga, T. Sato, M. Takeda, Y. Seki, Y. Sawada, K. Yubuta and T. Shishido. "Effects of silver deposition on 405 nm light-driven zinc oxide photocatalyst". *J. Vac. Sci. Technol.*, **28** (2010) 6p.
- 56.** R. R. Salinas-Guzmán, J. L. Guzmán-Mar, L. Hinojosa-Reyes, J. M. Peralta-Hernández and A. Hernández-Ramírez, "Enhancement of cyanide photocatalytic degradation using sol–gel ZnO sensitized with cobalt phthalocyanine", *J. Sol-Gel Sci. Technol.* **54** 1-7 .
- 57.** K. Nonomura, E. Ebel, T. Oekermann, T. Yoshida, H. Minoura, D. W. Hrlle and D. Schlettwein¹, 2003, "Spectral Sensitization of ZnO by Phthalocyanine and/or Porphyrin Molecules Attached by Electrochemical Self- Assembly", 203rd Meeting, April 27-May 2, 2003, Paris, France.

- 58.** M.K.I. Senevirathne, P.K.D.D.P. Pitigala, V. Sivakumar, P.V.V. Jayaweera, A.G.U. Perera and K. Tennakone, “Sensitization of TiO₂ and ZnO nanocrystalline films with acriflavine”, *J. Photochem. Photobiol. A*: **195** (2008) 364–367.
- 59.** H.Chen, A. Du Pasquier, G. Saraf , J. Zhong and Yi. Lu, “Dye-sensitized solar cells using ZnO nanotips and Ga-doped ZnO films”, *Semicond. Sci. Technol.* **23** (2008) 6pp.
- 60.** K. Hauffe, V. Martinez, H. Pusch, J. Range, R. Schmidt and R. Stechemesser, “Experiments on dye sensitization of zinc oxide”, *Appl Opt.* **8** (1969) 34-41 .
- 61.** S. Chakrabarti, B. Chaudhuri, S. Bhattacharjee, P.Das and BK. Dutta, “Degradation mechanism and kinetic model for photocatalytic oxidation of PVC-ZnO composite film in presence of a sensitizing dye and UV radiation”, *J Hazard Mater.* **15** (2008) 1-3.
- 62.** N. J. Cherepy, G. P. Smestad, M. Gratzel and J. Z. Zhang, “Ultrafast Electron Injection: Implications for a Photoelectrochemical Cell Utilizing an Anthocyanin Dye-Sensitized TiO₂ Nanocrystalline Electrode”, *J. Phys. Chem. B* **101** (1997) 9342-9351.
- 63.** A. Petrella, PD. Cozzoli, ML.Curri, M. Striccoli, P. Cosma and A. Agostiano, “Photoelectrochemical study on photosynthetic pigments-sensitized nanocrystalline ZnO films”, *Bioelectrochemistry.* **63** (2004) 99-102.

- 64.** E. Yamazaki, M. Murayama, N. Nishikawa, N. Hashimoto, M. Shoyama and O. Kurita, "Utilization of natural carotenoids as photosensitizers for dye-sensitized solar cells", *Sol. Energy*, **81** (2007) 512-516.
- 65.** K. Tennakone, A.R. Kumarasinghe, G.R.R.A. Kumara, K.G.U. Wijayantha and P.M. Sirimanne, "Nanoporous TiO₂ photoanode sensitized with the flower pigment cyaniding", *J. Photochem. Photobiol. A*, **108** (1997) 193-195.
- 66.** A. Kay and M. Graetzel, "Research Article Artificial photosynthesis. 1. Photosensitization of titania solar cells with chlorophyll derivatives and related natural porphyrins", *J. Phys. Chem.*, **23** (1993) 6272–6277.
- 67.** S. Benjamin, D.Vaya, P.B. Punjabi and S. C. Ameta, "Enhancing photocatalytic activity of zinc oxide by coating with some natural pigments", *Arabian J. Chem.* **4** (2011) 205-209.
- 68.** A. Zyoud. Nanoparticle CdS-Sensitized TiO₂ Catalyst for Photo-Degradation of Water Organic Contaminants: Feasibility Assessment and Natural-Dye Alternatives, Ph.D.Thesis, An-Najah National University, Palestine, 2009, 155p.
- 69.** J. Sullivan, September 1998, "Anthocyanin", *Carnivorous Plant Newsletter*, 27(3):86-88.
- 70.** J. M. R. C. Fernando and G. K. R. Senadeera, Natural anthocyanins as photosensitizers for dye-sensitized solar devices, *Curr. Sci.* **95** (2008) 663-666.

71. Reference 29, p257.
72. <http://www.svetila.com/en/ultra-vitalux-300w-1170.html>, (accessed 28 July 2011).
73. J.A MacLaughlin, R.R. Anderson and M.F.Holick, “Spectral character of sunlight modulates photosynthesis of previtamin D3 and its photoisomers in human skin”, *Science*. **216** (1982) 1001-1003.
74. J. M. Andrews, “BSAC standardized disc susceptibility testing method (version 4)”, *J. Antimicrob. Chemother.* **56** (2005) 60-76.
75. Current Protocols in Food Analytical Chemistry. Available at: <http://www.nshtvn.org/ebook/molbio/Current%20Protocols/CPFAC/faqf0101.pdf>. (Accessed 27 JAN 2012)
76. A. B. Moghaddam, T. Nazari, J. Badraghi and M. (Kazemzad, “Synthesis of ZnO Nanoparticles and Electrodeposition of Polypyrrole/ZnO Nanocomposite Film”, *Int. J. Electrochem. Sci.*, **4** (2009) 247 – 257.
77. Shape factor (X-ray diffraction), U.S. Department of Energy, Office of Scientific and Technical Information, available on: http://www.osti.gov/engage/rrpedia/Shape_factor_%28Xray_diffraction%29#cite_note-0, (accessed 30 July 2011).
78. http://depts.washington.edu/chemcrs/bulkdisk/chem364A_spr05/notes_Lecture-Note-11.pdf. (Accessed 15 Aug 2011).

- 79.** M. Frobisher, R. D Hinsdill, K. T Crabtree and P. R. Goodheart. In Fundamentals of Microbiology, Tokyo, Toppan Co Ltd, 1974, p137.
- 80.** B. A. Forbes, D. F. Sahm and A. S. Wissfeid, diagnostic microbiology. USA, Mosby. 2007. P 206.
- 81.** [http://teachers.usd497.org/agleue/Gratzel_solar_cell%20assets/ data%20and%20results%20and%20UV-Vis%20spectroscopy%20of%20the%20dyes.htm](http://teachers.usd497.org/agleue/Gratzel_solar_cell%20assets/data%20and%20results%20and%20UV-Vis%20spectroscopy%20of%20the%20dyes.htm). (Accessed 23 Aug 2011).
- 82.** C. Y. Lee, T. Y. Tseng, S. Y. Li and P. Lin, “Growth of Zinc Oxide Nanowires on Silicon (100)”, *TKJSE*. **6** (2003) 127-132.
- 83.** D. Sridevi and K. V. Rajendran, “Synthesis and optical characteristics of ZnO nanocrystals”, *Bull. Mater. Sci.*, **32** (2009) 165–168.
- 84.** C. Cheng and Z. Wang, “Bacteriostatic activity of anthocyanin of *Malva sylvestris*”, *Journal of Forestry Research*, **17** (2006) 83-85.
- 85.** W. A. Jacoby, P. C. Maness, E. J. Wolfrum, D. M. Blake and J. A. Fennel, “Mineralization of bacterial cell mass on a photocatalytic surface in air”, *Environ Sci Technol.* **32** (1998) 2650–2653.
- 86.** E. J. Wolfrum, J. Huang, D. M. Blake, P. C. Maness, Z. Huang, and J. Fiest, “Photocatalytic Oxidation of Bacteria, Bacterial and Fungal Spores, and Model Biofilm Components to Carbon Dioxide on Titanium Dioxide-Coated Surfaces”, *Environ. Sci. Technol.*, **36** (2002) 3412–3419.

- 87.** Kenneth Todar ,Todar's Online Textbook of Bacteriology: Madison University of Wisconsin, 2011, Nutrition and Growth of Bacteria (page 1), <http://textbookofbacteriology.net/index.html>.
- 88.** http://www.nanomt.com/sc_zno.asp. Accessed (24 SEP 2011).
- 89.** S. Hao, J. H. Wu, Y. Huang and J. Lin, “Natural dyes as photosensitizers for dye-sensitized solar cells”. *Sol. Energy.* **80** (2006) 209–214.
- 90.** W. Cuna, Z. Jincai, W. Xinming , M. Bixian ,S. Guoying , P. Ping’an and F. Jiamo, “Preparation, characterization and photocatalytic activity of nano-sized ZnO/SnO₂ coupled photocatalysts”. *Appl. Catal., B.* **39** (2002) 269–279.
- 91.** J.M. Oteiza, M. Peltzer, L. Gannuzzi and N. Zaritzky, Antimicrobial efficacy of UV radiation on Escherichia coli O157:H7 (EDL 933) in fruit juices of different absorptivities, *J Food Prot.* 2005 Jan; 68(1):49-58.
- 92.** S. Atmaca, K. Gul and R. Cicek, “The Effect of Zinc on Microbial Growth”, *Tr. J. of Medical Sciences*, **28** (1998) 595-597.
- 93.** H. Babich and G. Stotzky, “Toxicity of Zinc to Fungi, Bacteria, and Coliphages: Influence of Chloride Ions”, *Appl. Environ. Microbiol.* **36** (1978) 906-914.
- 94.** M.L. Paddock, M.S. Graige, G. Feher and M.Y Okamura, “Identification of the proton pathway in bacterial reaction centers:

inhibition of proton transfer by binding of Zn^{2+} or Cd^{2+} ". *Proc. Nat. Acad. Sci. USA*, **96** (1999) 6183–6188.

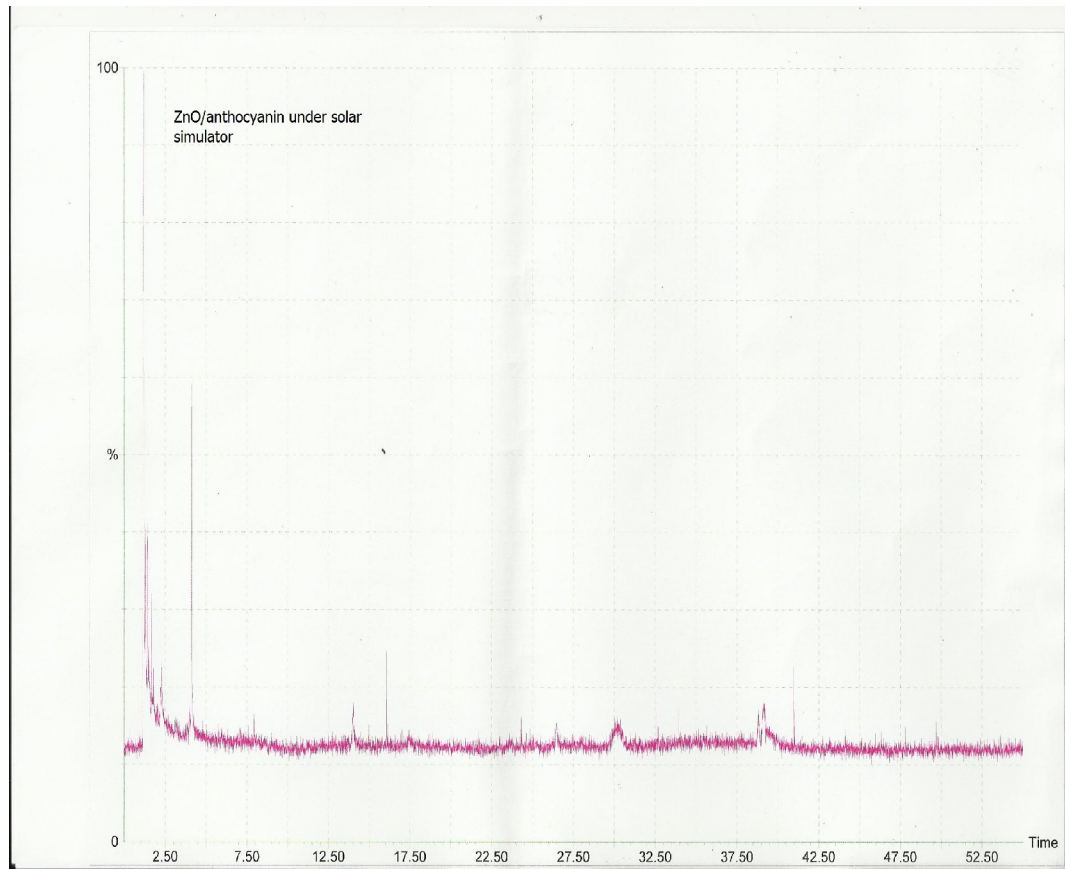
- 95.** L. S. Einbond, K. A. Reynertson, X. DongLuo, M. J. Basile and E. J. Kennelly, "Anthocyanin antioxidants from edible fruits". *Food Chem.* **84** (2004) 23–28.
- 96.** L. Majjad. Dye-Modified Nano-Crystalline TiO_2 Surfaces in Light-Driven Water Purification from Organic Contaminants, Ph.D. Thesis, An-Najah National University, Palestine, (2005), 166p.
- 97.** S. Mozia, M. Tomaszewska and A. W. Morawski, "Photocatalytic degradation of azo-dye Acid Red 18", *Desalination*, **185** (2005) 449-456.
- 98.** Y. Bessekhoud, N. Chaoui, M. Trzpit, N. Ghazzal, D. Robert and J.V. Weber, "UV-Vis versus visible degradation of Acid Orange II in a coupled CdS/ TiO_2 semiconductors suspension", *J. photochem. Photobiol. A*, **183** (2006) 218-224.
- 99.** N. Daneshvar, S. Aber, M. S. Seyed Dorraji, A. R. Khataee, and M. H. Rasoulifard, "Preparation and Investigation of Photocatalytic Properties of ZnO Nanocrystals: Effect of Operational Parameters and Kinetic Study", *Int J Chem Biomol Engg*, **1** (2008) 24-29.
- 100.** P. Gilbert, D.J. Evans, E. Evans, I.G. Duguid, M.R.W. Brown. "Surface characteristics and adhesion of *Escherichia coli* and *Staphylococcus epidermis*". *J Appl Bacteriol.* **71** (1991) 72_/77.

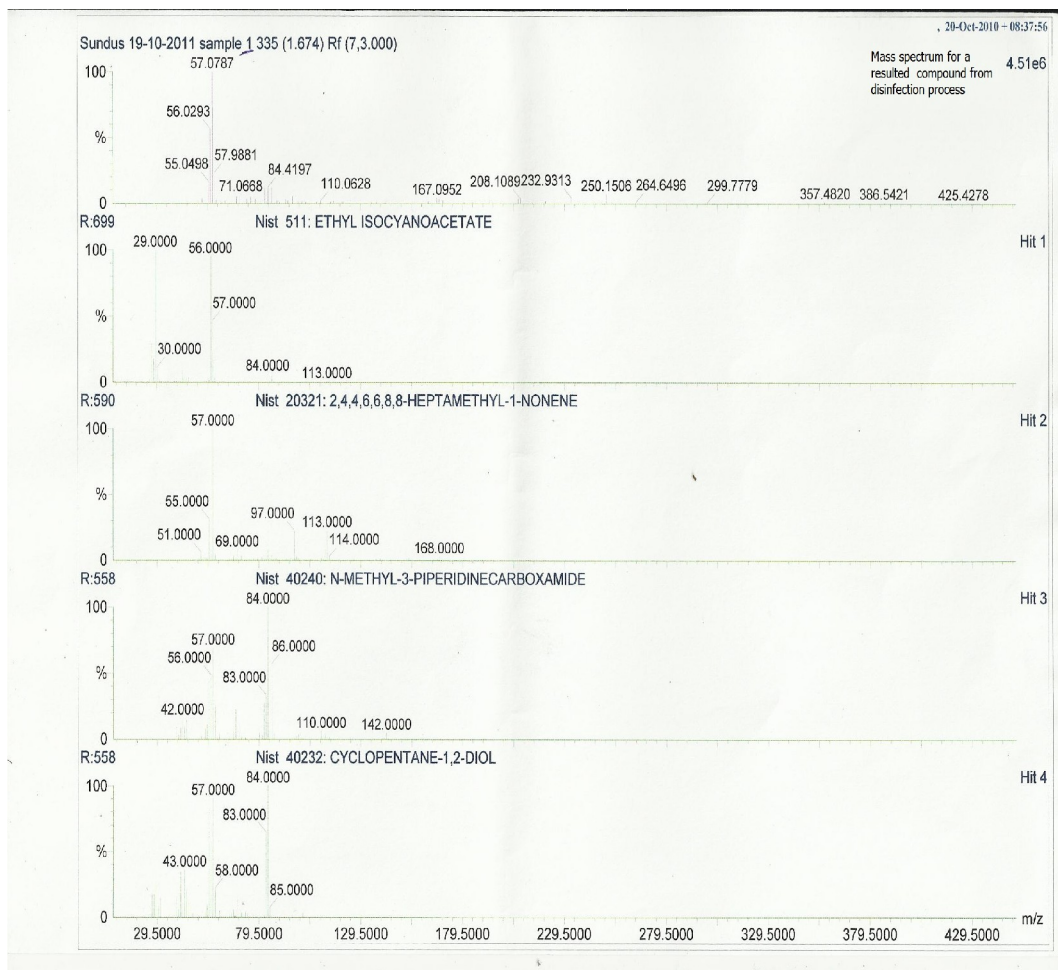
- 101.** G.H. Laleh, H. Frydoonfar, R. Heidary, R. Jameei and S. Zare, The Effect of Light, Temperature, pH and Species on Stability of Anthocyanin Pigments in Four *Berberis* Species, *Pakistan J Nutr*, 5 (1): 90-92, 2006.
- 102.** T. Matsunaga, R. Tomada, T. Nakajima and H. Wake. “Photochemical sterilization of microbial cells by semiconductor powders”, *FEMS Microbiol Lett.* **29** (1985) 211–214.
- 103.** T. Saito, T. Iwase and T. Morioka. “Mode of photocatalytic bactericidal action of powdered semiconductor TiO₂ on mutans streptococci”. *J Photochem Photobiol B Biol.* **14** (1992) 369–379.
- 104.** H. Sakai, R. Cai, K. Hashimoto, T. Kato, K. Hashimoto, A. Fujishima, Y. Kubota, E. Ito and T. Yoshioka. “Photocatalytic effect of TiO₂ particles on tumor cells—study on mechanism of cell death by measuring concentration of intracellular calcium ion”. *Photomed Photobiol.* **12** (1990) 135–138.
- 105.** H. Sakai, E. Ito, R-X. Cai, T. Yoshioka, K. Hashimoto and A. Fujishima, “Intracellular Ca⁺² concentration change of T24 cell under irradiation in the presence of TiO₂ ultrafine particles”. *Biochim Biophys Acta.* **1201** (1994) 259–265.
- 106.** K. Sunada, Y. Kikuchi, K. Hashimoto and A. Fujishima, “Bactericidal and detoxification effects of TiO₂ thin film photocatalysts”. *Environ Sci Technol.* **32** (1998) 726–728.

- 107.** K. Sunada, T. Watanabe, and K. Hashimoto, “Studies on photokilling of bacteria on TiO₂ thin film,” *J. Photochem. Photobiol. A*, **156** (2003) 227–233.
- 108.** E. C. Friedberg, G. C. Walker, and W. Siede. (1995). DNA and mutagenesis. ASM Press, Washington, D.C.
- 109.** K. M. Reddy, K. Feris, J. Bell, D. G. Wingett, C. Hanley, and A. Punnoose. *Appl Phys Lett.* **24** (2007) 8p.
- 110.** E. Kozawa, H. Sakai, T. Hirano, T. Kohno, T. Kakihara, N. Momozawa, M. Abe. “Photocatalytic activity of TiO₂ particulate films prepared by depositing TiO₂ particles with various sizes”. *J Microencapsul.* **18** (2001) 29_40.
- 111.** R. Brayner, R. Ferrari-Iliou, N. Brivois, Sh. Djediat, M. F. Benedetti, and F. Fievet, “Toxicological Impact Studies Based on Escherichia coli Bacteria in Ultrafine ZnO Nanoparticles Colloidal Medium”, *Nano Lett.*, **6** (2006) 866-870.
- 112.** A. A. Tayel, W. F. El-Tras, SH. Moussa, A. F. El-Baz, H. Mahrous, M. F. Salem, L. Brimer, “Antibacterial Action of Zinc Oxide Nanoparticles Against Foodborne Pathogens”, *J. Food Safety*, **31**, (2011) 211–218.
- 113.** N. Padmavathy and R. Vijayaraghavan, “Enhanced bioactivity of ZnO nanoparticles—an antimicrobial study”, *Sci. Technol. Adv. Mater.* **9** (2008) (7pp).

Appendix

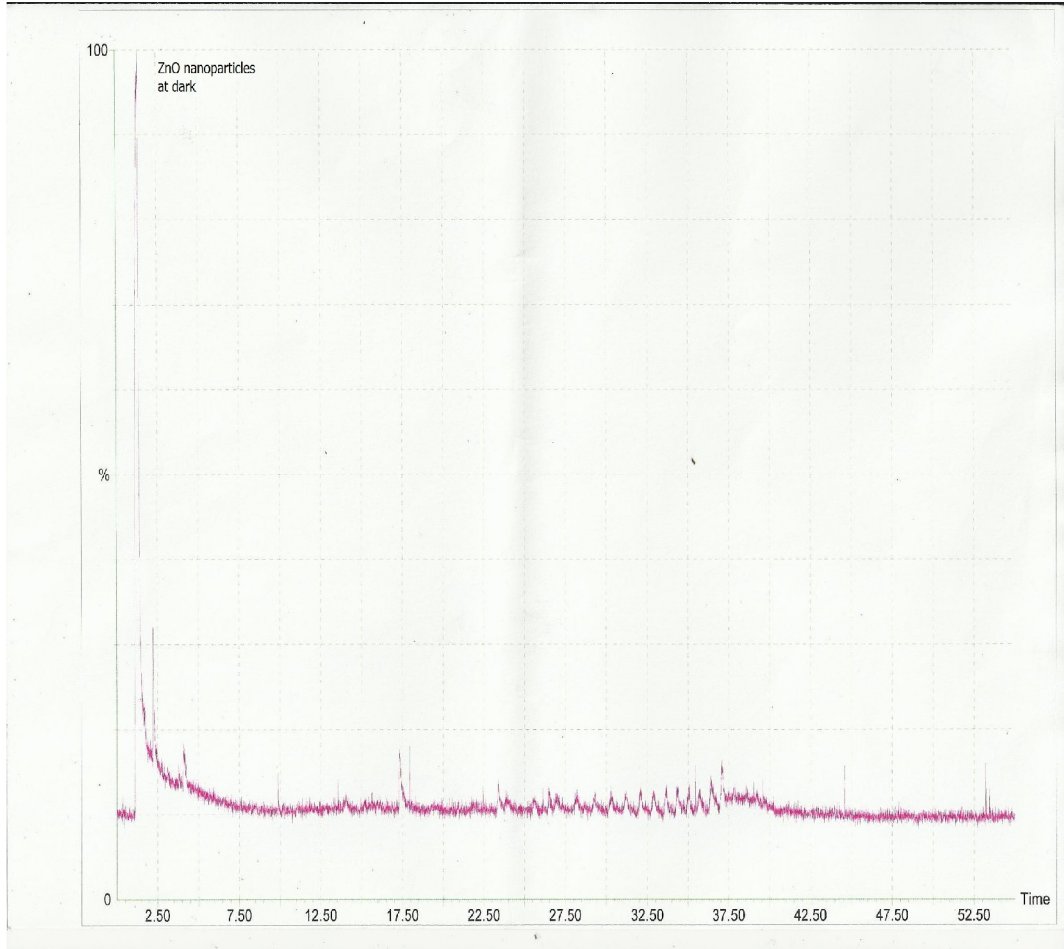
Appendix for the GC-MS analysis data





Hit	REV	for	Compound Name	M.W.	Formula	CAS	Library
1	699	521	ETHYL ISOCYANOACETATE	113	C5H7O2N	2999-46-4	Nist
2	590	484	2,4,4,6,6,8,8-HEPTAMETHYL-1-NONENE	224	C16H32	15796-04-0	Nist
3	558	440	N-METHYL-3-PIPERIDINECARBOXAMIDE	142	C7H14ON2	5115-98-0	Nist
4	558	430	CYCLOPENTANE-1,2-DIOL	102	C5H10O2	900194-24-0	Nist
5	530	381	N,N'-DI-TERT-BUTYL CARBODIIMIDE	154	C9H18N2	691-24-7	Nist
6	521	382	1,3-CYCLOPENTANEDIOL, TRANS-	102	C5H10O2	16326-98-0	Nist
7	508	374	1-AZETIDINECARBOXALDEHYDE, 2,2,4,4-TETRAMETHYL-	141	C8H15ON	50455-46-4	Nist
8	506	411	2-PROPANAMINE, N-(2,2-DIMETHYLPROPYLIDENE)-2-METHYL-	141	C9H19N	1432-48-0	Nist
9	497	397	N-NITROSO-2,4,4-TRIMETHYLOXAZOLIDINE	144	C6H12O2N2	96228-15-8	Nist
10	493	380	1,3-CYCLOPENTANEDIOL, CIS-	102	C5H10O2	16326-97-9	Nist
11	481	347	3-PENTANONE, O-METHYLOXIME	115	C6H13ON	15754-22-0	Nist
12	480	349	ALLYL N-OCTYL ETHER	170	C11H22O	3295-97-4	Nist
13	461	338	1,2-CYCLOPENTANEDIOL, TRANS-	102	C5H10O2	5057-99-8	Nist
14	449	315	N,N-DINITROPIPERAZINE	176	C4H8O4N4	4164-37-8	Nist
15	446	332	(S)-(-)-2-AZETIDINECARBOXYLIC ACID	101	C4H7O2N	2133-34-8	Nist
16	443	321	UREA, N,N'-BIS(1,1-DIMETHYLETHYL)-	172	C9H20ON2	5336-24-3	Nist
17	436	337	PIPERAZINE, 1,4-DIETHYL-	142	C8H18N2	6483-50-7	Nist
18	417	321	ETHANEDIOIC ACID, BIS(1-METHYLPROPYL) ESTER	202	C10H18O4	13784-89-9	Nist
19	409	335	2-(DIETHYLAMINO)-N-(9,10-DIOXOANTHRACENE-2-YL)-ETHANAMIDE	336	C20H20O3N2	225929-33-9	Nist
20	401	306	PROPAN-1-ONE, 1-(2,5-DIMETHYL-4-PROPYNYLPYPERAZIN-1-YL)-	226	C12H22O2N2	90043-72-4	Nist

Expected compounds at 1.674 min.



جامعة النجاح الوطنية

كلية الدراسات العليا

استخدام ZnO المطور بالأصبغ الطبيعية في تعقيم المياه بالتحطيم الضوئي للبكتيريا

إعداد

سندس عثمان عبد الهادي عتيق

إشراف

أ. د. حكمت هلال

د. مجدي دويكات

قدمت هذه الرسالة استكمالاً لمتطلبات الحصول على درجة الماجستير في الكيمياء بكلية الدراسات العليا في جامعة النجاح الوطنية في نابلس، فلسطين.

2012م

ب

استخدام ZnO المطور بالأصبغ الطبيعية في تعقيم المياه بالتحطيم الضوئي للبكتيريا

إعداد

سندس عثمان عبد الهادي عتيق

إشراف

أ. د. حكمت هلال

د. مجدي دويكات

الملخص

هناك الكثير من الوسائل والطرق المستخدمة في تعقيم الماء و تنقيته من الكائنات الدقيقة. لكن كل هذه الوسائل لها آثار سلبية، من أبرزها تكوين نواتج جانبية لا تقل في خطورتها عن الملوث الأساسي. لذلك يعد استخدام الحفازات الضوئية كأكسيد الزنك (ZnO) في عمليات تعقيم الماء بديلا ملائما. و أكسيد الزنك من أشباه الموصلات التي تمتلك فجوة طاقة (band gap) واسعة (3.2 eV)، لذلك فإن عملية تهيج الإلكترونات لديه تتطلب وجود الأشعة فوق البنفسجية، لكن استخدام بعض الأصباغ المثبتة على سطح جزيئات أكسيد الزنك تزيد من حساسيته للأشعة المرئية وبالتالي يمكننا من استخدام أشعة الشمس المتوفرة في عملية التحطيم الضوئي.

تم في هذه الدراسة تحسين حساسية أكسيد الزنك للضوء المرئي باستخدام صبغة الأنثوسيانين الطبيعية (anthocyanin) المستخلصة من أزهار نبات الكركديه، واستخدام هذا الحفاز المطور بالصبغة في تعقيم الماء من البكتيريا عن طريق التحطيم الضوئي لها بوجود ضوء مشابه لضوء الشمس، وذلك لأن فجوة الطاقة لجزيء الصبغة صغيرة و يمتص ضمن منطقة الضوء المرئي فيساعد على تهيج أكسيد الزنك باستخدام الأشعة المرئية. تنقية الماء باستخدام هذا الحفاز أدت إلى تحطيم أكثر من 90% من البكتيريا الموجودة في عينة الماء الملوث في 90 دقيقة بوجود ضوء مشابه لضوء الشمس، إذ أظهر أكسيد الزنك المطور بالصبغة زيادة في نسبة التحطيم بحوالي 10% أكثر من أكسيد الزنك المجرد. و أظهرت التجارب التي تمت باستثناء الحفاز أو الضوء نقصا قليلا في تركيز البكتيريا في عينة الماء الملوث. لم يؤثر

حجب الأشعة فوق البنفسجية التي ضمن الضوء الشمسي باستخدام فلتر ضوئي على عمل الحفاز المطور بالصبغة، بينما قلل كثيرا من فعالية أكسيد الزنك المجرد، مما يظهر دور الصبغة في زيادة حساسية أكسيد الزنك تجاه الأشعة المرئية وبالتالي زيادة فعاليته. و تم تحضير حبيبات أكسيد الزنك ذات الحجم الصغير جدا (نانو) التي يقدر قطرها ب 20 نم واستخدامها في تنقية الماء، و تشخيصها باستخدام تقنيات قياس الطيف المرئي وفوق البنفسجي و طيف اللعان الضوئي (photoluminescence spectrometry) و XRD و SEM. كانت فعالية حبيبات أكسيد الزنك (المحفز بالصبغة وغير المحفز) ذات الحجم الصغير (نانو) أكثر من فعالية الحبيبات ذات الحجم الكبير (مايكرو)، حيث أدت إلى التحطيم الكلي للبكتيريا ضمن الظروف نفسها المستخدمة. و تمت دراسة أثر بعض العوامل على فعالية الحفاز وسير تفاعل التحطيم الضوئي، مثل: مدة الإشعاع، و درجة الحرارة، و درجة الحموضة، وتركيز كل من الحفاز والملوث، وأثر وجود مواد عضوية وغير عضوية ذائبة في الماء المراد تعقيمه.

لم يكن لتغيير درجة الحرارة أثر كبير على فعالية الحفاز. و نظرا للطبيعية الأمفوتيرية لأكسيد الزنك فإن تغيير الرقم الهيدروجيني لوسط التفاعل كان له أثر بسيط جدا على فعالية الحفاز. كان لتغيير كمية الحفاز المستخدمة أثر على فعاليته، حيث لوحظت زيادة الفعالية مع زيادة الكمية المضافة حتى وصلت إلى حد معين، أي أن هناك كمية معينة من الحفاز يجب استخدامها للحصول على أفضل النتائج. كما أدت زيادة تركيز البكتيريا في عينة الماء المراد تعقيمها إلى زيادة في فعالية الحفاز. أما وجود شوائب عضوية وغير عضوية فقد أثر على فعالية الحفاز بشكل متفاوت. تمت إعادة استخدام الحفاز بعد انتهاء التفاعل في تعقيم عينات أخرى من الماء الملوث، حيث أظهر الحفاز المعاد استخدامه فعالية جيدة في تحطيم البكتيريا، كما أن إعادة صبغ الحفاز بعد استخدامه الأول و إعادة استخدامه في تنقية عينة أخرى من الماء الملوث أدت إلى استرجاع الفعالية الأصلية للحفاز.

This document was created with Win2PDF available at <http://www.win2pdf.com>.
The unregistered version of Win2PDF is for evaluation or non-commercial use only.
This page will not be added after purchasing Win2PDF.